UC San Diego
UC San Diego Electronic Theses and Dissertations

Title

Hypersensitivity of BRCA-Deficient Cancer Cells to FEN1 Inhibition

Permalink

https://escholarship.org/uc/item/951449g2

Author

Guo, Elaine Yiran

Publication Date

2020

Peer reviewed|Thesis/dissertation

UNIVERSITY OF CALIFORNIA SAN DIEGO

Hypersensitivity of *BRCA*-Deficient Cancer Cells to FEN1 Inhibition

A dissertation submitted in partial satisfaction of the requirements for the degree Doctor
of Philosophy

in

Biomedical Sciences

by

Elaine Y. Guo

Committee in charge:

      Professor Richard Kolodner, Co-chair
      Professor Jean Wang, Co-chair
      Professor Arshad Desai
      Professor Steven Dowdy
      Professor Paul Mischel

2020

The dissertation of Elaine Y. Guo is approved, and it is acceptable in quality and form for publication on microfilm and electronically:

_____

_____

_____

_____
                                                                    Co-chair

_____
                                                                    Co-chair

University of California San Diego

2020

iii

The dedicated life is worth living.
You must give with your whole heart.

Annie Dillard

TABLE OF CONTENTS

LIST OF ABBREVIATIONS

BRCA1	Breast Cancer Type 1 Susceptibility Gene
kDa	Kilodalton
DDR	DNA damage response
DSB	Double-strand DNA break
HR	Homologous recombination
NLS	Nuclear localization sequence
RING	Really Interesting New Gene
BARD1	BRCA1-Associated RING Domain 1
ERα	Estrogen Receptor alpha
CHK2	Checkpoint Kinase 2
ATM	Ataxia Telangiectasia Mutated
IR	Ionizing radiation
PALB2	Partner and Localizer of BRCA2
BRCT	BRCA1 C Terminus
BRIP1	BRCA1-Interacting Protein C-Terminal Helicase 1
CtIP	CtBP-Interacting Protein
MRN	Mre11, Rad50, and Nbs1
Mre11	Meiotic Recombination 11
Rad50	Radiation Sensitive 50
Nbs1	Nibrin
HBOC	Hereditary breast and ovarian cancer
BRCA2	Breast Cancer Type 2 Susceptibility Gene

RAD51	Radiation Sensitive 51
ssDNA	Single-strand DNA
BRC repeats	Breast Cancer Type 2 Susceptibility Protein repeats
dsDNA	Double-strand DNA
RPA	Replication Protein A
OB folds	Oligonucleotide binding folds
CDK	Cyclin-Dependent Kinase
RAD52	Radiation Sensitive 52
ABRAXAS	BRCA1 A Complex Subunit
RAP80	Receptor-Associated Protein 80
PARP	Poly (ADP-ribose) Polymerase
PARPi	PARP inhibitor
HU	Hydroxyurea
TP53	Tumor Protein 53
NHEJ	Non-homologous end joining
PARP1	Poly (ADP-ribose) Polymerase 1
SL	Synthetic lethality, synthetic lethal
PAR	Poly(ADP-ribose)
NAD$^+$	Nicotinamide adenine dinucleotide
FDA	Food and Drug Administration
53BP1	p53-Binding Protein 1
REV7	Revertibility Protein 7
RAD27	Radiation Sensitive 27

GIS	Genome instability suppressing
TCGA	The Cancer Genome Atlas
RAD55-RAD57	Radiation Sensitive 55-Radiation Sensitive 57
rad27Δ	rad27 deletion/ null allele
RAD2	Radiation Sensitive 2
FEN1	Flap Endonuclease 1
EXO1	Exonuclease 1
GEN1	Flap Endonuclease GEN Homolog 1
XPG	Xeroderma Pigmentosum
APC	Adenomatous Polyposis Coli
SGS1	Slow Growth Suppressor 1
BLM	Bloom Syndrome RecQ Like Helicase
EC50	Half maximal effective concentration
C_{max}	Maximum serum concentration
IC50	Half maximal inhibitory concentration
TERT	Telomerase Reverse Transcriptase
CRISPR	Clustered regularly interspaced short palindromic repeats
WT	Wildtype
eGIS1	Essential genome instability suppressing
DMSO	Dimethyl sulfoxide
CCLE	Broad Institute Cancer Cell Line Encyclopedia
siRNA	Small interfering RNA
siFEN1	FEN1-targeting siRNAs

siNT	Non-targeting control siRNAs
GAPDH	Glyceraldehyde 3-Phosphate Dehydrogenase
BrdU	5-bromo-2'-deoxyuridine
FACS	Fluorescence-activated cell sorting
γH2AX	Phosphorylated H2A Histone Family Member X
DAPI	4′,6-diamidino-2-phenylindole
mRFP	Mono red fluorescent protein
H2B	Histone 2B
PIKK	Phosphatidylinositol 3-Kinase-Related Kinase
ATR	Ataxia Telangiectasia and Rad3 Related
DNA-PK	DNA-Dependent Protein Kinase
Chk1	Checkpoint Kinase 1
DNA-PKcs	DNA-Dependent Protein Kinase, catalytic subunit
Ku	Non-homologous end joining protein
ATRIP	ATR-Interacting Protein
CDC25A	Cell Division Cycle 25 Homolog A
H2AX	H2A Histone Family Member X
pChk1	Phosphorylated Checkpoint Kinase 1
pChk2	Phosphorylated Checkpoint Kinase 2
DNA-PKi	DNA-PK inhibitor
ATMi	ATM inhibitor
ATRi	ATR inhibitor
BioGRID	Biological General Repository for Interaction Datasets

PBS	Phosphate buffered saline
EDTA	Ethylenediaminetetraacetic acid
HBSS	Hank's Balanced Salt Solution
FITC	Fluorescein isothiocyanate
7-AAD	7-aminoactinomycin D
HEPES	4-(2-hydroxyethyl)-1-piperazineethanesulfonic acid
CHAPS	3-((3-cholamidopropyl) dimethylammonio)-1-propanesulfonate
DTT	Dithiothreitol
BSA	Bovine serum albumin
FIJI	ImageJ
RIPA buffer	Radioimmunoprecipitation assay *buffer*
SDS-PAGE	Sodium dodecyl sulfate–polyacrylamide gel electrophoresis
PVDF	Polyvinylidene fluoride
HRP	Horseradish peroxidase
W/V	Weight/ volume
FBS	Fetal bovine serum
PSG	Penicillin-Streptomycin-Glutamine
ATCC	American Type Culture Collection
NEAA	Non-essential amino acid
Cas9	CRISPR associated protein 9
shRNA	Short hairpin RNA

LIST OF FIGURES

CHAPTER 1

CHAPTER 2

CHAPTER 3

LIST OF TABLES

CHAPTER 2

CHAPTER 3

CHAPTER 4

ACKNOWLEDGEMENTS

I would like to acknowledge my mentors Drs. Jean Wang and Richard Kolodner for guiding me and for challenging me to become a better scientist. My time in the Biomedical Sciences Graduate Program has allowed me to freely explore, learn, fail, and pick myself up again. It was through this process that I realized how much I love science, and for these opportunities, I'm truly grateful.

I'm thankful for members of the Kolodner and Wang Labs and neighboring labs for showing me the ropes and for their friendship. In particular, Dr. Anjana Srivatsan played a big part in helping me to troubleshoot experiments and provide feedback on my presentations. Our collaborators in the Ludwig San Diego Small Molecule Development Lab and at the Nikon Imaging Center have made many experiments possible as well. In addition, the NIH Cancer Biology Training Program has been one of my favorite parts of grad school; I've learned a lot from each discussion and from presenting my data in front of this supportive group. And of course, I'm also grateful for the guidance of my committee.

My friends and family, near and far, have been a foundation of my time here. I'm grateful to labmates, college and grad school friends for our countless conversations and adventures. And finally, I'm grateful to my family for their unwavering support from beginning to end, for knowing me best, for always listening and cheering me on.

Chapters 2 and 3, in part, are currently being prepared for submission for publication. Guo, Elaine; Ishii, Yuki; Mueller, James; Srivatsan, Anjana; Putnam, Christopher; Wang, Jean Y. J.; Kolodner, Richard. FEN1 is a potential therapeutic target for human cancers with defects in homologous recombination. The dissertation author is the co-author of this paper.

EDUCATION

2013-2020 University of California San Diego
PhD Candidate in Biomedical Sciences
Co-advisors Richard Kolodner and Jean YJ Wang

2009-2013 Rice University, TX
BS Chemistry, Specialization in Biological and Medicinal Chemistry
Distinction in Research and Creative Works

RESEARCH EXPERIENCE

2014-2020 University of California San Diego
PhD Thesis: Hypersensitivity of *BRCA*-Deficient Cancer Cells to FEN1 Inhibition
Co-advisors Richard Kolodner and Jean YJ Wang, Ludwig Institute for Cancer Research San Diego

2010-2013 Baylor College of Medicine, TX
Undergraduate Research Assistant
Advisor Choel Kim, Pharmacology

FUNDING

2015-2016 National Institutes of Health Cancer Cell Biology Training Grant

TEACHING & OUTREACH

2015-2016 UC San Diego Biomedical Sciences Graduate Student Council: Retreat Coordinator and Informal Seminar Coordinator

2015 Teaching Assistant for the UC San Diego undergraduate seminar: Introduction to Biomedical Research

2014-2015 Contributing writer for Science in the Classroom: **Guo E.** Annotations and teaching guides for "Sleep promotes branch-specific formation of dendritic spines after learning".

PUBLICATIONS

2020 **Guo E***, Ishii Y*, Mueller J, Srivatsan A, Putnam C, Wang JYJ, Kolodner R. "FEN1 is a potential therapeutic target for human cancers with defects in homologous recombination". In preparation for submission.

2015   Qin L, Reger AS, **Guo E**, Yang MP, Zwart P, Casteel DE, Kim C. "Structures of cGMP-Dependent Protein Kinase I alpha Leucine Zippers Reveal an Interchain Disulfide Bond Important for Dimer Stability". Biochemistry. 2015; 54(29):4419-22.

2014   Reger AS, Yang MP, Koide-Yoshida S, **Guo E**, Mehta S, Yuasa K, Liu A, Casteel DE, Kim C. "Crystal structure of the cGMP-dependent protein kinase II leucine zipper and Rab11b protein complex reveals molecular details of G-kinase-specific interactions". J Biol Chem. 2014; 289(37):25393-403.

ABSTRACT OF THE DISSERTATION

Hypersensitivity of *BRCA*-Deficient Cancer Cells to FEN1 Inhibition

by

Elaine Y. Guo

Doctor of Philosophy in Biomedical Sciences

University of California San Diego, 2020

Professor Richard Kolodner, Co-chair
Professor Jean Wang, Co-chair

Synthetic lethal strategies for cancer therapeutics seek to target genetic defects or vulnerabilities in tumor cells, while sparing normal cells. Here we identified that *RAD27/ FEN1*, which encodes Flap Endonuclease 1, has the greatest number of synthetic lethal interactions with *Saccharomyces cerevisiae* genome instability genes and is thus a potential target for an inhibitor-based approach to kill cancer cells with genome instability. FEN1 inhibition specifically targeted *BRCA1*- or *BRCA2*-defective members of matched pairs of human cell lines, and *BRCA*-deficient cancer cell lines tended to show increased sensitivity to FEN1 inhibition or knockdown, regardless of their olaparib sensitivity. Both

sensitive and resistant cell lines showed increased DNA damage responses upon FEN1 inhibition; however, sensitive cell lines were unable to recover and replicate DNA even when the drug was removed. Although FEN1 inhibition can induce an apoptotic response, inhibition of apoptosis did not rescue sensitive cell lines. Rather, we found that FEN1 inhibition increased chromosome breaks in sensitive cells characteristic of mitotic catastrophe. These results suggest that FEN1 inhibitors are potentially valuable for targeting cancers with defects in homologous recombination and that cycles of drug treatment could be effective for killing sensitive cells.

CHAPTER 1

INTRODUCTION

1-A. Breast Cancer Type 1 Susceptibility Gene (*BRCA1*)

In 1990, researchers established a concrete genetic link between early-onset familial breast cancer and chromosome 17q21 through linkage mapping (1). In the years that followed, both academic labs and private companies raced to identify and clone the gene responsible for inherited breast cancer, and in 1994, *BRCA1* was successfully identified by positional cloning methods (2).

1-A-1. BRCA1 functional domains and binding partners

BRCA1 is an 1863 amino acid or 208 kDa protein. It has many functional domains that interact with a wide range of binding partners (**Fig. 1-1**). Thus, BRCA1 has diverse functions ranging from hormone signaling to DNA damage response (DDR) coordination, playing roles in cell cycle checkpoint activation and double-strand DNA break (DSB) repair by homologous recombination (HR) (3-5).
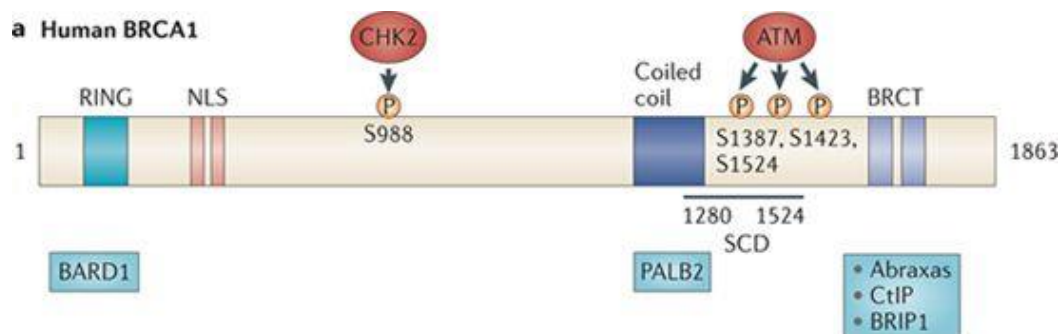
Figure 1-1. Human BRCA1 functional domains (6).

The N-terminus of BRCA1 contains a nuclear localization sequence (NLS) and a Really Interesting New Gene (RING) domain that heterodimerizes with BRCA1-associated RING domain protein 1 (BARD1) (7). One of the many functions of the BRCA1-BARD1 complex is regulation of estrogen signaling. Higher levels of estrogen increase risk of breast cancer (8) as estrogen promotes transcriptional activation of pro-proliferative genes. The BRCA1-BARD1 complex acts as an E3 ubiquitin ligase (9) and

can ubiquitinate and degrade estrogen receptor alpha (ERα) (10, 11) to regulate estrogen signaling and thus breast cancer proliferation.

BRCA1 is also phosphorylated in response to DNA damage. Located in its central region are multiple phosphorylation sites for the DDR kinases Checkpoint Kinase 2 (CHK2) and Ataxia Telangiectasia Mutated (ATM). CHK2 phosphorylation (on Serine 988 of BRCA1) is required for BRCA1-mediated HR (12); inhibition of this phosphorylation by mutating S988 disrupted regulation of HR. The central region also contains a SQ/TQ cluster domain with multiple ATM phosphorylation sites. These phosphorylation sites mediate G2/M and S phase checkpoint activation; a transfected BRCA1 mutant without 3 of these phosphorylation sites (Serine 1387, 1423, 1524) could not rescue defective checkpoint activation or ionizing radiation (IR) hypersensitivity in a BRCA1-deficient cell line (13, 14).

The C-terminus of BRCA1 contains a coiled-coil domain, which binds to partner and localizer of BRCA2 (PALB2). This interaction is important for loading of BRCA2-Radiation Sensitive 51 (RAD51) at DSB, a central step in HR (15, 16).

The C-terminus of BRCA1 also contains a BRCA1 C Terminus (BRCT) domain, an important phosphoprotein binding motif which is conserved in multiple DDR proteins (facilitates binding to proteins phosphorylated on serine motifs SXXF by ATM). Through its BRCT domain, BRCA1 forms distinct complexes that function in DDR. These binding partners include the BRCA1 A Complex Subunit (ABRAXAS), BRCA1-interacting protein C-terminal helicase 1 (BRIP1), and CtBP-interacting protein (CtIP) (17). The BRCA1–abraxas complex aids BRCA1 recruitment to sites of DNA damage (18-21), in part because this complex recognizes ubiquitylated histones, an important posttranslational

modification in DDR. The BRCA1–BRIP1 complex is required for HR (22, 23). Lastly, the BRCA1–CtIP complex acts as a molecular switch in DSB repair, promoting HR over DNA end-joining by associating with the MRN complex (Meiotic Recombination 11/ Mre11, Radiation Sensitive 50/ Rad50, and Nibrin/ Nbs1) to facilitate end resection (24, 25).

1-A-2. BRCA1 is a tumor suppressor

In the context of disease, BRCA1 is a tumor suppressor that follows the two-hit model, in which an inherited deleterious mutation in one allele is later combined with a somatic deleterious mutation in the other allele to cause cancer (26). BRCA1 deficiency is most prominently implicated in hereditary breast and ovarian cancer (HBOC) (27) but increases risk for other cancer types too. While many unique cancer-causing *BRCA1* mutations have been documented (28-30), they fall into two main groups.

The first group includes missense, deleterious mutations in the RING domain. These mutations can disrupt binding to BARD1 and thus also disrupt the E3 ubiquitin ligase activity of the BRCA1-BARD1 complex (31-33). The second group of cancer-associated mutations includes truncations and missense mutations of the C-terminal domain (34, 35). While all truncating mutations are considered functionally deleterious, missense mutations in the C-terminal BRCT domain can also contribute to BRCA1 loss of function or loss of binding to its interactors by causing protein misfolding and destabilization (24, 35). The presence of cancer-associated mutations in the RING and BRCT domains suggests that these sequences are important for mediating BRCA1 tumor suppressor function (28-30).

1-B. Breast Cancer Type 2 Susceptibility Gene (*BRCA2*)

Breast cancer is a complex disease, and studies in 1993 predicted the existence of multiple breast cancer susceptibility genes, beyond those at the 17q locus (36). In 1995, researchers identified another causative gene, *BRCA2*, at chromosome 13q12-q13 by studying families with multiple cases of early-onset breast cancer with clear linkage to *BRCA1* (37).

1-B-1. BRCA2 functional domains and binding partners.

BRCA2 is a 3418 amino acid or 384 kDa protein. It's a DNA binding and phosphoprotein that, in contrast to the multiple functions of BRCA1, is primarily involved in HR (**Fig. 1-2**).
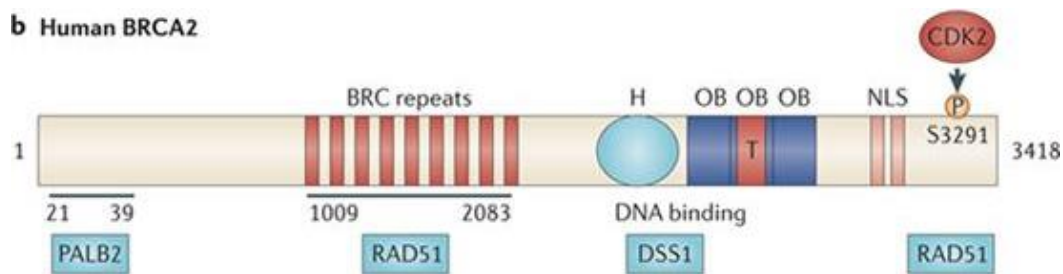
Figure 1-2. Human BRCA2 functional domains (6).

The N-terminus of BRCA2 binds the partner and localizer of BRCA2 (PALB2) (38). As its name implies, PALB2 association with BRCA2 is required for the localization of BRCA2 to sites of DNA damage during HR, where BRCA2 is then required for the assembly of RAD51 recombinase on single-strand DNA (ssDNA) at DSB (39, 40).

BRCA2 binds directly to RAD51 through its 8 conserved Breast Cancer Type 2 Susceptibility Protein (BRC) repeats. This interaction is required for the assembly of RAD51 in vivo as BRCA2-deficient cancer cells show aberrant RAD51 foci formation in response to IR (39). In addition to recruiting RAD51 to sites of DNA damage, the BRC repeats also regulate RAD51 DNA-binding selectivity, promoting the assembly of RAD51

onto ssDNA, not double-strand DNA (dsDNA). To target RAD51 onto ssDNA, the BRC repeats accelerate displacement of the abundant ssDNA binding protein, replication protein A (RPA), from ssDNA (37) and maintain the active ATP-bound form of the RAD51-ssDNA filament (by blocking ATP hydrolysis) (41). In conjunction, the BRC repeats also block RAD51 nucleation onto dsDNA (42). These steps promote DNA strand exchange by expanding the ssDNA in preparation for homology search and facilitating the interaction between invading and homologous template DNA strands.

BRCA2 also contains a DNA-binding domain that interacts with both ssDNA and dsDNA. This domain is divided into an α-helical domain and 3 oligonucleotide binding (OB) folds that bind ssDNA, and a tower domain that binds dsDNA (43, 44). During DNA repair, the BRCA2 OB folds target BRCA2 to ssDNA and in turn promote RAD51 recruitment to ssDNA (45). One study found that, in fact, a fusion protein of BRCA2 BRC repeats (which recruit RAD51) and the large RPA subunit (which binds ssDNA) was enough to partially restore HR in *Brca2*-mutant cells, suggesting that the ssDNA binding domains are important to the ability of BRCA2 to mediate HR.

The C-terminus of BRCA2 contains an NLS and additional binding sites for RAD51. C-terminal interactions between BRCA2 and RAD51 is regulated by a cyclin-dependent kinase (CDK) phosphorylation site (Serine 3291), which when phosphorylated, blocks BRCA2 interaction with RAD51 (46). During S phase or in the presence of DNA damage, phosphorylation of this site decreases, to stimulate interaction with RAD51, and increases as cells progress towards mitosis.

1-B-2. BRCA2 is a tumor suppressor

Similar to *BRCA1*, *BRCA2* is a tumor suppressor that follows the two-hit model. *BRCA2* mutations are also a predominant cause of HBOC (27) and increase risk of other cancer types as well. Cancer-causing mutations in *BRCA2* can be found as point mutations in BRC repeats that disrupt RAD51 binding (47) or mutations in the DNA binding domain (48) that are linked to defects in HR (49). Mutations in the BRC repeats and the DNA binding domain highlight the importance of the BRCA2-RAD51 and BRCA2-DNA interactions to tumor suppression.

1-C. BRCA1 and BRCA2 Function in Double-Strand Break Repair by Homologous Recombination

The initial clue for understanding the functions of BRCA1 and BRCA2 came from the observation that *Brca*-deficient mice are phenotypically similar to mice deficient in the *Rad51* recombinase. Homozygous mutations in *Brca1, Brca2, and Rad51* all lead to embryonic lethality (50-52), and the few respective early stage embryos that form all show hypersensitivity to IR and increased chromosome aberrations, which are characteristic of error-prone repair of chromatid breaks (53). These mouse models suggested that BRCA1 and BRCA2 could participate in the RAD51-mediated HR pathway (50, 51).

1-C-1. Homologous Recombination: An Overview

Homologous recombination (HR) is a mechanism for maintaining genome integrity that is found in all eukaryotes (**Fig. 1-3**). HR is required for repair of DSB (54) and can be initiated either at two-ended DSB or at one-ended DSB that are generated by nucleolytic cleavage of stalled replication forks. This pathway is active during S and G2 phases of the cell cycle when sister chromatids, or identical copies of a chromosome, are available as templates.
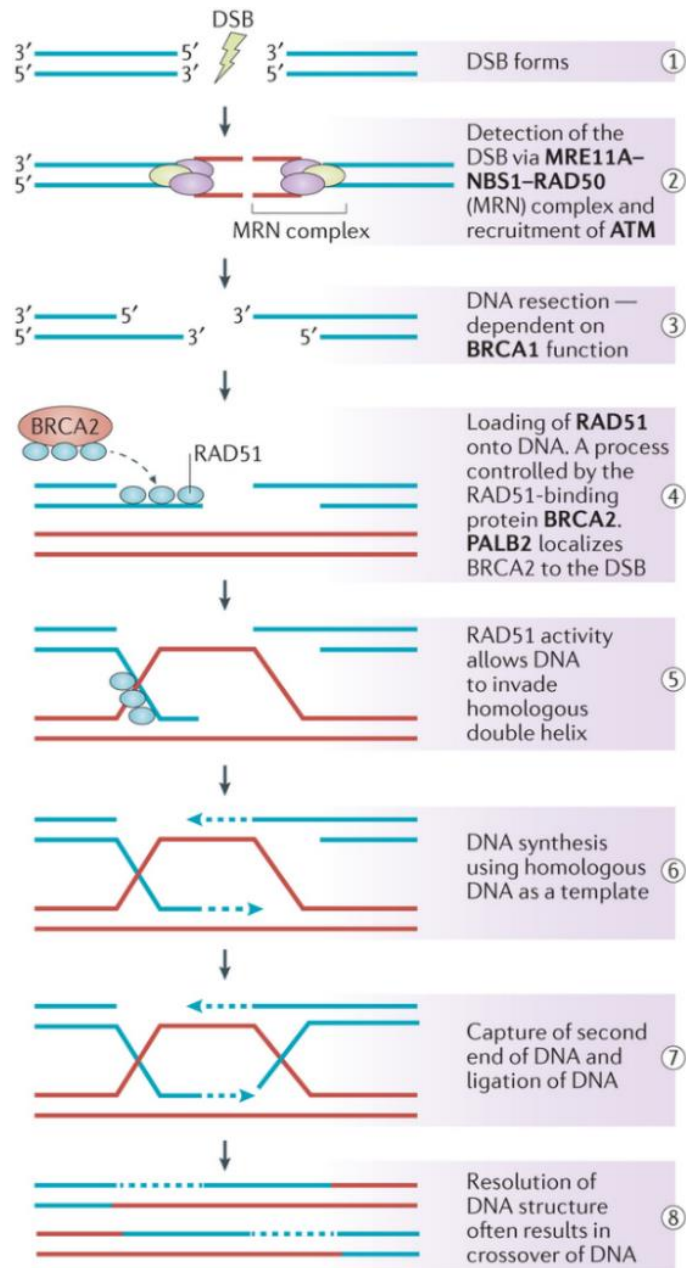
Figure 1-3. Homologous recombination pathway (55). *Step 1.* DSB formation. *Step 2.* Detection and binding of the broken ends by the MRN complex, which then leads to ATM recruitment and HR initiation. *Step 3.* Resection of 5′ DNA to expose two regions of ssDNA on either side of the DSB. This step is BRCA1-dependent. *Step 4.* BRCA2 localizes the DNA recombinase RAD51 to the exposed 3' overhanging ssDNA of the resected DSB. This step is dependent on PALB2. *Step 5.* RAD51 bound to DNA forms a nucleoprotein filament with the ability to invade an intact, homologous donor stretch of DNA (red). *Step 6.* DNA polymerases use the homologous DNA sequence as a template and the invaded ssDNA as a primer to synthesize new DNA. *Steps 7 and 8.* Lastly, DNA ligases and endonucleases resolve the resulting DNA structures to complete DSB repair. Tumor suppressor proteins are in bold.

Many key eukaryotic genes that act in HR were first identified in *Saccharomyces cerevisiae* by mutant isolation, epistasis analysis, and cloning of corresponding genes by complementation of the mutant phenotype (54). This work identified a panel of recombinases, or enzymes which mediate pairing and exchange of DNA strands and which catalyze HR, known as the Radiation Sensitive 52 (RAD52) epistasis group. These proteins are highly conserved in eukaryotes from yeast to man.

The most notable member of this group is the RAD51 recombinase. RAD51 is central to assembly of the presynaptic filament, a crucial step in HR. At resected DSB, RAD51 polymerizes onto the exposed ssDNA to form a highly ordered and helical presynaptic filament. This ssDNA filament then invades dsDNA in search of homology between recombining and donating DNA strands.

Loading of RAD51 onto ssDNA, however, is slow and competes with RPA, an abundant protein that binds ssDNA with high affinity. Although it's true that RPA can facilitate HR by removing secondary structures in ssDNA (56) and by sequestering ssDNA intermediates (57, 58), it can also strongly inhibit the function of recombinases by excluding their binding to ssDNA (59, 60). To overcome the inhibitory effect of RPA in the assembly of the RAD51 presynaptic filament, HR enlists the help of BRCA1 and BRCA2.

1-C-2. BRCA1 is an adaptor protein that facilitates HR

BRCA1 is directly involved in HR-mediated repair of DSB (18, 19, 61). BRCA1 is recruited to DNA damage sites through its direct interaction with the abraxas-Receptor-Associated Protein 80 (RAP80) complex (mediated by BRCT repeats), in part because this complex recognizes ubiquitylated histones, an important posttranslational modification in DDR (18).

BRCA1 also aids 5'-end resection of DSB during HR (25) through its interaction with CtIP and the MRN complex (also mediated by BRCT repeats). This process is abrogated by three independent tumor-associated mutations in the BRCT domain of BRCA1 (24, 62), suggesting that BRCA1-mediated end resection is important for tumor suppression.

Lastly, BRCA1 also aids BRCA2 recombination mediator function through its interactions with PALB2 (mediated by BRCA1's coiled-coil domain). PALB2 binds directly to both BRCA1 and BRCA2 (15, 16, 38, 63). The BRCA1-PALB2 interaction is a prerequisite for the recruitment of BRCA2 and RAD51 to sites of DNA damage during HR (15, 16), and the PALB2-BRCA2 interaction is required for BRCA2 to load RAD51 onto RPA-bound ssDNA (64). PALB2 depletion abolished the interaction between BRCA1 and BRCA2 and generated a phenotype resembling that of BRCA2 depletion.

Together, these data support the importance of BRCA1 in end resection and in cooperating with BRCA2 in loading RAD51. In this pathway, BRCA1 functions upstream of BRCA2, with the function of BRCA2 dependent on BRCA1.

1-C-3. BRCA2 is a recombination mediator that loads RAD51 in HR

The primary function of BRCA2 is to facilitate HR. As a recombination mediator in this pathway, BRCA2 increases the efficiency of RPA displacement from and Rad51 assembly onto ssDNA at DSB (44, 65). These steps expand the ssDNA in preparation for homology search and facilitate strand exchange between invading and homologous template DNA.

To do this, BRCA2 binds directly to Rad51 via its BRC repeats (66-69) and also via its C-terminal domain (70, 71). BRCA2 then targets Rad51 to ssDNA at DSB through its interaction with PALB2 and also with the help of its DNA binding domain (45).

BRCA2 is essential for efficient RAD51 assembly during HR (42, 72, 73) as cells deficient in BRCA2 showed impaired recruitment of RAD51 to the nucleus (74), defective nuclear RAD51 foci formation (39, 73), and defective repair of DSB by HR (39).

The roles that the BRCA proteins play in repairing DSBs through HR underlie the sensitivity of *BRCA1* or *BRCA2*-defective tumors to DNA damaging agents, such as Poly (ADP-ribose) Polymerase (PARP) inhibitors.

1-D. BRCA1 and BRCA2 Function in Replication Fork Protection

During S phase, DNA replication forks can encounter a variety of stresses such as template damage, unusual DNA secondary structures, slow-moving or paused transcription complexes, covalent protein-DNA complexes, or a shortage of deoxyribonucleotides (75, 76). These stresses can stall replication fork progression, and if left unresolved, exposed ssDNA at stalled forks are potential targets for endonucleases to generate DSBs. To ensure the completion of replication and genome integrity, the cell relies on DNA repair pathways that remodel and restart stalled replication forks (**Fig. 1-4**).

At the stalled fork, remodelers (such as RAD51 and DNA translocases) (77, 78) generate a reversed arm of nascent DNA. This reversed arm resembles single-ended DNA at a DSB, or a DNA break, and is vulnerable to excessive resection by nucleases. RAD51, a ssDNA binding protein recruited to DSB, is central in protecting these types of breaks as its binding prevents nuclease access (79-81).

11
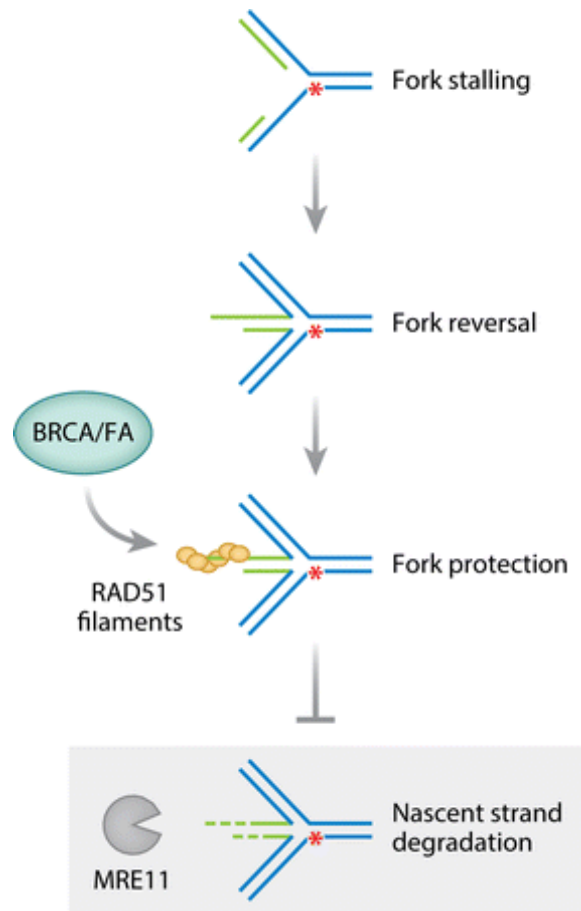
Figure 1-4. Protection of nascent DNA from degradation at stalled replication forks (82). A replication fork can stall when it encounters a lesion (red asterisk). Nascent strands (green) at a stalled fork can pair with each other such that the fork reverses. At the reversed fork, BRCA1 and BRCA2 protect nascent strands from degradation by stabilizing RAD51 filaments. Without these proteins (gray box), nascent strands can become substrates for degradation (by MRE11 and other nucleases) and lead to genome instability.

1-D-1. BRCA1 in replication fork protection

Recent work showed that BRCA1 plays a role in fork protection. BRCA1 is found at ongoing and stalled replication forks (83, 84), and in complex with BARD1, directly interacts with and recruits RAD51 (85, 86). In fork protection, the BRCA1-BARD1 complex acts independently of the canonical BRCA1–PALB2 interaction and the PALB2–BRCA2–RAD51 pathway (87).

Studies also identified a separation-of-function BRCA1 mutant (Serine 114A), which was HR proficient but fork protection deficient; these cells were resistant to PARP inhibitors (PARPi) and formed RAD51 foci after treatment with olaparib, but were sensitive to agents that induced replication fork stalling and collapse, such as hydroxyurea (HU) and aphidicolin.

1-D-2. BRCA2 in replication fork protection

BRCA2 plays a role in protecting stalled replication forks and does so also by assembling RAD51 filaments on the reversed arm of nascent DNA (86). Initial evidence for the role of BRCA2 in this process came from BRCA2-deficient cells that showed defects in maintaining the length of nascent DNA at stalled replication forks (based on single-molecule DNA fiber analysis) upon treatment with HU (80).

Crucial evidence supporting this role of BRCA2 was a separation-of-function mutant (Serine 3291A). This mutant affected the ability of BRCA2 to stabilize RAD51 filaments and thus was defective in protection of replication forks, but it did not affect the ability of BRCA2 to load RAD51 onto DNA, showed proficient HR and resistance to PARP inhibitors and crosslinking agents (80).

1-D-3. BRCA1 and BRCA2 in replication fork protection

BRCA1 and BRCA2 both protect stalled replication forks by stabilizing RAD51 filaments on nascent DNA and preventing its nucleolytic degradation (88) (80, 86, 89). These functions can prevent the formation of replication stress induced DSB.

1-E. BRCA1 and BRCA2 in tumorigenesis

The *BRCA* genes are frequently evaluated together in the context of disease because germline mutations in either gene are causative in the majority of inherited breast and ovarian cancers, or HBOC. This inherited disorder increases an individual's lifetime risk of developing breast (early-onset, or before the age of 50) and ovarian cancers, bilateral breast cancer, a second primary tumor in a different tissue, and cancer recurrence.

HBOC follows an autosomal dominant inheritance pattern, in which a mutation in only one copy of the gene is needed to increase risk of developing a disease. In this case, germline heterozygous mutations in either *BRCA1* or *BRCA2* cause haploinsufficiency in DNA repair and trigger subsequent genetic alterations that can lead to cancer. This is followed by loss of heterozygosity in the cancers that arise in mutation carriers. Additional alterations include loss of Tumor Protein 53 (TP53), ATM, or CHK2 functions. These alterations may allow cells to bypass checkpoint controls, evade apoptosis, and consequently initiate tumorigenesis.

5-10% of all breast cancers and 10-15% of all ovarian cancers are hereditary through HBOC, but individuals with HBOC have a lifetime risk of 50-80% for developing breast cancer and 30-50% for developing ovarian cancer (6). Although HBOC is most frequently associated with breast and ovarian cancer, it also increases risk for pancreatic, stomach, laryngeal, fallopian tube and prostate cancer. Additionally, individuals who

inherit two copies of mutant *BRCA2* develop Fanconi Anemia, a disease characterized by bone marrow failure, physical abnormalities, organ defects, and an increased risk of certain hematological cancers.

BRCA1 and BRCA2 protect the genome by 1) repairing DSB through HR and 2) preventing DNA lesions at stalled replication forks from becoming DSB. The loss of either protein can lead to DSB accumulation and cause cells to use error-prone DNA repair processes, such as non-homologous end joining (NHEJ), that increase mutations and chromosomal abnormalities. These alternatives can contribute to genome instability and subsequent tumorigenesis.

The role of BRCA proteins in mediating DSB repair, genome stability, and tumor suppression is supported by evidence from *Brca*-mutant mice. The mice used in these studies have a targeted null mutation in *Brca1* (*Brca1−/−*) restricted to the T-cell compartment and in a *p53−/−* background or they have a targeted, homozygous mutation in *Brca2* that results in truncations, from which partial transcripts are expressed. Both *Brca1*- and *Brca2*-mutant mice showed replication-associated DNA damage, such as chromatid aberrations including translocations, breaks and exchanges (90, 91). These *Brca1*- and *Brca2*-mutant mice also developed thymic lymphomas, a common tumor that arises due to defective DSB repair (90, 91). Furthermore, conditional expression of homozygous *Brca1* or *Brca2* mutants in mammary epithelium is sufficient to generate mammary cancers (92).

Loss of BRCA function leads to defects in HR and/ or replication fork protection, which can contribute to genome instability and tumorigenesis, reflected in both mouse models and in HBOC.

1-F. BRCA1 and BRCA2 Defects Sensitize Cancer Cells to PARP1 Inhibition

In 2005, studies reported that *BRCA1* and *BRCA2*-deficient cells are hypersensitive to PARP inhibitors (93, 94). This paved the way for using synthetic lethality (SL) as a therapeutic approach in cancer.

1-F-1. PARP1 is a signal transduction protein in DNA damage response

Poly(ADP-ribose) polymerase 1 (PARP1) catalyzes post-translational modifications important in DDR. PARP1 contains an N-terminal DNA binding, automodification, and C-terminal catalytic domain (95). The DNA binding domain has high affinity for DNA single-strand breaks, which mediates PARP1 to respond rapidly to damage. Upon DNA binding, the catalytic domain initiates poly(ADP-ribose) (PAR) synthesis, using nicotinamide adenine dinucleotide (NAD^+) as a donor of ADP-ribose (96, 97), on target proteins and on PARP1 itself. These negatively charged, branched PAR chains cause chromatin decondensation around damage sites and recruit additional repair proteins (98-101).

PARP1 is not essential to development; *Parp1* knockout mice develop normally (102), though they are sensitized to DNA damage (103). While PARylation is ubiquitous in higher eukaryotes, it is absent from yeast (104).

1-F-2. PARP inhibitors and mechanisms of action

In 2014, the PARPi olaparib became the first Food and Drug Administration (FDA) approved drug to exploit synthetic lethal targets. These inhibitors, olaparib and since then many others, trap PARP on DNA; these compounds interact with the catalytic site of PARP, preventing autoPARylation and subsequent PARP release from DNA (105-107) (as autoPARylation decreases PARP's affinity for DNA). This trapping mechanism is

supported by evidence showing that cells without PARP1 are resistant to PARPi (105, 108). Additionally, the potency of PARP trapping has become a predictor of cytotoxicity in BRCA-defective cells (105, 106, 109).

In the cell, trapping of PARP on DNA leads to the accumulation of single-strand DNA breaks that are predicted to collapse replication forks and trigger recombination repair (110). These DSB are most effectively repaired by HR. In the absence of HR, or in cancer cells that have lost BRCA1 or BRCA2 function, DSB repair is compromised and this can lead to chromosomal aberrations, genome instability, and cell death.

1-F-3. PARP inhibitors and clinical outcome

For olaparib, phase I trial in patients with ovarian, breast, or prostate cancers that carried germline *BRCA1* or *BRCA2* mutations found that 63% of patients showed clinical benefit and that side effects were less severe compared with chemotherapy (111). Phase II trials of olaparib also showed clinical benefit (112-114). One key finding from these trials though is that while olaparib increased progression free survival, it did not significantly improve overall survival (**Fig. 1-5**).

Some of these clinical challenges can be explained by mechanisms of resistance to PARPi. Studies have found that reversion mutations of *BRCA1* or *BRCA2* that restore HR led to resistance in vivo (115, 116). Other mechanisms of restoring HR, such as inactivation of p53-binding protein 1 (53BP1) (117) or Revertibility Protein 7 (REV7) (118), led to resistance as well in vitro. The development of PARP inhibitors for the treatment of BRCA-deficient tumors, despite ongoing challenges, establishes a paradigm for exploiting synthetic lethal targets in cancer therapy (119).

Because clinical challenges for using PARP inhibitors to treat *BRCA*-deficient cells remain, such as limited improvements in overall survival and drug resistance, the goal of my thesis project is to find other SL targets for *BRCA1* and *BRCA2*.

A.

No. at risk

Ovarian	193	131	85	56	29	16	10	4	2	0
Breast	62	32	15	9	5	3	2	2	1	0
Pancreas	23	13	8	3	1	1	1	0	0	0
Prostate	8	6	5	2	2	2	0	0	0	0

B.

No. at risk

Ovarian	193	172	154	139	117	78	53	27	14	0	0
Breast	62	50	43	33	25	17	10	6	4	2	0
Pancreas	23	17	14	12	9	6	4	3	1	0	0
Prostate	8	7	6	5	4	4	2	2	1	0	0
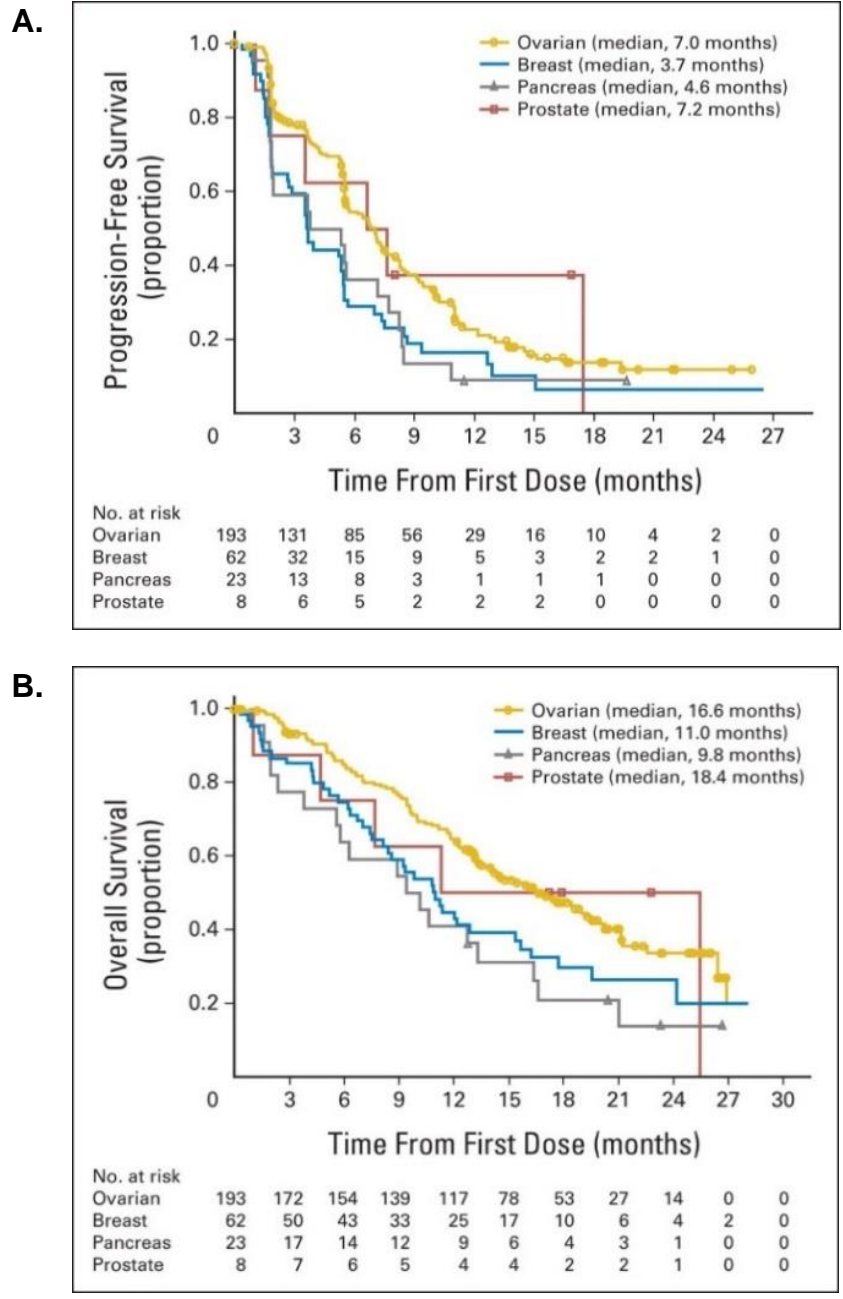
Figure 1-5. Olaparib increased progression free survival but did not significantly improve overall survival (114). **A.** Median progression free survival was 7, 3.7, 4.6, and 7.2 months in the ovarian, breast, pancreatic, and prostate cancer groups, respectively. The proportion of patients who were progression free at 6 months was 54.6%, 29.0%, 36.4%, and 62.5% in the ovarian, breast, pancreatic, and prostate cancer groups, respectively. **B.** Median overall survival was 16.6, 11, 9.8, and 18.4 months in the ovarian, breast, pancreatic, and prostate groups, respectively. The proportion of patients alive at 12 months was 64.4%, 44.7%, 40.9%, and 50.0% in the ovarian, breast, pancreatic, and prostate cancer groups, respectively.

19

1-G. SL Interactions of HR Genes with *RAD27* (Human *FEN1*) in *S. Cerevisiae*

1-G-1. Using SL networks in yeast to identify SL targets in human cells

Synthetic lethality (SL) or synthetic sickness is a genetic interaction in which the combination of two genetic events leads to cell death or impaired growth, whereas neither alone is sufficient (120). These genetic events can include loss of function mutations or chemical inhibition. Identifying SL gene pairs can enable selective targeting of cancer cells that are already defective in one of the genes, such as *BRCA1* or *BRCA2*, while sparing normal cells.

SL networks have been most systematically and comprehensively identified in *S. cerevisiae* using high-throughput genetic screens (121). In yeast, defects in DNA repair pathways exhibit extensive SL interactions, and since these pathways are highly conserved in eukaryotes, we hypothesized that their SL interactions are also conserved.

In a previous study, Putnam, Srivatsan, and Kolodner used SL relationships in *S. cerevisiae* and other functional genomics data sets to construct a network of genes that were predicted to act in the suppression of genome rearrangements. Validation studies identified 266 genome instability suppressing (GIS) genes and an additional 38 candidate GIS genes and then implicated their corresponding human homologs and pathway genes as candidate human GIS genes (122, 123). Analysis of The Cancer Genome Atlas (TCGA) data suggested that the human homologs of the GIS genes, which include recombination repair genes, are frequently defective in cancers that exhibit genome instability. These studies asked if *S. cerevisiae* SL networks can be used to predict possible therapeutic targets for cancers that have defects in GIS genes and identified *RAD27/ FEN1* as a candidate.

1-G-2. Yeast *RAD27* (human *FEN1*) is SL with HR genes

Yeast Radiation Sensitive 27 (*RAD27*) is a 5' flap endonuclease in Okazaki fragment processing and long-patch base-excision repair. Among its numerous SL interactions, *RAD27* is SL with DSB recombination repair genes *RAD51*, *RAD52* (124), and Radiation Sensitive 55-Radiation Sensitive 57 (*RAD55*-*RAD57)* in yeast (125, 126), which suggests that the majority of replication lesions that accumulate in *rad27Δ* strains are processed by HR (**Fig. 1-6**).

While *RAD27* is conserved in humans as *FEN1*, *RAD52* and *RAD55-RAD57* are functional analogs of the human HR and replication fork protection gene *BRCA2*. The goal of this thesis is to validate the predicted SL interactions between *FEN1* and HR genes and to understand the cell death mechanisms associated with these SL interactions.
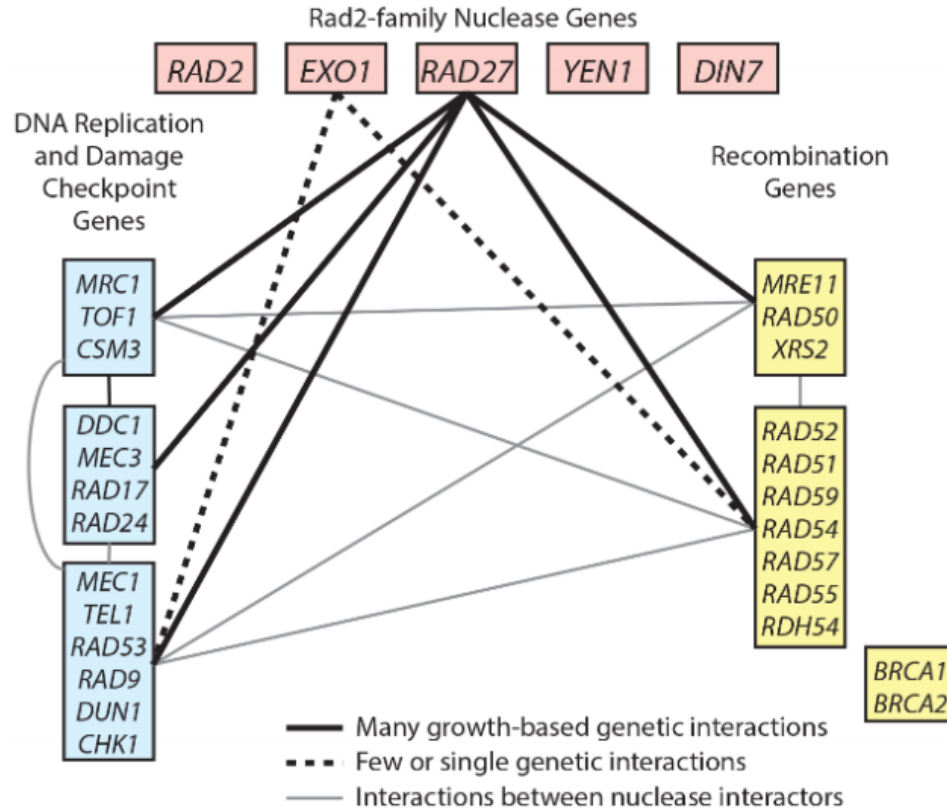
Figure 1-6. A subset of *RAD27* synthetic lethal interactions in *S. cerevisiae*. *RAD27*, part of the Radiation Sensitive 2 (Rad2) nuclease family, shows many growth-based genetic interactions with genes in DNA replication, cell cycle checkpoint, and recombination repair. Among its many SL interactions, *RAD27* is SL with *RAD52*, and the *RAD55-RAD57* complex in recombination. *RAD27* is homologous with human *FEN1* (not shown). While *RAD52* and the *RAD55-RAD57* complex don't have homologs in humans, they are functionally analogous with *BRCA2* in recombination.

1-G-3. Flap endonuclease 1 (FEN1) is an endonuclease in DNA replication and repair

FEN1 is a structure-specific endonuclease in DNA synthesis and repair. It is part of a family of conserved, structure-specific endo- and exonucleases including Exonuclease 1 (EXO1), Flap endonuclease GEN homolog 1 (GEN1), and Xeroderma Pigmentosum (XPG). FEN1 is a constitutively expressed nuclear protein active in the processing of the 5' ends of Okazaki fragments during lagging strand DNA synthesis (127-132) (**Fig. 1-7**) and in the processing of branched structures during long-patch base-excision repair (133-136).

To do this, FEN1 specifically recognizes dsDNA with 5' unannealed ssDNA flaps, binds both the flap and duplex regions of the substrate (137), and cleaves at the base of the flap (135, 138). During lagging strand synthesis, this removes the RNA primer (FEN1 can cleave both DNA and RNA (135, 138, 139)) and generates a nick in the phosphodiester backbone for DNA ligase I to form an intact DNA strand (140).

In addition to FEN1's role in Okazaki fragment maturation, studies have proposed that FEN1 may play a role in restarting stalled replication forks via the break-induced recombination pathway, in which a DSB is created on the stalled fork to convert the stalled fork into a recombination substrate (141). In this process, FEN1 cleaves the chicken foot structure associated with a regressed replication fork, which would generate a DSB (142).

DNA replication

Key: 〰〰 RNA primer
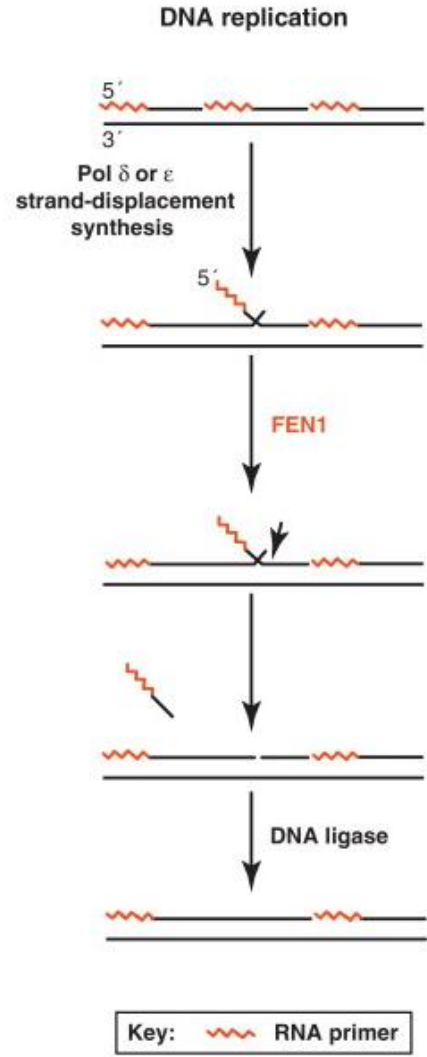
Figure 1-7. FEN1 functions in lagging strand DNA synthesis (143). During polymerase δ or polymerase ε-mediated strand-displacement synthesis on the lagging strand, 5' flaps are created on the Okazaki fragments when the elongating DNA displaces the 5' end of the downstream strand. This flap, which contains the RNA primer, must be removed to allow ligation of the newly synthesized DNA. FEN1 removes this 5' flap and leaves behind nicked DNA that is a substrate for ligation.

24

In the absence of FEN1, ssDNA flaps on Okazaki fragments or at stalled replication forks accumulate, which when combined with cleavage of the parental strand by nucleases, can lead to DSB or equilibrate into structures that lead to duplications and repeat sequence expansions (144). The activity of FEN1 prevents the direct accumulation of ssDNA flaps and indirect accumulation of mutations or DSB to maintain genome integrity.

FEN1 is conserved through evolution. Its biological importance was primarily revealed by studies of its *S. cerevisiae* homolog *RAD27*. The *rad27* null genotype shows a spontaneous mutator phenotype with increased rates of microsatellite instability (133, 145-147). In addition, *rad27* mutants undergo S phase arrest, chromosome loss, and slowed growth (145-151).

The mammalian homolog of yeast *RAD27* is mouse *Fen1* or human *FEN1*. Fen1 is essential in development. *Fen1* homozygous knockout mice (*Fen1-/-*) are embryonically lethal (152, 153); *Fen1* null blastocysts that form can't enter S phase to carry out DNA synthesis and are arrested in the endocycle (152). These *Fen1-/-* cells also undergo extensive IR-induced apoptosis (152), suggesting that they cannot maintain normal DNA replication and repair. Fen1 is critical for normal cell cycle progression in the mouse embryo.

Fen1 heterozygote animals appear normal, but *Fen1* haploinsufficiency contributes to genome instability and tumor progression. Studies found that *Fen1* heterozygous knockout mice that are also heterozygous for adenomatous polyposis coli (*APC*) develop adenocarcinomas that contain microsatellite instability (153). These

results suggest that, in mammals, *Fen1* is essential for embryonic development and later acts as a tumor suppressor by maintaining genome integrity.

Although *Fen1* haploinsufficiency can promote tumor progression in mice, other studies found that FEN1 overexpression may support malignancy as well. FEN1 is overexpressed in small cell lung cancer cell lines compared to control (154) and also in other cancer types (155-157). The level of FEN1 expression has been correlated with tumor grade and aggressiveness (155). This suggests that FEN1 may provide a proliferative advantage by supporting replication or repairing damaged DNA. Since FEN1 may play a dual role in tumorigenesis, it's important to understand the genetic context when targeting FEN1 in cancer therapy.

While FEN1 is essential in development, gene essentiality projects have shown that it is not essential in cell lines such as DLD1 colorectal cancer cells (158). Furthermore, FEN1 knockouts in human cell lines have also been published (159).

1-H. Goals of Thesis Research: To identify and characterize SL targets as a therapeutic approach in cancer

Previously observed SL interactions between *RAD27* and DSB repair genes *RAD51*, *RAD52*, *RAD55-RAD57* in yeast (125, 126) suggests that the majority of replication lesions that accumulate in *rad27Δ* strains are processed by DSB repair. In mammalian cells, the DNA repair protein FEN1 (RAD27 homolog) and the DSB repair and replication fork protection proteins BRCA1 and BRCA2 (RAD52 and RAD55-RAD57 are BRCA2 functional equivalents) contribute to the maintenance of genome integrity.

FEN1 catalyzes the removal of ssDNA flaps on replication intermediates, preventing unrepaired flaps from being converted into DSB by nucleases. FEN1 also

plays a role in restarting stalled replication forks via the break-induced recombination pathway, in which a DSB is created on the stalled fork to initiate recombination (141, 142, 160).

In a FEN1 deficient system, we hypothesize that BRCA1 and BRCA2 are required for DSB repair and/ or resolution of stalled replication forks. We expect that the loss of FEN1 and BRCA proteins would lead to DSB accumulation, replication fork stalling, cell cycle arrest, chromosomal aberrations, and cell death.

The goals of this thesis are 1) to determine whether FEN1 is a SL target for killing *BRCA1/ BRCA2*-deficient cancer cells and 2) to understand the mechanisms of cell death in human cancer cells with combined defects in FEN1 and BRCA1/ BRCA2.

CHAPTER 2

HYPERSENSITIVITY OF BRCA1 OR BRCA2 DEFICIENT CELLS TO FEN1 INHIBITION OR DEPLETION

Chapter 2 Introduction

To determine whether FEN1 is a SL target for killing *BRCA1* or *BRCA2*-deficient cells, we tested the effects of FEN1 inhibition using a small molecule inhibitor C8 and FEN1 knockdown by siRNAs in *BRCA*-deficient and proficient cancer cell lines and matched cell line pairs with *BRCA*-deficient derivatives.

2-A. Identification of *RAD27/ FEN1* as a genome instability suppressor (GIS) gene synthetic lethal target.

Previous work in the Kolodner Lab identified 266 GIS genes and an additional 38 candidate GIS genes in *S. cerevisiae,* and analysis of TCGA data suggested that the human homologs of GIS genes are frequently defective in cancers that exhibit genome instability. Evaluation of known SL interactions in yeast demonstrated that *RAD27* had the greatest number of SL relationships with identified GIS genes, closely followed by *SGS1* (**Fig. 2-1-A**). Because the human homolog of *SGS1*, *BLM*, is a human disease gene, we focused subsequent studies on *RAD27* and its human homolog *FEN1*, which encodes Flap Endonuclease 1. FEN1 acts during Okazaki fragment maturation and long-patch base-excision repair. The majority of *RAD27* SL genes encoded proteins that function in chromosome metabolism, including homologous recombination (HR)/ double-strand break repair (DSB repair), DNA damage checkpoints, chromatin assembly, chromatin remodeling, chromosome cohesion and the nuclear pore (**Fig. 2-1-B**); identification of nuclear pore genes could reflect the role of the nuclear pore in DSB repair.

2-B. FEN1 inhibitors selectively kill *BRCA1/BRCA2* defective cell lines.

To determine if *RAD27* SL relationships with HR defects were recapitulated in human cells, we synthesized 4 previously published FEN1 inhibitors: C2, C8, C16, and

C20 (**Fig. 2-2-A**) (161) and tested their ability to kill PEO1 and PEO4 cells as assessed by clonogenic survival assays after a 3-day exposure to the inhibitor.

PEO1 is a *BRCA2*-defective cell line derived from an ovarian tumor; PEO1 has a nonsense mutation in *BRCA2* that led to loss of BRCA2 expression and function, causing sensitivity to cisplatin and PARP inhibition. PEO4 is a cell line derived from a relapse tumor from the same patient as PEO1 in which the initial *BRCA2* mutation was reverted (162). This secondary mutation restored BRCA2 expression and function; PEO4 is cisplatin and PARP inhibitor resistant.

The *BRCA2*-mutant PEO1 cells were more sensitive to killing by the FEN1 inhibitor C8 than the *BRCA2*-revertant PEO4 cells (**Fig. 2-2-B**); PEO1 showed an EC50 value of 3 µM, in contrast to PEO4 with a 5-fold higher EC50 of 15 µM. In addition, PEO1 cells were more sensitive to killing by the other three FEN1 inhibitors than PEO4 cells, with the relative sensitivity C8>C16>>C2>C20 (**Fig. 2-2-C**). C8 was used in all subsequent experiments because, in comparison with the next most potent inhibitor C16, C8 had a greater half-life in serum after intraperitoneal administration to a mouse (1.6 hr half-life, C_{max} = 16 μM vs no measurable exposure, data not shown).

FEN1 is a member of a family of nucleases, including XPG, EXO1, and GEN1, with conserved active site residues. Since C8 binds to the active site, we determined the IC50 of C8 for FEN1 and its family members in vitro. Of these enzymes, FEN1 is the most sensitive target with an IC_{50} of 1 nM (**Table 2-1**, in collaboration with the Small Molecule Discovery Lab, Ludwig San Diego, CA).

The effect of C8 on cell proliferation in PEO1 and PEO4 was also measured using the trypan blue exclusion assay. Two concentrations of C8 that showed differential

clonogenic survival responses between PEO1 and PEO4 were chosen: 12.5 and 25 μM. Cells were treated with C8 for 3 days and then grown in drug-free media for 6 more days. Viable cell counts showed that at 12.5 μM of C8, both cell lines proliferated after drug removal. But at 25 μM C8, viable cell counts decreased over time in PEO1 cells even after drug removal, in contrast to PEO4 cells.

Two additional pairs of matched cell lines were examined for their sensitivity to C8: 1) Tert-transformed, p53-null retinal pigmental epithelial (RPE) cells and a derivative in which *BRCA1* was inactivated with CRISPR; and 2) DLD1 colorectal tumor cells and a derivative in which the wild type copy of *BRCA2* was inactivated by gene disruption. In each case the *BRCA*-deficient derivative cell lines were more sensitive to killing by C8 than the matched *BRCA*-WT or proficient parental cell lines by clonogenic survival assays (**Fig. 2-4**).

To determine whether differential survival to C8 could be repeated in other *BRCA*-deficient and *BRCA*-proficient cell lines, a larger panel of human breast (**Fig. 2-5-A**), ovarian (**Fig. 2-5-B**), colorectal (**Fig. 2-5-C**) and lung cancer cell lines (**Fig. 2-5-D**) was tested. The ability of C8 to kill was assessed by clonogenic survival assay. Cells were treated with 12.5 μM C8 for 3 days; this C8 concentration was between the EC_{50} values for PEO1 and PEO4 cells. For cell lines derived from each tumor type, the response to C8 treatment ranged from highly sensitive to completely resistant. When the data for all of the cancer cell lines are combined, those with reported *BRCA* mutations tend to be more sensitive to C8 treatment than those without reported *BRCA* mutations (**Fig. 2-5-E**; p=0.0015, Kolmogorov-Smirnov test).

Many cell lines were sensitive to killing by C8 and had mutations in *BRCA1* (HCC1954, MDA-MB-436, UWB1.289, JHOS-2) or *BRCA2* (HCC1395, HCC1599, PEO1, Kuramochi, Ovmana, IGR-OV1, OVCAR-4), including the olaparib-resistant *BRCA1*-mutant cell line HCC1937.

Despite this, there were other tumor cell lines whose reported *BRCA* mutation status was not predictive of their sensitivity to killing by C8. Cell lines with *BRCA* mutations without C8 sensitivity may contain mutations that do not substantially affect the HR proficiency of these cell lines, whereas cell lines without *BRCA* mutations with C8 sensitivity may contain other genetic or epigenetic defects affecting HR or other pathways that are required in the absence of normal FEN1 activity. Among these latter C8-sensitive cell lines is the breast cancer cell line MDA-MB-468, which is not sensitive to killing by olaparib.
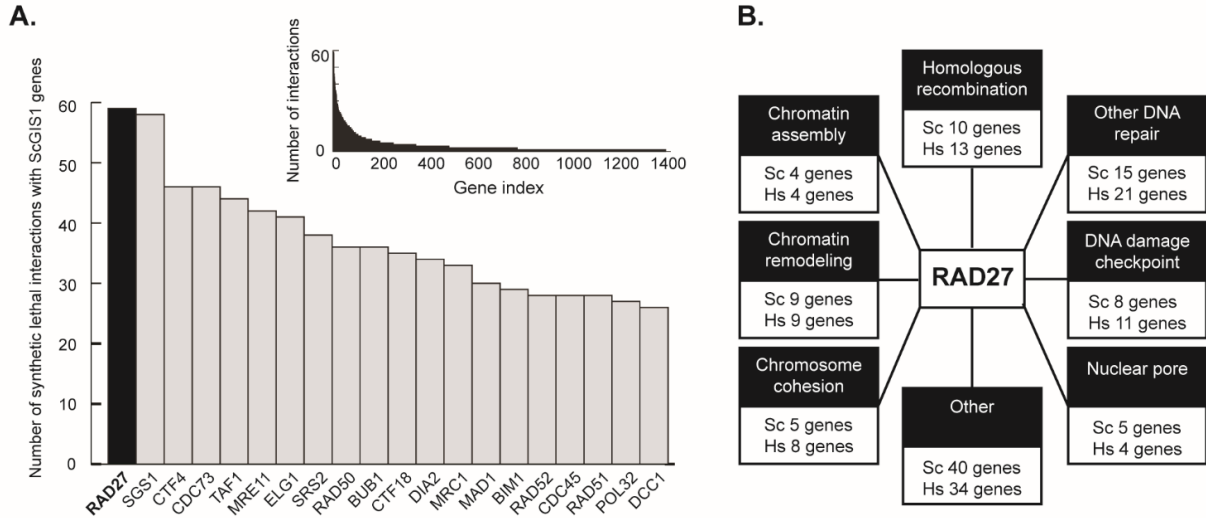
Figure 2-1. *RAD27* **shares the greatest number of known SL interactions with** *S. cerevisiae* **GIS genes. A.** The number of reported SL interactions of genes with the 266 *S. cerevisiae* non-essential GIS and essential GIS (eGIS1) genes; inset shows the entire distribution for all interactors**. B.** *RAD27* SL interactors (Sc genes) fall into common pathways, which are often conserved in humans (Hs genes).

A.

C2   C8   C16   C20
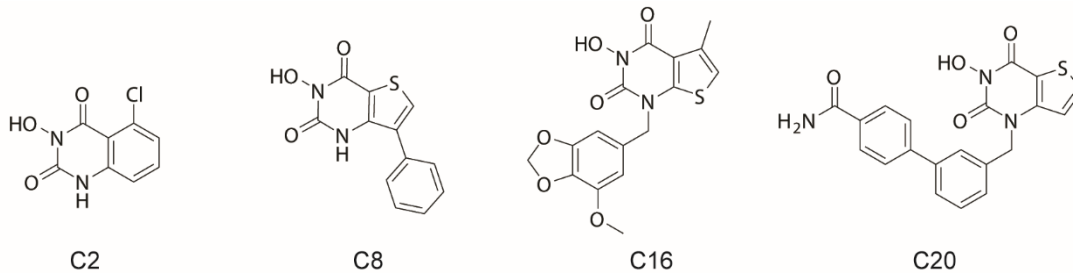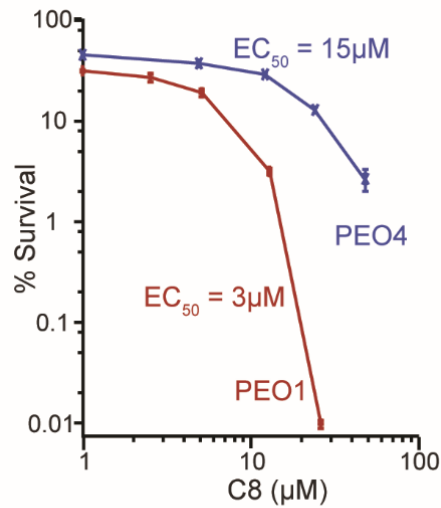
B.   **C.**
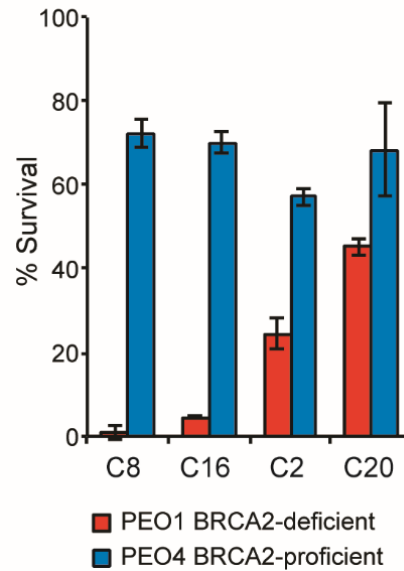
Figure 2-2. *BRCA*-**deficient cancer cell lines are hypersensitive to FEN1 inhibition. A.** Structures of the synthesized FEN1 inhibitors. **B.** Clonogenic survival of *BRCA2*-deficient PEO1 and *BRCA2*-revertant PEO4 cells demonstrates that PEO1 cells are more sensitive to a 3-day exposure to the C8 FEN1 inhibitor. **C.** Clonogenic survival demonstrates that PEO1 cells are more sensitive than PEO4 cells to all of the FEN1 inhibitors, with C8 and C16 causing the greatest reduction in percent survival. Cells were treated for 3 days with compounds 2 and 20 at 25 μM, 8 and 16 at 12.5 μM.

Table 2-1. C8 inhibits FEN1 and family member nucleases. (In collaboration with the Small Molecule Development Lab, Ludwig San Diego, CA)

FEN nuclease family	C8 IC$_{50}$ (nM)	Function
FEN1	1	Replication, base excision repair
XPG	5	Nucleotide excision repair
EXO1	45	Mismatch repair, double-strand break repair
GEN1	750	Homologous recombination
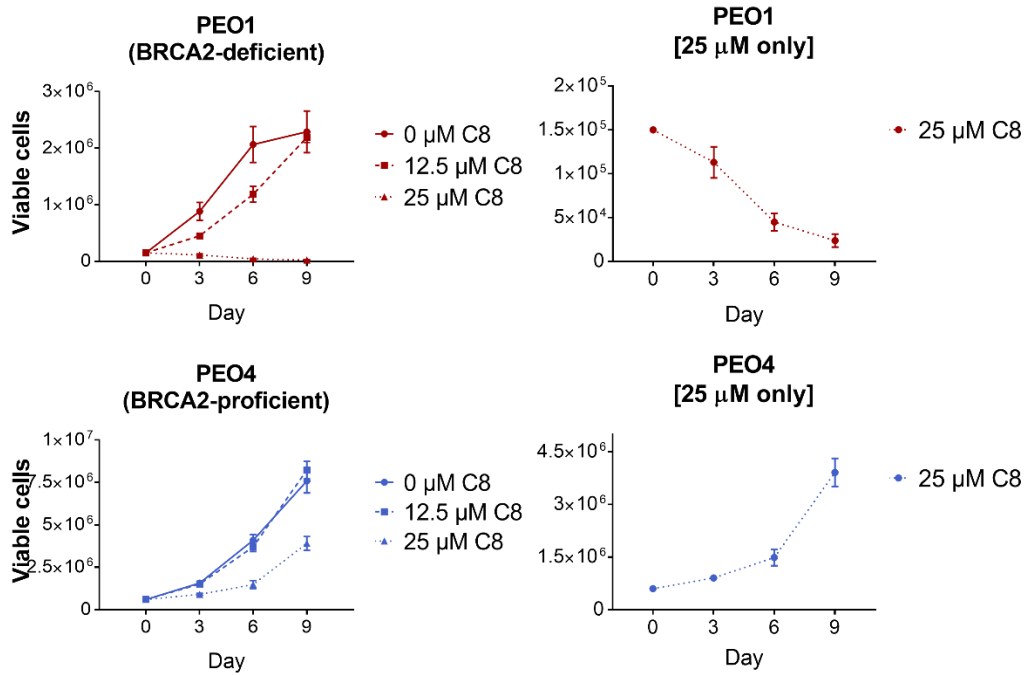
Figure 2-3. *BRCA2*-deficient cells are hypersensitive to C8 even after drug removal. PEO1 and PEO4 cells were treated with C8 for 3 days and then grown in drug-free media for 6 more days. Two concentrations of C8 that showed differential clonogenic survival responses between PEO1 and PEO4 were chosen: 12.5 and 25 µM. The number of viable cells was measured using the trypan blue exclusion assay (n=9). The 25 µM condition is highlighted on the right, where the scale is magnified to show the differential responses more clearly.
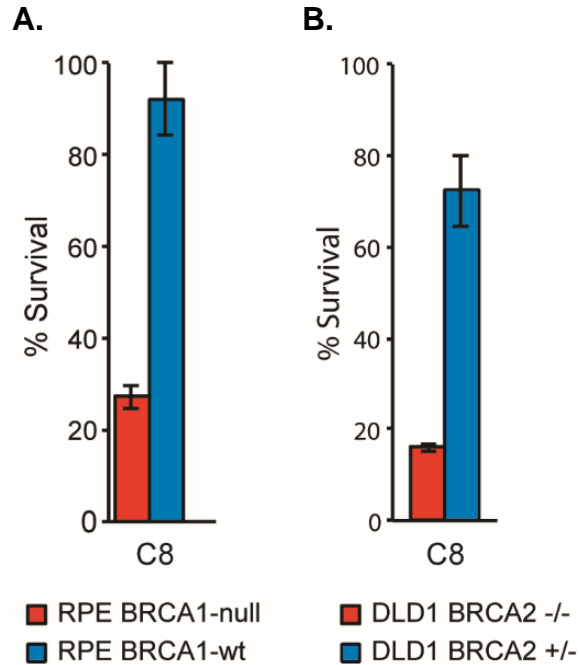
Figure 2-4. *BRCA1* or *BRCA2*-deficient cells are hypersensitive to C8 compared to parental *BRCA*-WT or proficient cells. A. Tert-transformed and p53-null RPE cells with a *BRCA1* disruption are more sensitive to C8 than the parental *BRCA1*-wildtype cells. Percent clonogenic survival of RPE1 hTERT p53-/- BRCA1-/- and BRCA1+/+ cells after exposure to 11.1 µM C8 for 3 days compared to DMSO. Cell survival was measured by crystal violet staining 4 days post drug removal for BRCA1+/+ cells and 5 days post drug removal for BRCA1-/- cells (n=3). **B.** DLD1 cells with a *BRCA2* disruption are more sensitive to the C8 FEN1 inhibitor than the parental BRCA2 proficient cells. Percent clonogenic survival of DLD-1 BRCA2-/- and BRCA2+/- cells after exposure to 7 µM C8 for 3 days compared to DMSO. Cell survival was measured by crystal violet staining 3 days post drug removal for BRCA2+/- cells and 5 days post drug removal for BRCA2-/- cells (n=3).
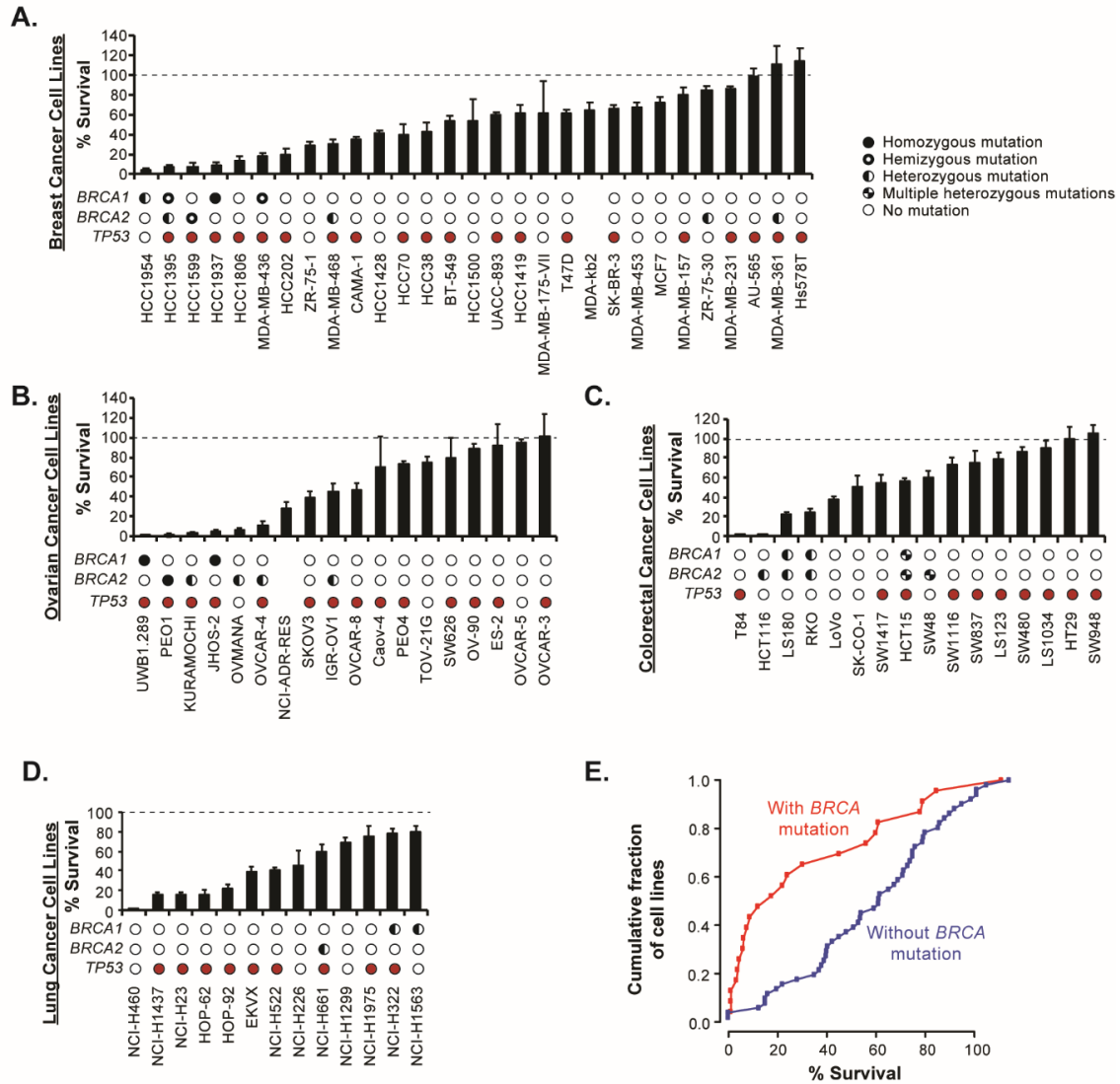
Figure 2-5. Sensitivity of breast, ovarian, colorectal, and lung cancer cell lines to the C8 FEN1 inhibitor. Clonogenic survival of breast cancer cell lines (**A**), ovarian cancer cell lines (**B**), colorectal cancer cell lines (**C**), and lung cancer cell lines (**D**) treated with 12.5 μM C8 for 3 days are displayed as bars (n=12). The *BRCA1* and *BRCA2* mutation status information from the Broad Institute Cancer Cell Line Encyclopedia (CCLE (163)); zygosity was inferred from mutant vs. wild-type read counts and copy number information. Homozygous mutations are solid black circles, hemizygous mutations are black circles with a central white spot, heterozygous mutations are half-filled circles, multiple heterozygous mutations are displayed as split filled circles, and no mutations are displayed as empty circles. Cell lines with *TP53* mutations are shown with filled red circles and those without *TP53* mutations are shown with empty circles. Cell lines with no data in the CCLE are shown without circles. **E.** Cumulative percent survival of cell lines with and without *BRCA* mutations after 12.5 μM C8 for 3 days. The breast, ovarian, colorectal, and lung cancer cell lines were separated into two groups. One group of cell lines with *BRCA* mutations (including homozygous, hemizygous, heterozygous, and multiple heterozygous) and the other without. The cumulative fraction of cell lines was plotted in increasing order of % survival.

38

2-C. *BRCA*-deficient cell lines are sensitive to FEN1 siRNA knockdown

In addition to the FEN1 inhibitor C8, we used an orthogonal approach to target FEN1 expression by siRNA. siRNA knockdown of *FEN1* was examined in 2 *BRCA1*-deficient (UWB1.289, HCC1937), 1 *BRCA2*-deficient (PEO1) and 3 *BRCA*-proficient (PEO4, OV-90, OVCAR-3) cancer cell lines.

Three days after transfection of *FEN1*-targeting siRNAs (siFEN1) or non-targeting control siRNAs (siNT), siFEN1 treatment caused FEN1 protein levels to be reduced by 40 to 80% in both *BRCA*-deficient and *BRCA*-proficient cell lines (**Fig. 2-6**) and the number of viable cells were reduced specifically in the *BRCA*-deficient cell lines (**Fig. 2-7-A**).

To test whether the effects of FEN1 knockdown persist over time or whether siFEN1-treated cells recover, the ability of FEN1 knockdown cells to form colonies was measured. Six cultures of each cell line were treated for 1 day with siFEN1 or siNT. The cells were then cultured in fresh media for 2 days and then the media was changed every 3 days for a total of 15 to 21 days after which colonies were counted (**Fig. 2-7-B,C**) and colony sizes were determined (**Fig. 2-8**).

In comparison to the siNT control, siFEN1 treatment resulted in large and significant decreases in colony numbers for the *BRCA*-deficient cell lines, whereas only one of the *BRCA*-proficient cell lines (OVCAR-3) had a small decrease in colony number (**Fig. 2-7-C**). Similarly, siFEN1 treatment resulted in decreases in colony size in *BRCA*-defective cell lines but little if any decrease in colony size in *BRCA*-proficient cell lines (**Fig. 2-8**). Remarkably, the short-term effect of siFEN1 treatment on cell viability was not as large as seen in the clonogenic survival assays, suggesting that many of the siFEN1

treated *BRCA*-deficient cells that were viable after 3 days either died over time or could not undergo additional cell divisions.

Experiments with the FEN1 inhibitor C8 and with FEN1 siRNAs showed that FEN1 is a SL target for killing *BRCA1* or *BRCA2*-deficient cells. *BRCA*-deficient cells are hypersensitive to C8, and FEN1 siRNAs reduced viability, clonogenic survival, and colony size in *BRCA*-deficient cells.

Chapter 2 is currently being prepared for submission for publication. Guo, Elaine; Ishii, Yuki; Mueller, James; Srivatsan, Anjana; Putnam, Christopher; Wang, Jean Y. J.; Kolodner, Richard. FEN1 is a potential therapeutic target for human cancers with defects in homologous recombination. The dissertation author is the co-author of this paper.
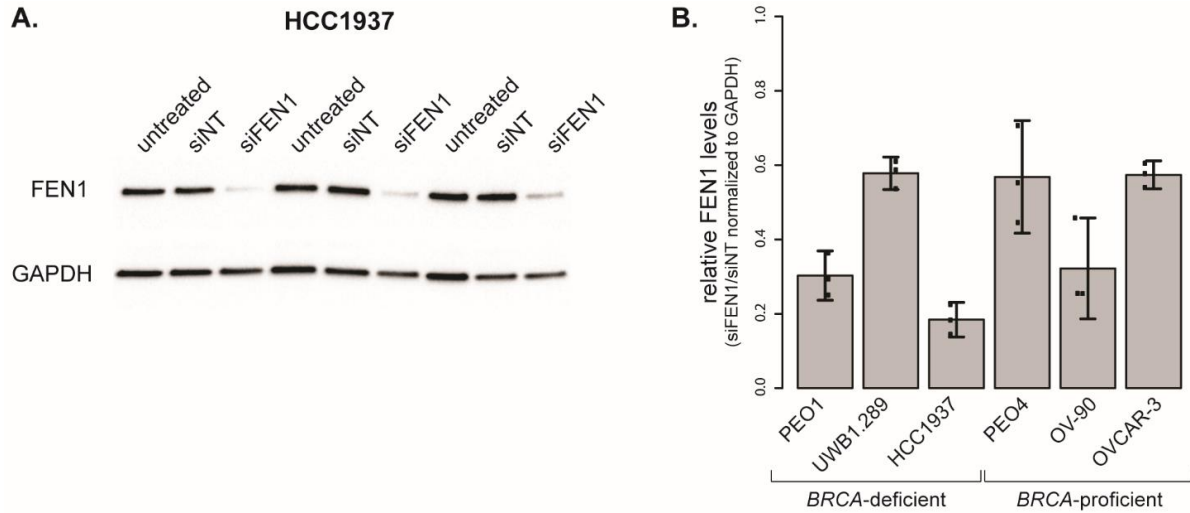
Figure 2-6. siFEN1 reduces the expression of FEN1 in both *BRCA*-deficient and *BRCA*-proficient cell lines. A. FEN1 and GAPDH levels in HCC1937 after no treatment, siNT treatment, or siFEN1 treatment. Three technical replicates are shown. **B.** The average FEN1 expression in the siFEN1 treated cells relative to siNT treated cells after normalization to GAPDH levels are displayed as bars. Individual measurements are shown as points (n=3). Error bars correspond to 2 times the standard error of the mean.
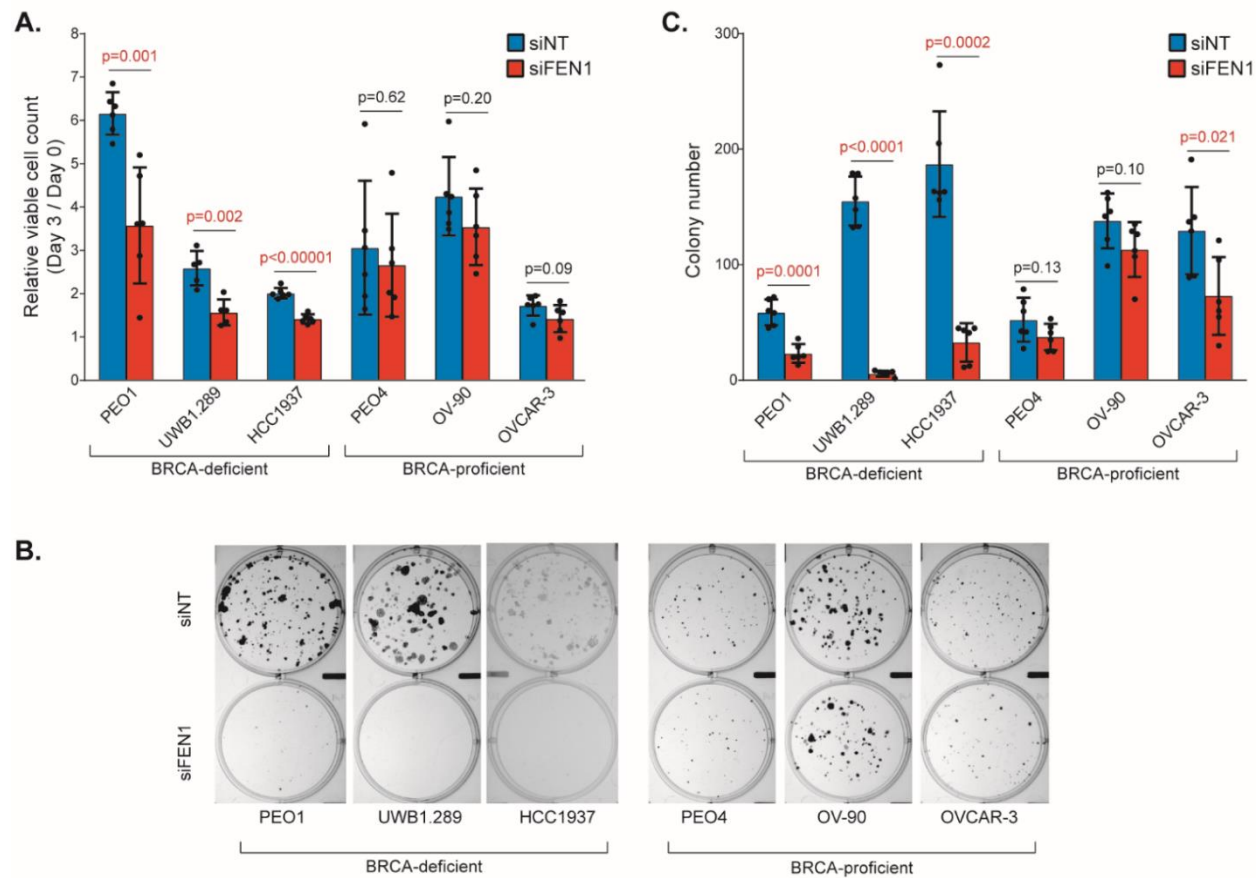
Figure 2-7. Treatment of *BRCA*-deficient cell lines with siFEN1 decreased viable cell numbers and reduced clonogenic survival. A. The number of viable cells is reduced 3 days post siFEN1 treatment relative to 3 days post control siNT treatment for *BRCA*-deficient cell lines but not BRCA-proficient cell lines (n=6, except for UWB1.289 where n=5). P-values were calculated using the 2-tailed t-test. **B.** Example images of the clonogenic survival assay of BRCA-deficient and BRCA-proficient cell lines treated with siNT or siFEN1. **C.** The number of colonies in the clonogenic survival assay 15-21 days post transfection were reduced with siFEN1 treatment relative to siNT treatment in *BRCA*-deficient cell lines and OVCAR-3, but not PEO4 or OV-90 (n=6). P-values were calculated using the 2-tailed t-test.
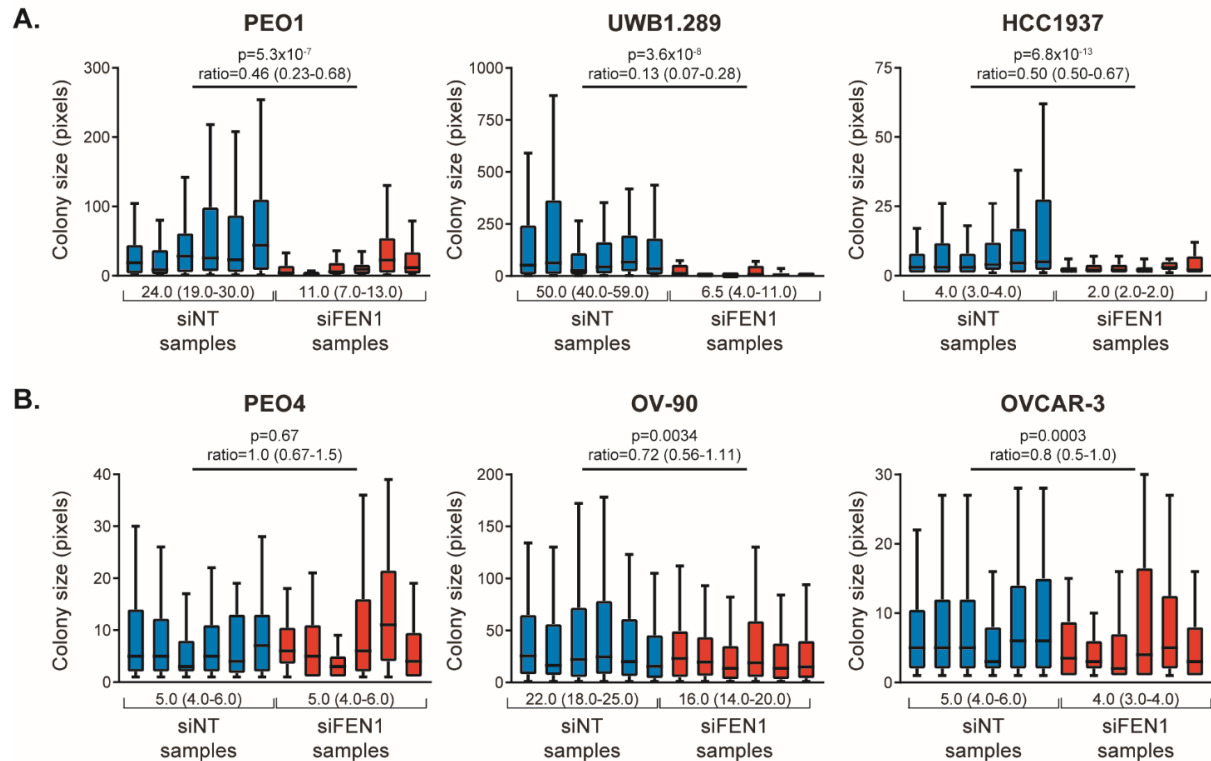
Figure 2-8. FEN1 inhibition reduces the size of colonies in clonogenic survival assays in *BRCA*-deficient cell lines. The sizes of the colonies arising during a clonogenic survival assay after treatment with siNT (blue) or siFEN1 (red) were determined for *BRCA*-deficient (**A.**) and *BRCA*-proficient (**B.**) cell lines (n=6). Reduced colony sizes were observed for the *BRCA*-deficient and two *BRCA*-proficient cell lines (OV-90 and OVCAR-3); however, the reduction in colony size was much greater for the *BRCA*-deficient cell lines. The median colony size and 95% confidence interval for the median (below x-axis) were determined for all of the observed colonies; the 95% confidence interval was determined by a bootstrap approach from which random samples (n=20,000) were taken with replacement and a new median was taken for each random sample. The 95% confidence interval was taken at the 2.5% and 97.5% percentiles of the medians from the randomized samples. The ratio of the colony sizes and range of the ratio were calculated from the medians and the 95% confidence intervals of the medians. The p-values for the difference between colony sizes of the siNT and siFEN1 treated samples were calculated using a 2-sided Kolmogorov-Smirnov test.

CHAPTER 3

MECHANISMS OF FEN1 INHIBITION INDUCED

CELL DEATH

Chapter 3 Introduction

FEN1 inhibition increases flaps on lagging strands during DNA replication, which in combination with nucleolytic cleavage on the template strand, can lead to potentially lethal DSBs. We first tested the effects of C8 on DNA damage levels and cell cycle progression in both *BRCA*-proficient and *BRCA*-deficient cells and asked whether these changes were dependent on *BRCA* mutation status or function. To understand the mechanism of FEN1 inhibition induced cell death, we measured the effects of C8 on caspase activity, chromosomal phenotype, and checkpoint pathway activation in *BRCA*-deficient and *BRCA*-proficient cells, also asking if the results were dependent on *BRCA* mutation status or function.

3-A. C8 differentially affects cell cycle and cell death in *BRCA*-deficient and *BRCA*-proficient cells.

To determine how FEN1 inhibition might affect the cell cycle, a panel of 6 cell lines, 3 *BRCA*-deficient and 3 *BRCA*-proficient, was treated with 25 μM C8 for 3 days. At the end of drug treatment, these cells were pulsed with BrdU (5-bromo-2'-deoxyuridine) for 45 minutes to identify cells undergoing active DNA synthesis. BrdU incorporation by DNA synthesis was measured by FACS.

Treatment of the *BRCA*-defective PEO1, UWB1.289, and HCC1937 cells with C8 resulted in cells with a decreased ability to synthesize DNA and an increased sub-G1 DNA content, which indicates dying cells, relative to untreated controls (**Fig. 3-1, Table 3-1**; sub-G1 content is qualitative). Similar effects were observed with other C8-sensitive cell lines both with and without *BRCA* defects (HCT116, Ovmana, Kuramochi, NCI-H460, OVCAR-4 and JHOS-2; **Fig. 3-2, Table 3-2**).

In contrast, C8 treatment of the *BRCA*-proficient and C8-resistant PEO4, MDA-MB-231, OVCAR-3, and MCF7 cells resulted in little change in the ability of the cells to synthesize DNA and in the number of sub-G1 cells compared to untreated controls (**Fig. 3-1; Fig. 3-2**). FEN1 inhibitor-sensitive cell lines showed strong defects on cell cycle progression after inhibitor treatment.

To determine if the loss of DNA replication was only an acute response to FEN1 inhibition, we tested the ability of *BRCA2*-mutant PEO1 cells and *BRCA2*-revertant PEO4 cells to recover from treatment by C8. Both PEO1 and PEO4 cells were treated with 25 µM C8 for 3 days followed by incubation in either C8-free or C8-containing medium for an additional 3 days; the ability of the cells to incorporate BrdU was analyzed by FACS at each step (**Fig. 3-3, Table 3-3**). C8-treated PEO4 cells had a modest increase in sub-G1 cells and decrease in S-phase cells relative to control that was more pronounced after 6 days of C8 treatment than after 3 days of C8 treatment (**Fig. 3-3**). PEO4 cells, however, had a robust restoration of S-phase cells after 3 days of C8 treatment and 3 days in C8-free medium (**Fig. 3-3**).

In contrast, at the end of both 3 and 6 days of C8 treatment, PEO1 cells had severe defects in their ability to incorporate BrdU. Moreover, after drug removal for 3 days, the % of BrdU-incorporating PEO1 cells continued to decrease while the % of subG1 cells continued to increase, compared to PEO1 cells after only 3 days in C8 containing medium.

PEO1 cells were unable to recover their ability to incorporate BrdU even after drug removal, while PEO4 cells continued to incorporate BrdU at each time point. These results suggest that FEN1 inhibitor sensitive cell lines cannot recover the ability to

46

replicate their DNA and that exit from the cell cycle is permanent after inhibitor treatment

(**Fig. 3-3**).
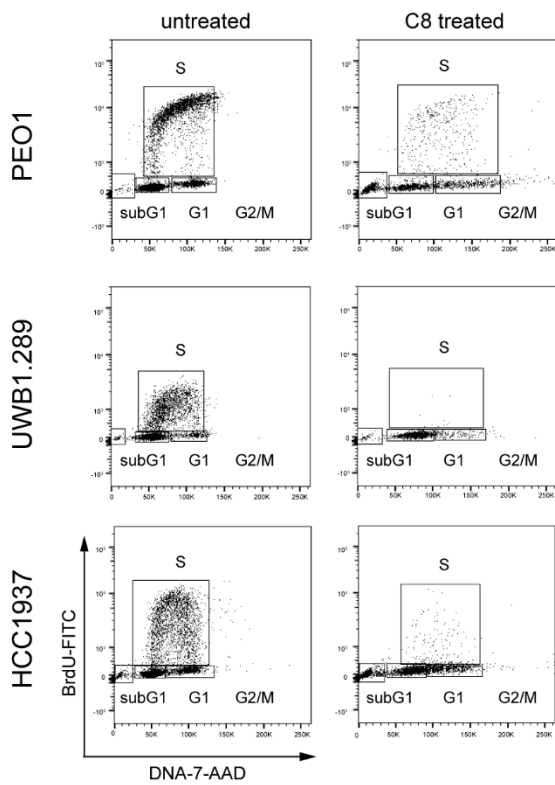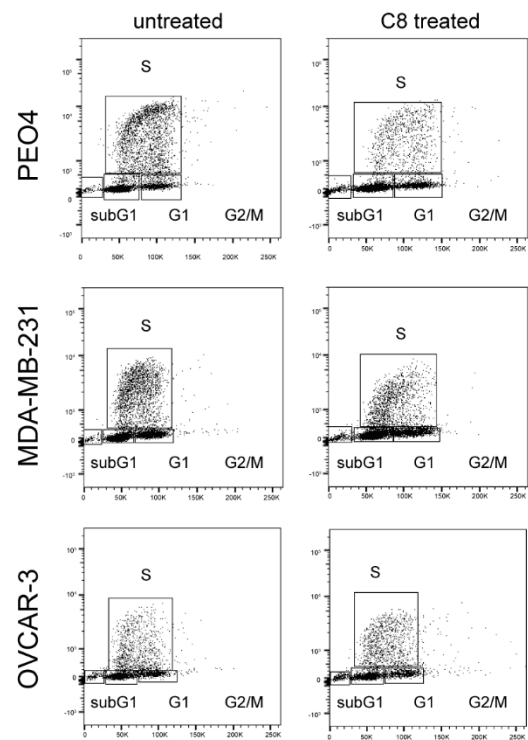
Figure 3-1. Treatment of BRCA-deficient cell lines with C8 leads to cell cycle progression defects. FACS profiles of total DNA (x-axis) and incorporated BrdU (y-axis) of *BRCA*-deficient (**A.**) and *BRCA*-proficient (**B.**) cells treated with 25 µM C8 for 3 days. Rectangles depict the gates used to determine cell cycle distribution percentages.

Table 3-1. Treatment of *BRCA*-deficient cell lines with C8 leads to cell cycle progression defects: quantified cell cycle distributions. Percentages of cells in different phases of the cell cycle are shown for *BRCA*-deficient (**A.**) and *BRCA*-proficient (**B.**) cells treated with 25 µM C8 for 3 days.

A.

		S	G1	G2/M
PEO1	untreated	36%	53%	11%
	C8 treated	16%	47%	37%
UWB1.289	untreated	38%	56%	6%
	C8 treated	1%	87%	12%
HCC1937	untreated	39%	46%	15%
	C8 treated	7%	60%	32%

B.

		S	G1	G2/M
PEO4	untreated	28%	58%	13%
	C8 treated	18%	65%	18%
MDA-MB-231	untreated	23%	62%	16%
	C8 treated	22%	57%	21%
OVCAR-3	untreated	25%	56%	19%
	C8 treated	31%	50%	19%
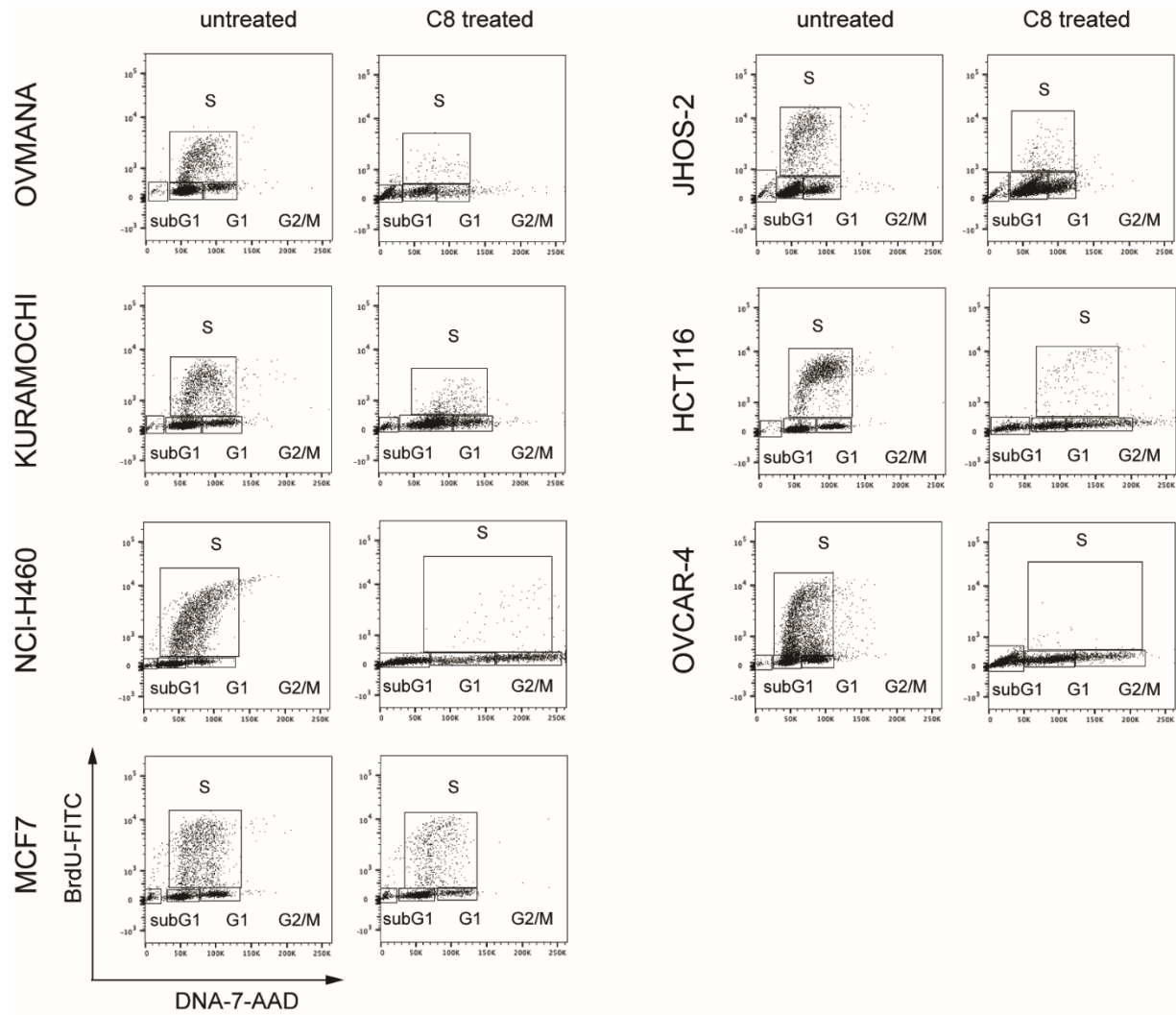
Figure 3-2. Treatment of BRCA-deficient cell lines with C8 leads to cell cycle progression defects. FACS profiles of total DNA (x-axis) and incorporated BrdU (y-axis) of cells treated with 25 µM C8 for 3 days. Rectangles depict the gates used to determine percentages.

Table 3-2. Treatment of *BRCA*-deficient cell lines with C8 leads to cell cycle progression defects: quantified cell cycle distributions. Percentages of cells in different phases of the cell cycle are shown after treatment with 25 µM C8 for 3 days.

		S	G1	G2/M
OVMANA	untreated	20%	70%	10%
	C8 treated	8%	70%	22%
KURAMOCHI	untreated	18%	71%	11%
	C8 treated	8%	75%	17%
NCI-H460	untreated	33%	60%	7%
	C8 treated	4%	43%	53%
MCF7	untreated	28%	56%	16%
	C8 treated	24%	63%	13%

		S	G1	G2/M
JHOS-2	untreated	15%	71%	14%
	C8 treated	3%	82%	15%
HCT116	untreated	22%	65%	13%
	C8 treated	8%	50%	42%
OVCAR-4	untreated	39%	43%	18%
	C8 treated	1%	74%	25%
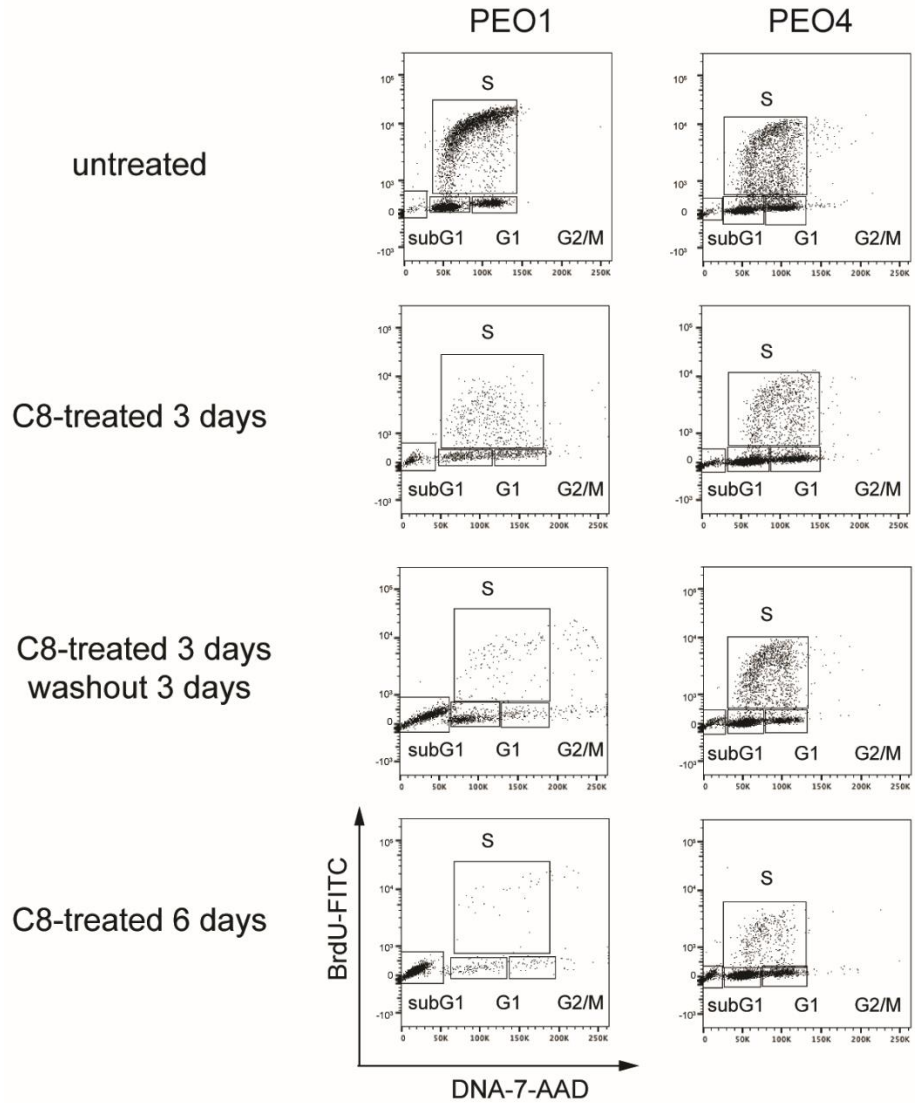
Figure 3-3. PEO1 cells do not recover from C8 treatment after drug removal. Both PEO1 and PEO4 cells were treated for 3 days with 25 µM C8 and then shifted to drug-free medium or left in the same C8-containing medium for an additional 3 days. At each time point, cells were shifted into BrdU-containing medium (10 µM) for 45 minutes, and BrdU incorporation was then analyzed by FACS. FACS profiles are displayed with total DNA along the x-axis and incorporated BrdU along the y-axis. Rectangles depict the gates used to determine percentages.

Table 3-3. PEO1 cells do not recover from C8 treatment after drug removal: quantified cell cycle distributions. Percentages of cells in different phases of the cell cycle are shown for PEO1 and PEO4 cells treated for 3 days with 25 μM C8 and then shifted to drug-free medium or left in the same C8-containing medium for an additional 3 days.

PEO1	S	G1	G2/M
Untreated	37%	53%	9%
C8 treated 3 days	26%	40%	34%
C8 treated 3 days + washout 3 days	16%	72%	13%
C8 treated 6 days	14%	61%	26%

PEO4	S	G1	G2/M
Untreated	25%	60%	15%
C8 treated 3 days	18%	65%	17%
C8 treated 3 days + washout 3 days	30%	56%	14%
C8 treated 6 days	10%	75%	15%

3-B. C8 induces DNA damage in *BRCA*-deficient and *BRCA*-proficient cell lines.

To test if the observed replication defects were associated with increased levels of DNA damage, PEO1 and PEO4 cells were treated with C8 for 3 days and then monitored for histone γH2AX levels, histone γH2AX foci, and 53BP1 foci. In both PEO1 and PEO4 cells, C8 treatment caused increased levels of histone γH2AX protein levels (**Fig. 3-4-A**), an increase in the percent of cells with > 25 histone γH2AX foci per nucleus (**Fig. 3-4-B,C**), and an increase in the number of cells with > 25 53BP1 foci per nucleus (**Fig. 3-4-D,E**) relative to untreated controls. PEO1 cells, however, had more pronounced levels of these DNA damage markers after C8 treatment than PEO4 cells.

These results suggest that treatment of cells with FEN1 inhibitors results in increased DNA damage, including DSBs, in both *BRCA*-proficient PEO4 and *BRCA*-deficient PEO1 cells. Additionally, the higher levels of 53BP1 foci in PEO1 cells compared to PEO4 cells is consistent with reduced HR and increased unrepaired DSBs in PEO1 cells lacking functional BRCA2.

3-C. C8 treatment induces caspase activity in PEO1 cells.

C8 treatment caused increased caspase 3 activity in PEO1 cells relative to PEO4 cells (**Fig. 3-5-A**). The level of caspase 3 activation increased between 1 and 3 days of treatment with C8, in contrast to treatment with staurosporine which resulted in more rapid caspase 3 activation (**Fig. 3-5-B**). Addition of the pan-caspase inhibitor ZVAD-fmk caused a decrease in caspase 3 activation in both PEO1 and PEO4 cells after treatment by C8 but did not increase clonogenic survival of these treated cells (**Fig. 3-5-C**).

Together, these results suggest that the replication defects and resulting DNA damage caused by FEN1 inhibition can induce apoptotic pathways, but that FEN1

inhibition alone is sufficient to prevent cell proliferation and cause cell death even when

apoptosis is inhibited.
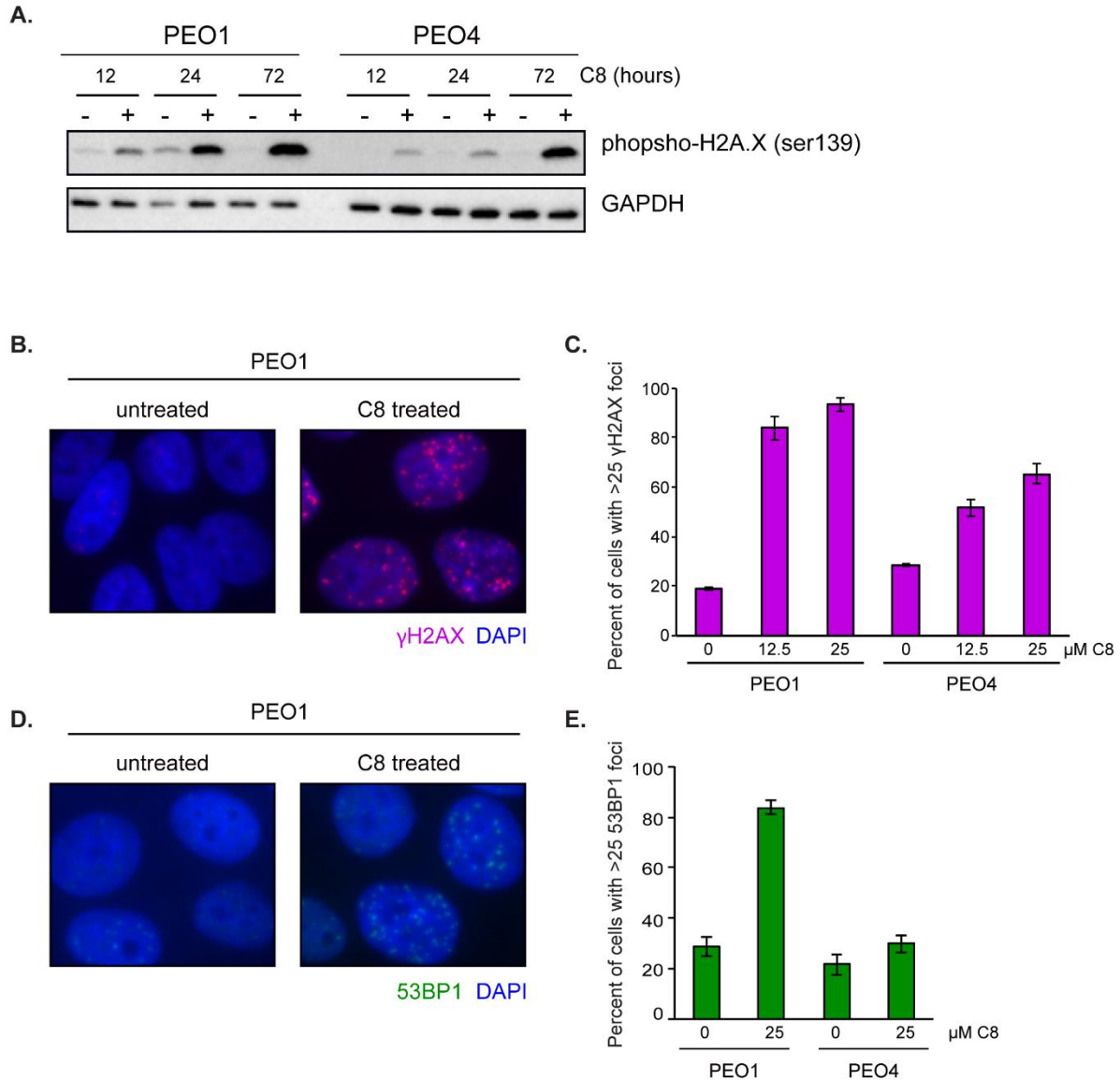
Figure 3-4. C8 induces DNA damage markers in both PEO1 and PEO4 cells. A. PEO1 and PEO4 cells were treated for 12, 24, and 72 hours with medium containing 25 µM C8. Cells were then lysed, and the protein extracts were analyzed by western blot using a phospho-specific γ-H2AX antibody and a GAPDH antibody (loading control). Both PEO1 and PEO4 showed induction of γ-H2AX formation upon prolonged exposure to C8. **B.** Representative images of PEO1 cells treated for 2 days with vehicle or 25 µM C8, then stained with DAPI (blue) and an antibody against γ-H2AX (pink). **C.** Quantification of the percent of PEO1 or PEO4 cells containing greater than 25 nuclear γ-H2AX foci after being treated for 2 days with 0, 12.5, or 25 µM C8. (n=3, with n>100 nuclei per condition). **D.** Representative images of PEO1 cells treated for 1 day with vehicle or 25 µM C8, then stained with DAPI (blue) and an antibody against 53BP1 (green). **E.** Quantification of the percent of PEO1 or PEO4 cells containing greater than 25 nuclear 53BP1 foci after being treated for 1 day with vehicle or 25 µM C8 (n=2, with n>100 nuclei per condition).

56
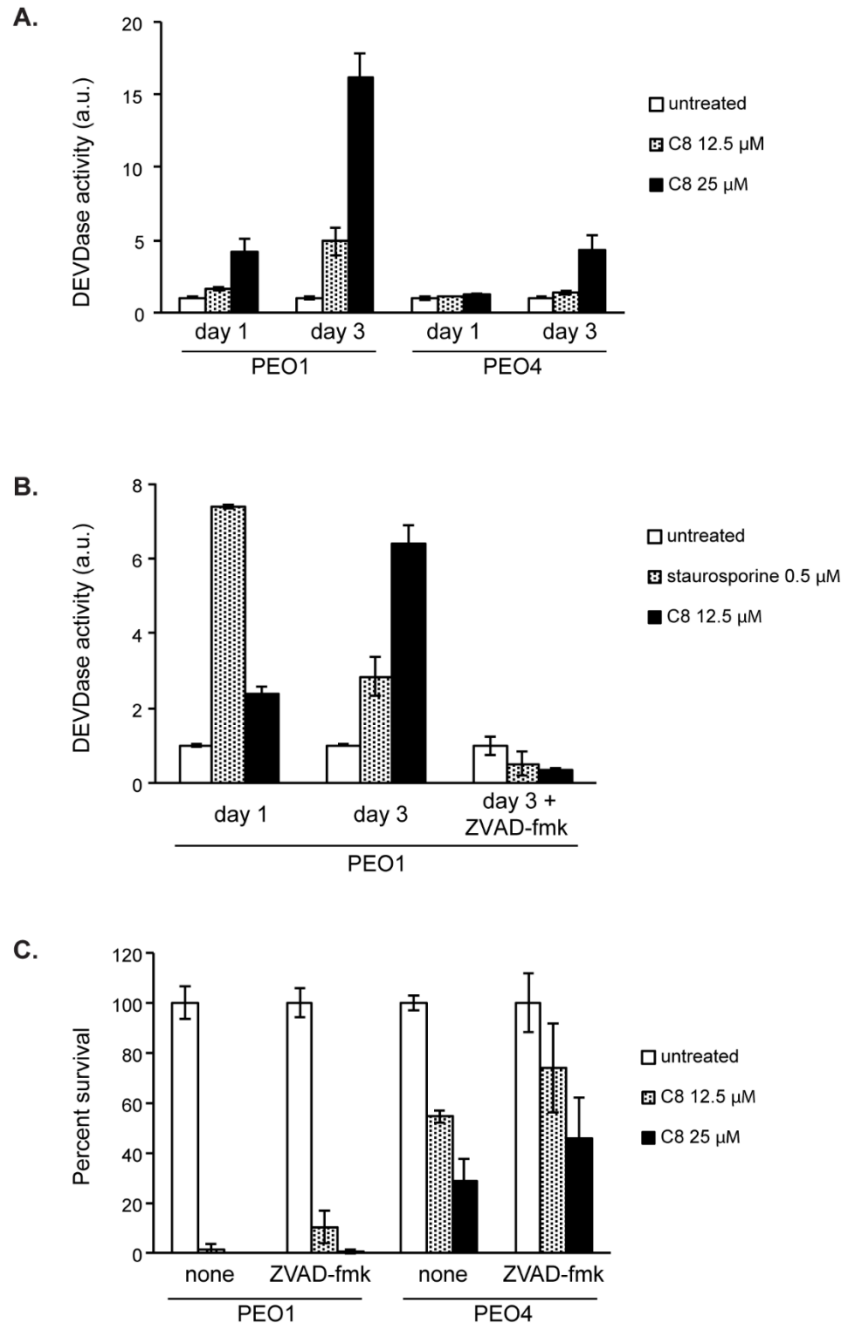
Figure 3-5. C8 induces caspase activity in PEO1 cells. A. Caspase activity was measured for PEO1 and PEO4 cells at 1 day and 3 days in 0, 12.5, or 25 µM C8 (n=3). Higher caspase induction was observed with PEO1 cells than PEO4 cells after 1 day and 3 days of treatment. **B.** Caspase activity was measured in PEO1 cells after 1 day or 3 days when untreated, treated with 0.5 µM staurosporine, or treated with 12.5 µM C8 (n=3). Caspase activity was highest in day 1 with staurosporine, whereas it was highest in day 3 with C8. Caspase activity at day 3 was suppressed by addition of 20 µM ZVAD-fmk caspase inhibitor (ZVAD-fmk was added 1 hour before C8). **C.** Clonogenic survival of PEO1 and PEO4 cells was measured. Cells were treated simultaneously with 0, 12.5, or 25 µM C8 and 0 or 20 µM ZVAD-fmk for 3 days (ZVAD-fmk was added 1 hour before C8). After 3 days of treatment, both C8 and ZVAD-fmk were washed out. PEO1 and PEO4 cells were re-plated in fresh media and allowed to grow for 14 days (n=2). Addition of the ZVAD-fmk caspase inhibitor only modestly increased the survival in C8-treated PEO1 and PEO4 cells.

3-D-1. C8 treatment decreased mitotic entry in both C8-hypersensitive and non-hypersensitive cell lines.

In addition to changes in S and subG1 cell cycle distributions, C8 treatment followed by drug removal led to a decrease in G2/M content in PEO1 cells (**Fig. 3-3**). This led us to next test whether C8 affects mitotic entry and/ or exit. Two cancer cell lines, one hypersensitive and one non-hypersensitive to C8, HCT116 and MDA-MB-231, respectively, were chosen because versions of these cell lines that contain mono red fluorescent protein (mRFP) tags on their H2B histones were available from the laboratories of Karen Oegema and Arshad Desai (Ludwig Institute for Cancer Research, UC San Diego, CA).

We monitored the chromatin of these cell lines by fluorescence microscopy to observe whether C8-treated cells could enter and/ or complete mitosis. HCT116 H2B-mRFP and MDA-MB-231 H2B-mRFP cells were treated for 2 days with 12.5 μM C8 (enough time for asynchronized cells to go through S phase at least once), released into drug-free media and imaged by fluorescence microscopy every 10 minutes for 3 days (or at least two cell cycles). The fates of individual nuclei were followed to determine the timing and fraction of nuclei that entered and completed the first mitosis after release from C8.

We observed two major phenotypes: mitotic nuclei and aberrant nuclei. Mitotic nuclei are defined by frames that contain chromatin condensation, which indicate mitotic entry, followed by chromatin decondensation and generation of daughter nuclei about 5 frames or 50 minutes later, which indicate mitotic exit (**Fig 3-6**). The majority of the remaining fraction of nuclei are aberrant nuclei, which are defined as nuclei that

fragmented, that condensed in size, or that cycled through mitosis but then almost immediately fragmented (data not shown).

For both cell lines, most cells in DMSO-treated conditions completed the first mitosis within one cell cycle time. 12.5 µM C8 decreased the ability of HCT116 H2B-mRFP cells to undergo mitosis, but caused a similar defect in MDA-MB-231 H2B-mRFP cells too.

For C8-hypersensitive HCT116 H2B-mRFP cells treated with 12.5 µM C8 for 2 days, 63% (n=40) completed the first mitosis, compared to 94% of control (n=117). In C8-treated samples, additional phenotypes included 31% that fragmented into aberrant nuclei and a remaining fraction that showed no change (data not shown).

For C8-non-hypersensitive MDA-MB-231 H2B-mRFP cells, 68% of C8-treated cells (n=30) completed the first mitosis, compared to 87% of control (n=74). In the C8-treated sample, another 23% fragmented into aberrant nuclei and the remaining showed no change in phenotype (data not shown).

3-D-2. In contrast to MDA-MB-231 cells, HCT116 cells do not continue to divide to form colonies after C8 treatment.

For MDA-MB-231 H2B-mRFP, 68% of cells completed the first mitosis after 12.5 µM C8 for 2 days. Taken in parallel with clonogenic survival results of MDA-MB-231 cells that showed 85% recovery after 12.5 µM C8 for 3 days (**Fig. 2-5-A**), these data suggest that C8-treated cells that were able to divide at day 2 continued to divide to form colonies.

Clonogenic survival recovery of C8-treated HCT116 cells, however, was only 1% (**Fig. 2-5-C**), compared to 63% of HCT116 H2B-mRFP cells that completed the first

mitosis after 2 days of C8 at the same concentration. These data suggest that while nuclei divided at 2 days after drug treatment, they did not continue to divide to form colonies.

What might explain the difference in clonogenic survival between these two cell lines, despite comparable ability to enter mitosis at 2 days after C8 treatment? MDA-MB-231 cells have intact G2/M checkpoints (164, 165) so that C8-treated cells might have activated G2/M to allow DNA repair and long-term survival of colonies. While HCT116 cells also have intact G2/M checkpoints (166-168), which might have been activated, DNA damage was not repaired in this cell line and led to permanent exit from the cell cycle. The ability to repair DNA damage prior to mitotic entry underlies the differential sensitivity between HCT116 and MDA-MB-231 cells to C8.
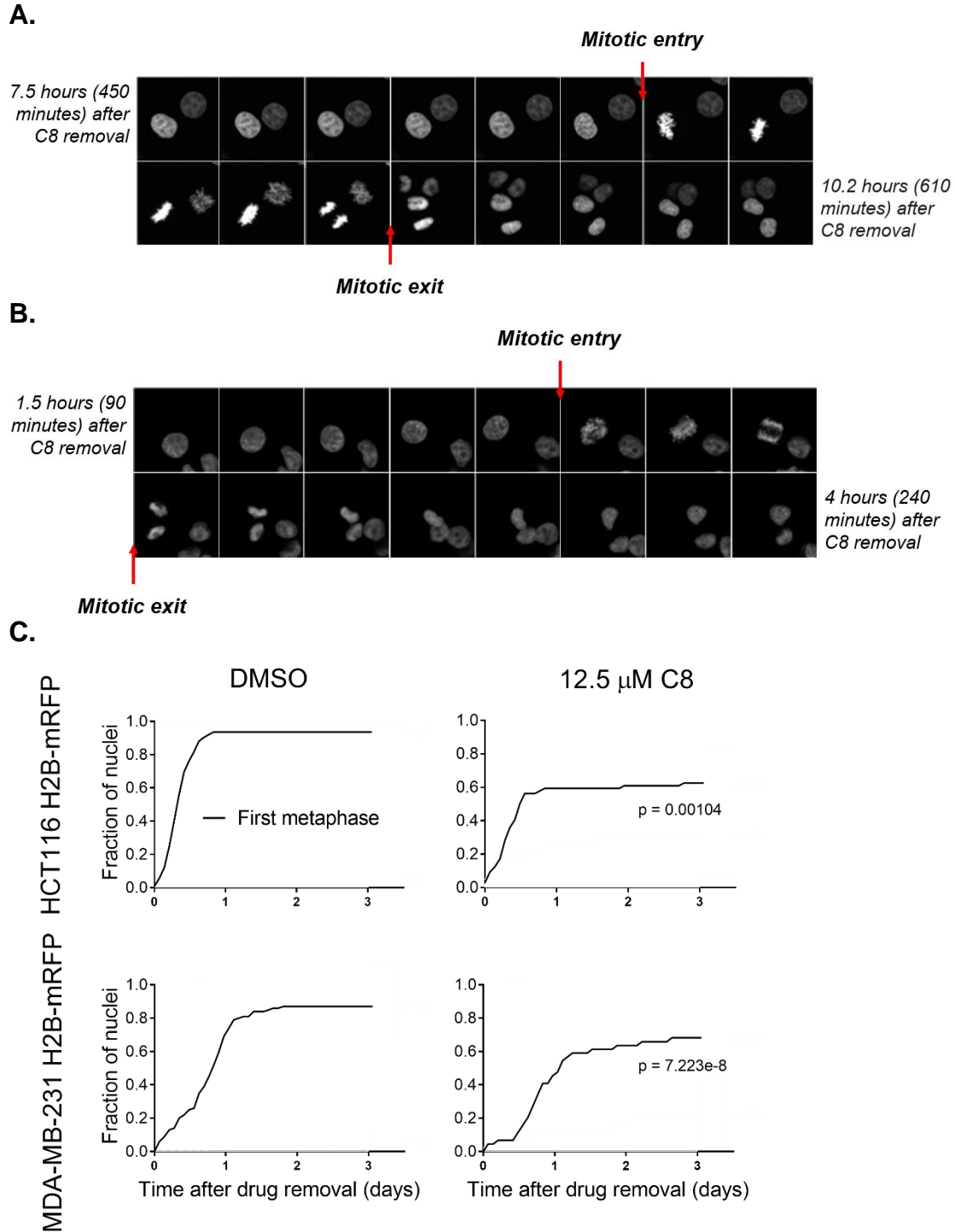
Figure 3-6. C8 inhibits mitotic entry and exit in both C8-hypersensitive and non-hypersensitive cells. HCT116 H2B-mRFP and MDA-MB-231 H2B-mRFP cells were treated for 2 days, then imaged every 10 minutes in fresh media for 3 more days. Representative time lapse images of nuclei undergoing mitosis for HCT116 H2B-mRFP (**A.**) and MDA-MB-231 H2B-mRFP (**B.**) are shown. Each montage follows the same field from left to right, top to bottom; frames were captured every 10 minutes. **C.** Individual nuclei (n>40) were followed by eye and the fraction of nuclei that entered and exited mitosis was quantified and the timing of the first metaphase graphed. P-values of C8-treated samples compared to control were calculated using the Freeman-Halton extension of the Fisher Exact, 2-tailed.

3-E. C8 increases fragmented chromosomes and chromatid breaks in *BRCA*-deficient more so than in *BRCA*-proficient cells.

We hypothesize that C8 induces DNA damage that remains unrepaired in BRCA-deficient or C8-sensitive cells. These cells cannot complete replication and re-enter the cell cycle with damaged DNA to undergo mitosis. The cells accumulate DNA damage and as they undergo one or more defective mitoses, they die. Cell death caused by premature entry into mitosis before replication is complete in the presence of severe DNA damage is defined as mitotic catastrophe (169-171).

To test whether C8-treated cells that enter mitosis contain chromosomal abnormality, we looked directly at the chromosomes using the metaphase spread assay. C8-sensitive, *BRCA2*-deficient PEO1 and C8-resistant, *BRCA*-WT OV-90 cancer cell lines were treated with DMSO or 25 μM C8 for 3 days and then released into drug-free media for 0-16 hours, after which the cells were incubated in hypotonic solution, fixed, and their DNA prepared and stained for metaphase spread imaging.

C8 significantly increased chromosomal aberrations, including fragmented chromosomes and chromatid breaks, in PEO1 cells (**Fig. 3-7**); all metaphase spreads in C8-treated samples showed >5 aberrations, in contrast to control, in which most metaphase spreads had 0-5 aberrations. The majority of metaphases in C8-treated OV-90 cells, on the other hand, contained 0-5 aberrations per metaphase. These results suggest that treatment with C8 leads to the accumulation of unrepaired DNA breaks, followed by shattered chromosomes in mitosis, and eventual cell death.

To extend this experiment, results from these two cell lines will be expanded to a panel of 3 *BRCA*-deficient (PEO1, UWB1.289, HCC1937) and 3 *BRCA*-proficient (PEO4,

OV-90, OVCAR-3) cell lines. To increase the fraction of metaphase cells, the cell lines will be treated with C8 for two cell cycles and then arrested with colcemid for 1 hour before fixing and staining for imaging.
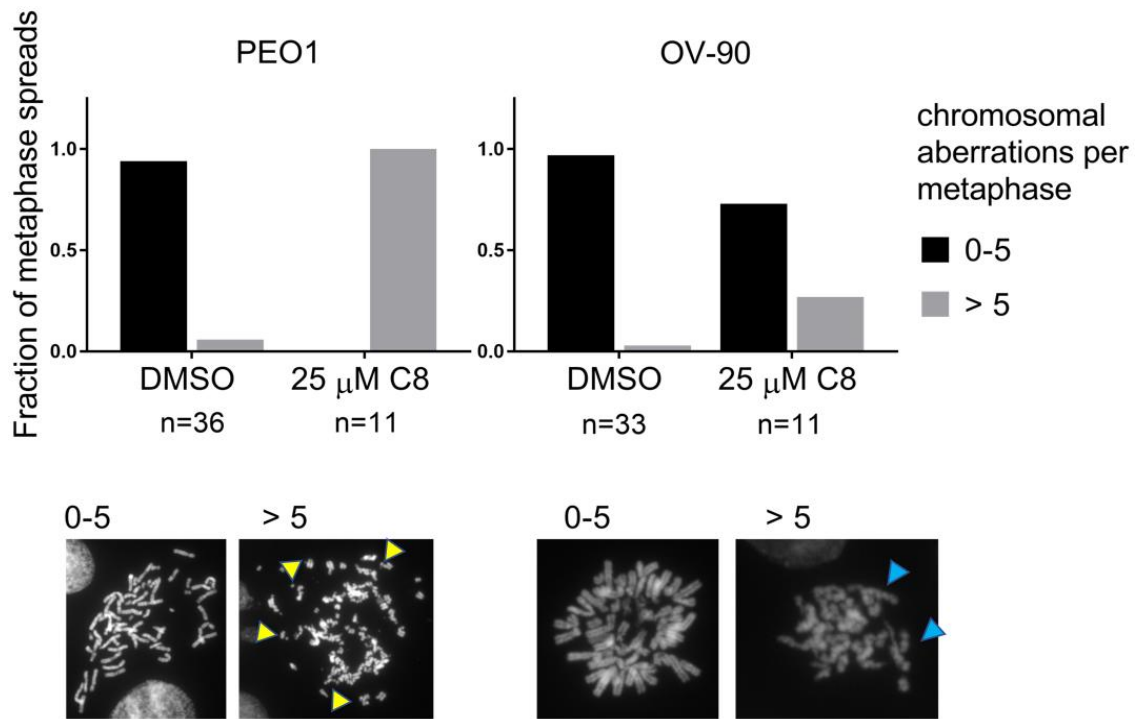
Figure 3-7. C8 increases chromosomal aberrations in *BRCA*-deficient cells. PEO1 and OV-90 cells were treated with vehicle or 25 µM C8 for 3 days. Cells were then released into drug-free media for 0-16 hours and then prepared for metaphase spread imaging. Metaphases were analyzed for chromosomal aberrations, which included fragmented chromosomes or chromatid breaks. Representative metaphase spreads are shown for each cell line, where examples of fragmented chromosomes (yellow arrows) and chromatid breaks (blue arrows) are marked.

3-F. C8 differentially activates checkpoint pathways triggered by DSB or stalled replication forks in PEO1 and PEO4 cells.

3-F-1. Introduction to PIKKs

In mammalian cells, the DDR is controlled by three PIKKs: ATM, ATR, and DNA-PK (**Fig. 3-8**). Upon DNA damage recognition, these kinases are activated and then phosphorylate hundreds of substrates to initiate cellular signaling cascades that promote a variety of processes, including checkpoint activation and DNA repair.

The ATM-Chk2 pathway is primarily activated by DSBs and promotes HR. ATR is recruited to regions of RPA-coated ssDNA, which are found at stalled replication forks; the ATR-Chk1 pathway mainly responds to DNA replication stress. DNA-PKcs is also activated by DSB; DNA-PKcs is recruited and activated by Ku-bound DSB ends to promote NHEJ (172). Because FEN1 inhibition induces DNA damage and chromosomal aberrations, we next asked how FEN1 inhibition affects PIKK activation. In the context of *BRCA*-deficient cells, we are interested in the effects of FEN1 inhibition on ATM and ATR signaling.

ATM is responsible for the global regulation of cellular responses to DSB.

ATM is recruited to and activated by the MRN complex at DSB (173, 174). Active ATM then phosphorylates hundreds of DDR substrates and induces a DNA damage signaling cascade, which includes activation of cell cycle checkpoints and DSB repair.

ATM is needed for the initiation and completion of DSB repair by HR (175). In this process, ATM triggers DSB end resection by stimulating the nucleolytic activities of CtIP and MRE11 to generate 3'-ssDNA overhangs, which then promotes HR over NHEJ.

(Upon ATM inhibition, ATR can compensate in part for the deficiency in early, but not later steps of HR after RAD51 nucleofilament formation.)

ATM, along with BRCA1, BRCA2, and PALB2, regulate the G2/M checkpoint.

In addition to DSB repair, ATM also regulates cell cycle checkpoints, including G2/M. The G2/M checkpoint inhibits mitotic entry upon DNA damage to minimize the segregation of broken chromosomes into daughter cells. Both ATM and BRCA1, in particular the phosphorylation of BRCA1 by ATM, are required for effective G2/M checkpoints (176). The expression of BRCA1 variants defective for ATM-mediated phosphorylation is associated with a defect in G2/M arrest (13).

In addition to ATM and BRCA1, recent studies also established BRCA2 and PALB2 as regulators in G2/M checkpoint maintenance. PALB2 links BRCA1 and BRCA2 in G2/M checkpoint control (177), where the BRCA1-PALB2 interaction is important for checkpoint activation, and PALB2-BRCA2 formation is more critical for G2/M checkpoint maintenance.

ATR is an essential kinase involved in the DNA replication stress response.

ATR coordinates DNA replication origin firing and guards replication fork stability. ATR is recruited, by ATRIP, to extended tracts of ssDNA coated with RPA (178) found at stalled replication forks or resected DSB. Activated ATR phosphorylates CHK1, which then promotes degradation of CDC25A (179), followed by inhibition of CDK activity, inhibition of late-origin firing, and slowing of replication to prevent premature mitotic entry.
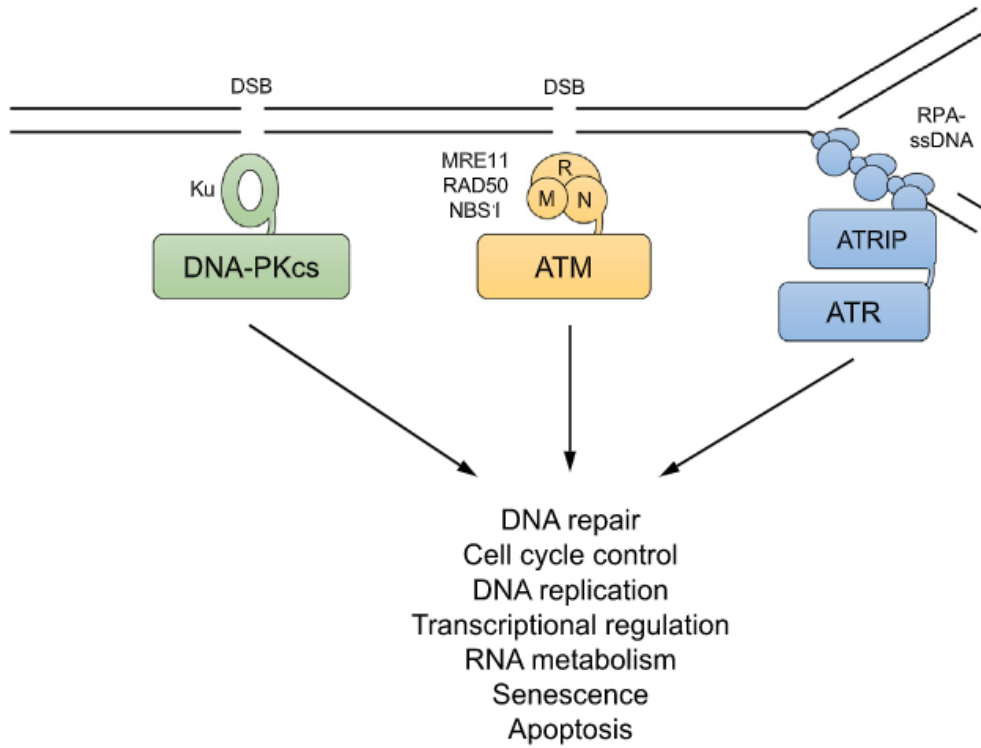
Figure 3-8. PIKK recruitment and activation in response to DSB and stalled replication forks (180). DNA-PKcs is recruited and activated by Ku-bound DSB ends. ATM is activated and recruited to DSB by the MRE11-RAD50-NBS1 (MRN) complex. ATR is recruited to RPA-coated ssDNA by its stable binding partner ATRIP.

3-F-2. C8 differentially activates checkpoint kinases in PEO1 and PEO4 cells.

To determine the effect of C8 on activation of these three kinases in a *BRCA*-deficient vs. *BRCA*-proficient background, I treated PEO1 and PEO4 cells with C8, followed by PIKK inhibitors, and then monitored the phosphorylation of three PIKK substrates by immunoblotting.

PEO1 and PEO4 cells were treated for 2 days with DMSO, 25 µM C8, or left untreated. At 2 days, cells were additionally treated for 3.5 hours with DMSO, individual, or a combination of inhibitors against ATM, ATR, and DNA-PK (all at 2 µM) before being harvested for immunoblotting.

The substrates include: H2AX/ γH2AX, Chk1/ pChk1 (Serine 317) and Chk2/ pChk2 (Threonine 68). H2AX can be phosphorylated by all three PIKKs. Chk1 is primarily the substrate of ATR (181), while phosphorylation of Chk2 involves primarily ATM (182, 183). Although the PIKKs have distinct modes of activation and different interacting proteins, they share certain substrates and have overlapping functions.

In *BRCA2*-deficient PEO1 cells, C8 increased γH2AX, as previously shown (**Fig. 3-4-A**). This phosphorylation was reduced by DNA-PKi, combined ATMi and ATRi, combined ATRi and DNA-PKi, and all 3 inhibitors, suggesting that C8 activated all 3 PIKKs in PEO1 cells (**Fig. 3-9**).

C8 also increased pChk1 levels that were decreased by ATRi and all combinations that included ATRi; these results confirm that ATR is responsible for Chk1 phosphorylation, which is consistent with the literature (184). The increase in pChk1 due to ATR activation suggest that stalled replication forks might have been present in C8-treated *BRCA2*-deficient PEO1 cells. ATR-Chk1 activation is also responsible for

inhibition of late-origin firing and slowing of replication, which would be consistent with the previously shown S phase progression defects in C8-treated PEO1 cells (**Fig. 3-1**).

Interestingly, C8 did not increase pChk2 in PEO1 cells. One interpretation of this data is that cells with high levels of DSBs induced by C8 did not survive.

C8 also increased γH2AX levels in *BRCA2*-proficient PEO4 cells, which was reduced by ATRi, DNA-PKi, and ATMi (compare combined ATRi and DNA-PKi with all three), suggesting that C8 also activates all 3 PIKKs in PEO4 cells (**Fig. 3-9**).

Unlike in PEO1 cells though, C8 increased pChk2 in PEO4 cells and did not change pChk1 levels. Phosphorylation of Chk2 was reduced by ATMi, DNA-PKi, combined ATMi and ATRi, ATMi and DNA-PKi, ATR and DNA-PKi, and all 3 inhibitors. This result suggests that ATM and DNA-PK both phosphorylate Chk2, which is consistent with previous results showing DSB are present in C8-treated PEO4 cells (**Fig. 3-4-A**).

In addition, ATM activation, which is needed for the initiation and completion of HR and which works together with BRCA1, BRCA2, and PALB2 to maintain the G2/M checkpoint, might indicate G2/M checkpoint activation and proficient HR in PEO4 cells. These pathways would allow cells to repair damaged DNA and continue to progress through the cell cycle.

C8 activated all 3 PIKKs in both PEO1 and PEO4 cells, as seen by increased γH2AX levels that were reduced with combinations of PIKK inhibitors (**Table 3-4**). There was, however, differential phosphorylation of Chk1 and Chk2 between the two cell lines. Phosphorylation of Chk1 through ATR is mainly in response to stalled forks, while phosphorylation of Chk2 through ATM and DNA-PK is mainly in response to DSB.

Differences in checkpoint kinase phosphorylation may suggest the presence of different forms of DNA damage and repair activity in C8-treated PEO1 and PEO4 cells.

3-F-3. Model for FEN1 inhibition induced synthetic lethal mechanism.

Our proposed model suggests that FEN1 inhibition by C8 increases DSB in both *BRCA*-proficient and *BRCA*-deficient cells. In a *BRCA*-proficient background, normal checkpoint signaling can occur, and DSB can be repaired by HR and replication fork protection pathways, leading to cell survival. In a *BRCA*-deficient background, however, the lack of checkpoint signaling and the lack of DSB repair and/ or stalled fork protection leads to cell lethality (**Fig. 3-10**).

Future studies are needed to determine whether C8 increases stalled replication forks or ssDNA in either *BRCA*-proficient or *BRCA*-deficient cells. To test this, we would initiate experiments to measure RPA foci using immunofluorescence or monitor nascent DNA lengths using DNA fiber assays.

If stalled replication forks are present in C8-treated cells, do they require activation of *BRCA*-dependent replication fork protection pathways? To test this, one approach we could use is separation-of-function *BRCA* mutants, such as the *BRCA1* (Serine 114A) and the *BRCA2* (Serine 3291A) mutants; both are HR proficient but defective in protection of stalled replication forks. Would cell lines with these *BRCA* mutants be able to as effectively repair C8-induced DNA damage?

Additional questions remain about whether the G2/M checkpoint is activated in and whether activation is required for survival of C8-treated, *BRCA*-proficient cells. Experiments that inactivate the G2/M checkpoint and measure survival could clarify these questions.

Lastly, to confirm HR activation in C8-treated, *BRCA*-proficient cells and the lack thereof in *BRCA*-deficient cells, we would measure RAD51 foci by immunofluorescence and resistance to PARP inhibition.

Chapter 3, in part, is currently being prepared for submission for publication. Guo, Elaine; Ishii, Yuki; Mueller, James; Srivatsan, Anjana; Putnam, Christopher; Wang, Jean Y. J.; Kolodner, Richard. FEN1 is a potential therapeutic target for human cancers with defects in homologous recombination. The dissertation author is the co-author of this paper.
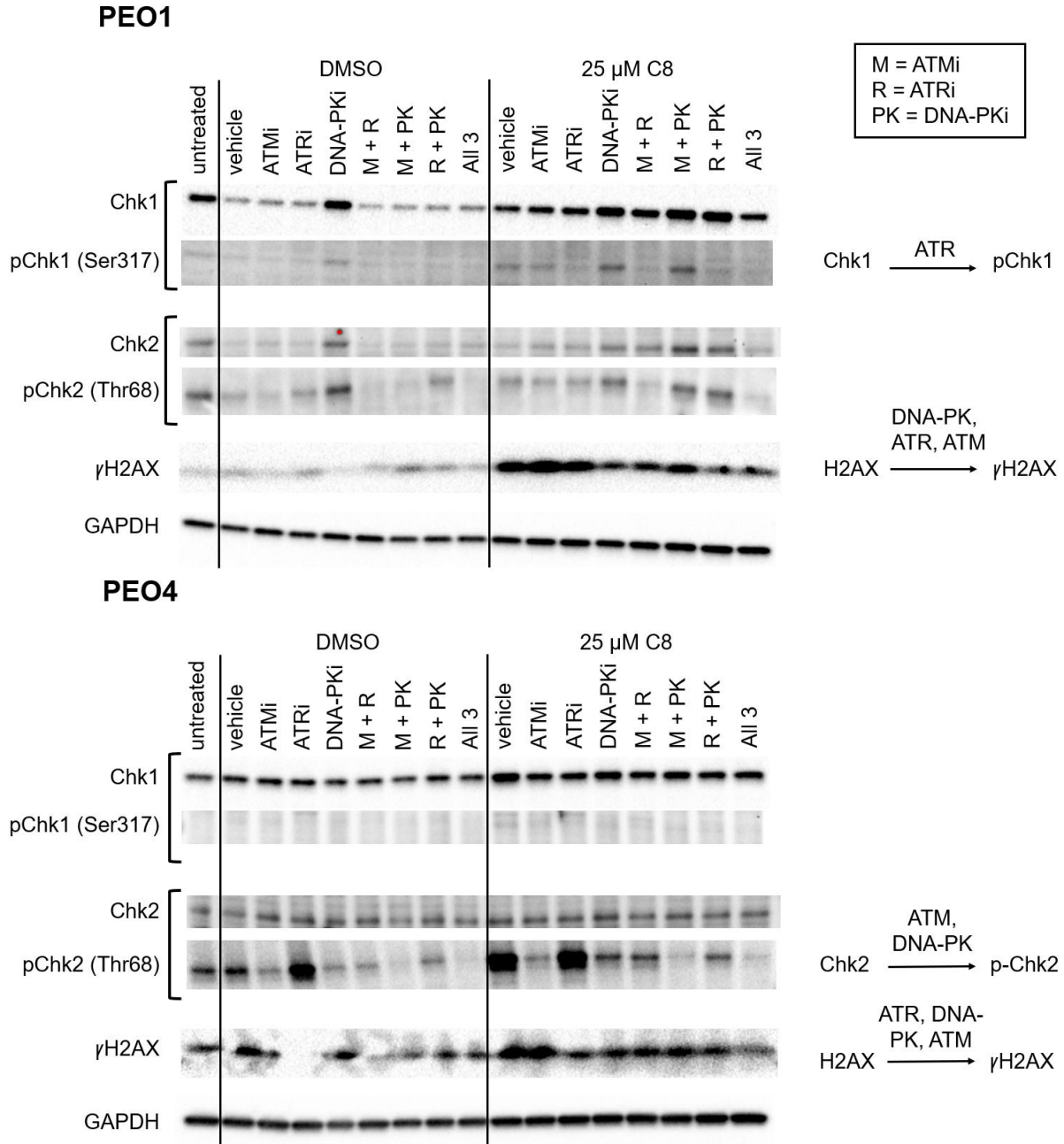
Figure 3-9. C8 differentially activates PIKK kinases in PEO1 and PEO4 cells. PEO1 and PEO4 cells were treated for 2 days (or at least one cell cycle, PEO1 doubling time=37 hours, PEO4=46 hours) with either vehicle, 25 μM C8, or left untreated. At 2 days, the cells were additionally treated for 3.5 hours with vehicle, individual, or a combination of inhibitors against ATM, ATR, and DNA-PK (all at 2 μM). Samples were then harvested at 2 days and 3.5 hours for immunoblotting.

72

Table 3-4. Summary of Differential Checkpoint Kinase Activation by C8 in PEO1 and PEO4 Cells. PEO1 and PEO4 cells were treated for 2 days with either vehicle, 25 µM C8, or left untreated. At 2 days, the cells were additionally treated for 3.5 hours with vehicle, individual, or a combination of inhibitors against ATM, ATR, and DNA-PK (all at 2 µM). Samples were then harvested at 2 days and 3.5 hours for immunoblotting.

	ATR	ATM	DNA-PK
PEO1 (*BRCA2*-deficient)	γH2AX pChk1	γH2AX	γH2AX
PEO4 (*BRCA2*-proficient)	γH2AX	γH2AX pChk2	γH2AX pChk2

FEN1 Inhibition Induced Synthetic Lethal Mechanism

FEN1 inhibition

Accumulation of flaps on lagging strands

Double-stranded breaks

BRCA-proficient

| Checkpoint activation | Homologous recombination, replication fork protection |

Repair

Survival

BRCA-deficient

| Stalled replication | Loss of homologous recombination and replication fork protection |

No repair

Lethality
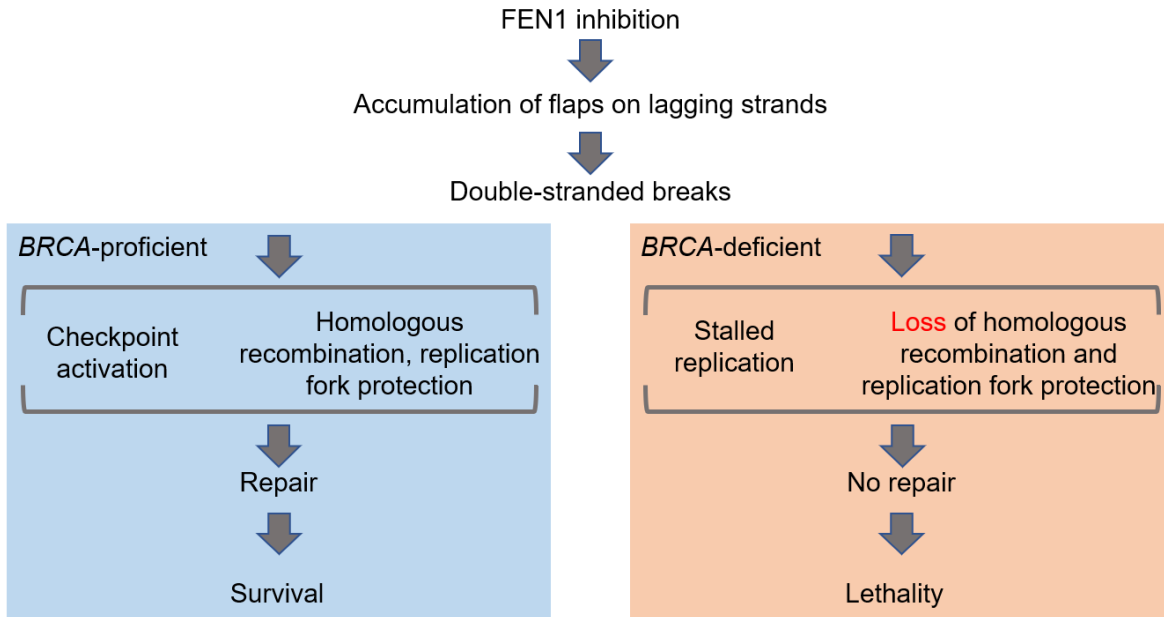
Figure 3-10. Model for FEN1 inhibition induced synthetic lethal mechanism. FEN1 inhibition in the cell leads to an accumulation of flaps on lagging strands during DNA replication, which in combination with nucleolytic cleavage on the template strand, can lead to DSB. In a *BRCA*-proficient background, normal checkpoint signaling can occur, and DNA double stranded breaks can be repaired by homologous recombination, leading to cell survival. In a *BRCA*-deficient background, DSB and stalled forks are not repaired, leading to cell lethality.

74

CHAPTER 4

MATERIALS AND METHODS

Identification of the *S. cerevisiae* GIS gene interaction network.

SL interactions that were not conditional SL interactions and not SL interactions involving three or more mutations (also called "genetic complex" interactions) were extracted from the BioGRID database version 3.5.168 (https://thebiogrid.org/). The numbers of SL interactions that each gene had with the 266 *S. cerevisiae* GIS genes were counted, and genes were sorted based on this count.

C8 clonogenic survival assays.

Breast, ovarian, colorectal, and lung cancer cell lines were cultured in the media listed (**Tables 4-1, 4-2, 4-3**, **4-4**) following American Type Culture Collection (ATCC) passaging and splitting guidelines.

Cells in log phase were plated in 12-well plates at 5×10^3 cells/well (n=3) and incubated at 37°C, 5% CO_2, in a humidified chamber. After 24 hours of growth, the cells were treated with 12.5 µM C8 or DMSO. After 3 days of incubation with C8 in DMSO, the media was aspirated and 1 ml of PBS was gently added per well and aspirated to wash the cells. The cells were trypsinized by addition of 100 µl/well of 0.25% W/V Trypsin [2.21 mM] EDTA in HBSS followed by incubation for 5 minutes at 37°C, 5% CO_2, in a humidified chamber. 900 µl of media was added per well and the cells were gently resuspended. The resuspended cells were then re-plated in 2 ml of media in 6-well plates at two different dilutions (4-fold difference) per condition. Plates were then incubated for 1-2 weeks.

Media was replenished every 3 days. After 1-2 weeks the media was aspirated and the wells washed with 2 ml/well of PBS. 2 ml/well of fixative (10% acetic acid, 10% methanol, 80% PBS) was then added, followed by incubation at room temperature for 5

minutes. The fixative was aspirated from each well and the wells washed by 2 ml/well of PBS. To stain the fixed cells, 0.5 ml/well of crystal violet (1% W/V in methanol) was then added and the plates incubated at room temperature for 5 minutes. Finally, the crystal violet solution was aspirated from each well and the plates washed by immersing in 1L of water three times. Colonies were counted and the % survival relative to control determined.

C8 trypan blue exclusion assay.

Cells were seeded at $1.5x10^5$ cells/6-cm dish for DMSO or at $1.5x10^5$ cells/6-well plate well for 12.5 and 25 µM C8-treated conditions (n=3). Cells were treated with C8 or DMSO for 3 days and then grown in drug-free media for 6 more days. DMSO-treated cells were split at days 3 and 6, while C8-treated conditions were not split. Media was changed every 3 days for all conditions.

To determine the number of viable cells, equal volumes of cell suspension and trypan blue solution (0.4% in 0.81% sodium chloride and 0.06% potassium phosphate dibasic solution, Bio-Rad) were mixed and the samples counted using a TC20 Automated Cell Counter (Bio-Rad). Each biological replicate was counted 3 times.

BrdU incorporation assay.

DNA synthesis was quantified by analyzing incorporated bromodeoxyuridine (BrdU) using a BrdU Flow Kit (BD Pharmingen) according to the manufacturer's instructions. Cells were treated with 25 µM of C8 or DMSO for 3 days, pulse-chased with BrdU (10 µM) for 45 min at the end of treatment, then fixed and permeabilized. The

subsequent double staining of cells with FITC-conjugated anti-BrdU antibody and 7-aminoactinomycin D (7-AAD), which binds to total DNA, allowed the determination of BrdU incorporation at each step of the cell cycle. Stained cells were acquired with the LSRII flow cytometer (BD Biosciences), and the results were analyzed using FlowJo software (FlowJo, LLC, Ashland, OR).

Measurement of caspase 3 activity.

Cells were washed with PBS at the end of treatment, lysed in a lysis buffer (50 mM HEPES pH 7.5, 100 mM NaCl, 2 mM EDTA, 0.1% CHAPS, 10% sucrose) and the protein concentration was measured. Next, 30 µg of each sample was incubated with 20 µg/ml of Ac-DEVD-AMC caspase-3 fluorogenic substrate (BD Pharmingen) in the lysis buffer supplemented with 10 mM of DTT for 1 hour at 37 ºC. Fluorescent AMC liberated from Ac-DEVD-AMC was detected using a fluorometer with excitation at 380 nm and emission at 440 nm.

Immunofluorescence.

Cells were plated on sterile Poly-L-Lysine coated cover slips (Fisher Scientific) and left to grow overnight. Following treatment with DMSO, 12.5 or 25 µM C8 for the indicated times, cells were fixed in 4% paraformaldehyde, permeabilized in 0.1% Triton-X/0.5% BSA, and blocked in 2% BSA.

After incubation with primary antibodies against γH2AX (Millipore Sigma 05-636) and 53BP-1 (Novus Biologicals NB100-304) at concentrations of 1:1000 overnight at 4 ºC, secondary antibodies at concentrations of 1:1000 (Alexa Fluor 594 for γH2AX, Alexa

Fluor 488 for 53BP-1, Thermo Fisher Scientific) were applied, followed by an 1 hour incubation at room temperature. Coverslips were mounted using ProLong Gold Antifade Mountant with DAPI (Life Technologies). Images were collected using a Nikon ECLIPSE TE2000-S fluorescence microscope at 60X and processed using FIJI.

siRNA treatment for immunoblotting and short-term survival assays.

Cells were seeded at 1×10^5 cells/well in 6-well plates and then transfected with either non-targeting pooled siRNA (Dharmacon ON-TARGETplus) or FEN1 SMARTpool siRNA (Dharmacon ON-TARGETplus) at 50 nM following the manufacturer's instructions. At 1 day post transfection, media containing OPTIMEM (Gibco) and Lipofectamine RNAiMAX (Thermo Fisher Scientific) were replaced with fresh media. For immunoblotting, at 3 days post transfection, cells were scraped in ice cold PBS, centrifuged at 4ºC, and the pellet stored at -80ºC. For trypan blue exclusion assays, at the time of transfection and at 3 days post transfection, trypsinized cell suspensions were mixed with equal volumes of 0.4% trypan blue solution (Bio-Rad) and viable cells were counted using a TC-20 Automated Cell Counter (Bio-Rad).

Immunoblotting.

Pellets were lysed in RIPA buffer with protease and phosphatase inhibitor cocktails (Cell Signaling Technology), sonicated for 5 pulses at 50% duty cycle (Ultrasonics, Inc), cleared by centrifugation at 17,900 xg for 10 minutes at 4ºC, and the protein concentration was quantified using a modified Lowry protein assay (Bio-Rad DC Protein Assay). Total cell lysates, prepared with 4X Laemmli buffer (Bio-Rad), were separated by SDS-PAGE

on 4-15% gradient gels (Bio-Rad TGX) and transferred to PVDF membranes (Bio-Rad) using a Trans-Blot Turbo (Bio-Rad).

Blots were incubated with primary antibodies against FEN1 (Abcam ab462), Chk1 (Cell Signaling Technology 2360, 1:1000), phospho-Chk1 (Ser317) (Cell Signaling Technology 2344, 1:1000), Chk2 (Cell Signaling Technology 2662, 1:1000), phospho-Chk2 (Thr68) (Cell Signaling Technology 2197, 1:1000), GAPDH (Cell Signaling Technology 2118S, 1:1000), and phospho-histone H2A.X (Ser139) (Cell Signaling Technology 2577, 1:1000), followed by incubation with HRP-linked rabbit or mouse secondary antibodies (Cell Signaling Technology). Blots were developed using the HRP substrate and detected using a ChemiDoc MP (Bio-Rad).

Clonogenic survival assays for siRNA-treated cells.

Single cells were seeded at low density in 6-well plates and then transfected with either non-targeting pooled siRNA or FEN1 SMARTpool siRNA at 50 nM. Media containing OPTIMEM and transfection reagents were replaced with 2ml fresh media at 1 day post transfection. At 3 days post transfection, an additional 2ml fresh media was added per well. Every 3 days thereafter, media was completely replaced with 2ml fresh media, and every 6 days thereafter, 2ml of fresh media was added to the 2ml already in each well. Cells were cultured for a total of 15 or 21 days, depending on the cell line, and then fixed (10% acetic acid, 10% methanol in PBS) and stained with crystal violet (1% W/V in methanol).

Colony count and size determination.

Colony counts and sizes were determined using FIJI. To provide a gold standard for calibrating FIJI though, colonies were first counted by eye (n=8 wells per cell line), regardless of colony size. To use FIJI, plates were first imaged using the AlphaImager HP (ProteinSimple). The background for each image was then subtracted and the image inverted. Thresholding was applied to convert the image to binary; this step was optimized for each cell line so that the automated colony counts reflected counts determined by eye. Watershed function was next applied to separate overlapping objects. Finally, particle counts and sizes were calculated; this step was also optimized for each cell line based on size and circularity. The data was displayed using GraphPad Prism software (GraphPad Software, La Jolla, CA).

Live cell imaging.

MDA-MB-231 H2B-mRFP and HCT116 H2B-mRFP cell lines were generously provided by the Karen Oegema and Arshad Desai (Ludwig Institute for Cancer Research, San Diego, CA). MDA-MB-231 H2B-mRFP was cultured in RPMI 1640 media (Gibco), supplemented with 10% Fetal Bovine Serum (FBS, Atlanta Biologicals) and 1% Penicillin-Streptomycin-Glutamine (PSG, Thermo Fisher Scientific). HCT116 H2B-mRFP was cultured in McCoy's 5A phenol red free media (HyClone), supplemented with 10% FBS and 1% PSG. Cells were maintained at 37 ºC with 5% CO_2 in a humidified chamber.

The cells were seeded into 96-well plates with MDA-MB-231 H2B-mRFP at 2,000 cells/well and HCT116 H2B-mRFP at 750 cells/well. Cells were treated for 2 days with DMSO or 12.5 µM C8, at the end of which, drug was washed out and fresh media added. Cells were then immediately imaged in fresh media at 10 minute intervals for 72 hours

using the Yokogawa CQ1 Confocal Imager (in collaboration with the Small Molecule Development Lab, Ludwig Institute for Cancer Research, San Diego, CA). The fate of each nuclei was tracked by eye.

Metaphase spread assay.

Cells were seeded at 9.6×10^4 cells/well in a 6-well plate. The cells were treated with DMSO or 25 µM C8 for 3 days and then harvested by trypsin and centrifugation at 1000 rpm for 5 minutes. Hypotonic, pre-warmed 0.075M KCl solution was added dropwise to the cells while vortexing the cells slowly, followed by incubation in this solution for 6 minutes at 37 ºC. Ice-cold Carnoy fixative (3:1 methanol: acetic acid) was then added to the cells in KCl at a ratio of 1:5, and the cells were centrifuged to remove the supernatant. The pellet was washed again in ice-cold Carnoy fixative before final resuspension in ice-cold Carnoy fixative.

10 µl per sample was dropped from 2 inches high onto glass slides, allowed to air dry, and stained with Hoechst 33342 (Thermo Fisher Scientific). ProLong Gold Antifade mounting media (Life Technologies) was added and the slides imaged the next day using a GE Life Sciences DeltaVision Elite microscope at 60X. Images were scored based on the methods described in Theunissen and Petrini (185).

PIKK inhibitor treatment for immunoblotting.

PEO1 cells were seeded at 3.15×10^5 cells/6-cm dish, and PEO4 cells were seeded at 7.5×10^5 cells/6-cm dish. Cells were treated the following day with DMSO or 25 µM C8 for 2 days. At 2 days, they were additionally treated with DMSO or checkpoint inhibitors

AZD156 (ATMi), AZD6738 (ATRi), NU7441 (DNA-PKi) at 2 μM for 3.5 hours. At the end

of treatment, cells were harvested by scraping in ice cold PBS, centrifuged at 4ºC, and

the pellets stored at -80ºC.

Table 4-1. Breast Cancer Cell Lines and Media. Fetal bovine serum (FBS).

AU-565	RPMI-1640, 10% FBS
BT-549	RPMI-1640, 10% FBS, 0.023 IU/mL bovine insulin
CAMA-1	Eagles Minimum Essential Medium, 10% FBS
HCC1395	RPMI-1640, 10% FBS
HCC1419	RPMI-1640, 10% FBS
HCC1428	RPMI-1640, 10% FBS
HCC1500	RPMI-1640, 10% FBS
HCC1806	RPMI-1640, 10% FBS
HCC1937	RPMI-1640, 10% FBS
HCC1954	RPMI-1640, 10% FBS
HCC202	RPMI-1640, 10% FBS
HCC38	RPMI-1640, 10% FBS
HCC70	RPMI-1640, 10% FBS
Hs 578T	DMEM, 10% FBS, 0.01 mg/mL bovine insulin
MCF7	Eagle's Minimum Essential Medium, 10% FBS, 0.01 mg/mL bovine insulin
MDA-kb2	Leibovitz's L-15, 10% FBS
MDA-MB-134-VI	Leibovitz's L-15, 20% FBS
MDA-MB-157	Leibovitz's L-15, 10% FBS
MDA-MB-175-VII	Leibovitz's L-15, 10% FBS
MDA-MB-231	Leibovitz's L-15, 10% FBS
MDA-MB-361	Leibovitz's L-15, 20% FBS
MDA-MB-436	Leibovitz's L-15, 10 mcg/mL insulin, 16 mcg/mL glutathione, 90%; 10% FBS
MDA-MB-453	Leibovitz's L-15, 10% FBS
MDA-MB-468	Leibovitz's L-15, 10% FBS
SK-BR-3	McCoy's 5A, 10% FBS
T47D	RPMI-1640, 0.2 U/mL bovine insulin, 10% FBS
UACC-893	Leibovitz's L-15, 10% FBS
ZR-75-1	RPMI-1640, 10% FBS
ZR-75-30	RPMI 1640, 10% FBS

Table 4-2. Ovarian Cancer Cell Lines and Media. Fetal bovine serum (FBS), non-essential amino acid (NEAA).

Caov-3	DMEM, 10% FBS
Caov-4	Leibovitz's L-15, 20% FBS
ES-2	McCoy's 5A, 10% FBS
IGR-OV1	RPMI-1640, 10% FBS
NCI-ADR-RES	RPMI-1640, 10% FBS
OV-90	1:1 mix of MCDB 105 1.5 g/L sodium bicarbonate and Medium 199 2.2 g/L sodium bicarbonate, 15% FBS
OVCAR-3	RPMI-1640, 20% FBS, 0.01 mg/mL bovine insulin
OVCAR-4	RPMI-1640, 10% FBS
OVCAR-5	RPMI-1640, 10% FBS
OVCAR-8	RPMI-1640, 10% FBS
PEO1	DMEM, 10% FBS
PEO4	DMEM, 10% FBS
SKOV3	McCoy's 5A, 10% FBS
SW626	Leibovitz's L-15, 10% FBS
TOV-21G	1:1 mix of MCDB 105 1.5 g/L sodium bicarbonate and Medium 199 2.2 g/L sodium bicarbonate, 15% FBS
UWB1.289	1:1 mix of RPMI-1640, MEGM and SingleQuot additives, 3% FBS
KURAMOCHI	RPMI-1640, 10% FBS
OVMANA	RPMI-1640, 10% FBS
JHOS-2	1:1 mix of DMEM and Ham-F12, 10% FBS, 0.1 mM NEAA

Table 4-3. Colorectal Cancer Cell Lines and Media. Fetal bovine serum (FBS).

HCT-116	McCoy's 5A, 10% FBS
HCT-15	RPMI-1640, 10% FBS
HT29	McCoy's 5A, 10% FBS
LoVo	F-12K, 10% FBS
LS 180	Eagle's Minimum Essential Medium, 10% FBS
LS1034	RPMI-1640, 10% FBS
LS123	Eagle's Minimum Essential Medium, 10% FBS
RKO	Eagle's Minimum Essential Medium, 10% FBS
SK-CO-1	Eagle's Minimum Essential Medium, 10% FBS
SW1116	Leibovitz's L-15, 10% FBS
SW1417	Leibovitz's L-15, 10% FBS
SW48	Leibovitz's L-15, 10% FBS
SW480	Leibovitz's L-15, 10% FBS
SW837	Leibovitz's L-15, 10% FBS
SW948	Leibovitz's L-15, 10% FBS
T84	DMEM-F12, 5% FBS

Table 4-4. Lung Cancer Cell Lines and Media. Fetal bovine serum (FBS).

EKVX	RPMI-1640, 10% FBS
HOP-62	RPMI-1640, 10% FBS
HOP-92	RPMI-1640, 10% FBS
NCI-522	RPMI-1640, 10% FBS
NCI-H1299	RPMI 1640, 10% FBS
NCI-H1437	RPMI 1640, 10% FBS
NCI-H1563	RPMI 1640, 10% FBS
NCI-H1975	RPMI 1640, 10% FBS
NCI-H226	RPMI-1640, 10% FBS
NCI-H23	RPMI-1640, 10% FBS
NCI-H322M	RPMI-1640, 10% FBS
NCI-H460	RPMI-1640, 10% FBS
NCI-H661	RPMI 1640, 10% FBS

CHAPTER 5

SUMMARY AND DISCUSSION

5-A. Identifying synthetic lethal targets as a therapeutic approach in cancer.

The introduction of the first synthetic lethal drug (the PARP inhibitor olaparib in ovarian cancers with *BRCA1* or *BRCA2* mutations) has increased interest in applying SL to the development of cancer therapeutics. This approach is particularly useful in targeting cells that have lost a tumor suppressor gene, such as *BRCA1* or *BRCA2*, and that may have gained an increased dependence on other genes.

PARP inhibitors established using SL as a therapeutic approach, but clinical challenges, such as limited improvements in overall survival and drug resistance, remain unresolved. Our studies aimed to find other SL targets for *BRCA1* and *BRCA2*.

Many tools are available for identifying SL gene targets, including screens using CRISPR-Cas9, shRNA, and small molecule inhibitor libraries. Another approach is to use the knowledge gained from yeast genetics, in which extensive screens have already been performed to map SL networks. The Kolodner Lab's expertise in yeast genetics guided us to use this last approach.

5-B. *RAD27/ FEN1* is a SL target for genome instability suppressor (GIS) genes, including HR genes.

The Kolodner Lab has identified 266 GIS genes in *S. cerevisiae*, which include genes that encode proteins that act in or that function in DNA replication, checkpoints, and recombination and which are often conserved in humans, and then documented their SL interactions. Analysis of this data showed that *RAD27* (human *FEN1*) had the greatest number of SL interactions with GIS genes, including the HR genes *RAD52* and *RAD55-RAD57* (that encode proteins that are to some extent functionally equivalent to BRCA2).

5-C. FEN1 is a SL target for killing *BRCA1/ BRCA2*-deficient cancer cells.

To determine whether the SL interactions identified in yeast are conserved in humans, we treated *BRCA1/ BRCA2*-defective cell lines with a FEN1 inhibitor C8, the most potent of four compounds tested, and measured their clonogenic survival responses.

Initial experiments using two ovarian cancer cell lines derived from the same patient, *BRCA2*-deficient PEO1 and *BRCA2*-proficient PEO4, the latter which carries a secondary mutation that restored BRCA2 function, showed that PEO1 cells are more sensitive to killing by C8. Additionally, cell proliferation assays showed that, in contrast to PEO4 cells, PEO1 cells do not recover from drug treatment; C8 induces irreversible damage in PEO1 cells that leads to cell death over a period of up to 9 days.

In addition, matched cell line pairs, the RPE *BRCA1*-null or WT retina cell lines and the DLD1 *BRCA2*-null or proficient colorectal cancer cell lines, showed that the *BRCA*-deficient derivatives are more sensitive to killing by C8 than the parental cell lines. These results increased the confidence that hypersensitivity to C8 was due to *BRCA1* or *BRCA2* mutation status, rather than another property of the cell lines.

Larger panels of human breast, ovarian, colorectal, and lung cancer cell lines showed there was a range of responses to C8. Many cell lines that were sensitive to killing by C8 had mutations in *BRCA1* or *BRCA2*, including the olaparib-resistant *BRCA1*-mutant cell line HCC1937. But *BRCA* mutation status was not entirely predictive of sensitivity. Cell lines with *BRCA* mutations without sensitivity to C8 may contain mutations that do not significantly affect HR activity; consistent with this, some of these cell lines contain heterozygous *BRCA1* or *BRCA2* missense mutations of unknown functional significance. On the other hand, cell lines without BRCA mutations with sensitivity to C8 may contain

90

mutations in other SL gene targets, as predicted by the spectrum of genetic alterations SL with *RAD27*. Alterations may include various genetic or epigenetic defects affecting HR or other DNA metabolism pathways that are required in the absence of normal FEN1 activity. Cell lines without *BRCA* mutation that are C8-sensitive include the olaparib sensitive HCC1806 and the olaparib resistant MDA-MB-468 (186).

An orthogonal approach, using FEN1 knockdown by siRNAs, showed that in a subset of 6 *BRCA*-deficient and *BRCA*-proficient cancer cell lines tested, FEN1 siRNAs differentially reduced viability, clonogenic survival, and colony size in *BRCA*-deficient cells vs. *BRCA*-proficient cells. The effect of siFEN1 on clonogenic survival was also more significant than on short-term cell viability, suggesting that many of the siFEN1 treated *BRCA*-deficient cells that were viable at 3 days either died over time or could not undergo additional cell divisions; siFEN1-treated *BRCA*-deficient cells also do not recover.

Experiments with the FEN1 inhibitor C8 and with FEN1 siRNAs showed that FEN1 is a SL target for killing *BRCA1* or *BRCA2*-deficient cells. In addition, both C8-treated and siFEN1-treated *BRCA*-deficient cells do not recover from FEN1 inhibition or depletion. The range of sensitivities to C8 in the large panel of cancer cell lines highlight other defects besides mutations in *BRCA1* and *BRCA2* that increase killing by FEN1 inhibitors. Lastly, cell lines that are resistant to PARP inhibitors but sensitive to C8 suggest that PARP inhibitor resistance mechanisms do not necessarily cause resistance to C8.

5-D. FEN1 inhibition induces toxic replication intermediates that require HR to resolve.

FEN1 catalyzes the removal of ssDNA flaps on replication intermediates, preventing unrepaired flaps from being converted into DSB by nucleases and/ or stalling

replication forks. Our data shows that FEN1 inhibition by C8 leads to DSB accumulation in both *BRCA*-proficient and *BRCA*-deficient cells. But specifically, in *BRCA*-deficient cells, C8 leads to strong, irreversible defects on cell cycle progression, increased chromosome breaks, and increased cell death. These data suggest that defects in HR-related genes and inhibition of the compensatory process carried out by FEN1, leads to high levels of DNA damage, cell cycle arrest, and cell death.

FACS data of *BRCA*-defective or C8-sensitive cells showed that C8 decreases DNA synthesis and increases sub-G1 DNA content, whereas *BRCA*-proficient or C8-resistant cells showed little change in cell cycle distribution when treated with C8. Importantly, this strong defect on cell cycle progression in *BRCA*-deficient cells is irreversible; specifically, PEO1 cells do not recover the ability to incorporate BrdU, even after drug removal, and exit the cell cycle, in contrast to PEO4 cells that continued to incorporate BrdU at each time point.

These replication defects were associated with increased levels of DNA damage, including DSB, in both *BRCA*-proficient PEO4 and *BRCA*-deficient PEO1 cells, as shown by the DNA damage markers histone γH2AX and 53BP1. PEO1 cells, though, had more pronounced levels of these DNA damage markers.

In *BRCA*-deficient cells, changes in S and subG1 cell cycle distributions resulting from C8 treatment and release are also accompanied by decreases in G2/M cells, suggesting potential defects in mitotic entry. C8 treatment decreases mitotic entry but did so in both C8-hypersensitive and non-hypersensitive cell lines, based on time lapse imaging of H2B-mRFP tagged cells. Although C8 does not differentially affect mitotic entry in C8-hypersensitive vs. non-hypersensitive cells, we found that C8 leads to higher levels

92

of chromosome breakage during mitosis in *BRCA*-deficient cells than *BRCA*-proficient cells, as shown by metaphase spread assays.

Consistent with previous data, C8 activated the DDR, which is regulated by the PIKKs: ATM, ATR, and DNA-PK. C8 activated all 3 PIKKs in both PEO1 and PEO4 cells, as seen by increased γH2AX levels that were reduced with combinations of PIKK inhibitors. There was, however, differential phosphorylation of Chk1 and Chk2 between the cell lines. Increased phosphorylation of Chk1 through ATR in C8-treated PEO1 cells suggests that stalled replication forks might have been present, whereas the lack of phospho-Chk2 may suggest that cells with high levels of DSB did not survive. Increased phosphorylation of Chk2 through ATM and DNA-PK in C8-treated PEO4 cells suggest that DSBs are recognized and repair pathways activated.

The differential activation of checkpoint pathways in PEO1 and PEO4 cells require further investigation to determine whether stalled replication forks are present in C8-treated *BRCA*-proficient or *BRCA*-deficient cells, play a role in sensitivity to C8, and require activation of replication fork protection pathways in addition to HR to resolve.

FEN1 inhibition leads to an accumulation of flaps on lagging strands during DNA replication, which in combination with nucleolytic cleavage on the template strand, can lead to potentially lethal DSBs in both *BRCA*-proficient and *BRCA*-deficient cells. In a *BRCA*-proficient background, DSBs can be repaired by HR and cells survive. But in a *BRCA*-deficient background, C8-induced DSBs are not repaired. These cells cannot complete replication and enter mitosis with damaged DNA. As the cells accumulate DNA damage with one or more cell cycles and undergo one or more defective mitoses characterized by shattered chromosomes, they die by mitotic catastrophe.

5-E. Therapeutic potential of FEN1 inhibitors.

These results suggest that FEN1 inhibitors are potentially valuable for the treatment of cancers with defects in HR and possibly other repair and checkpoint pathways. The compounds used in our studies are unlikely to translate into the clinic due to insufficient potency and low stability because they are likely a target for glucuronidation. Efforts to develop more potent, longer half-life inhibitors are needed and are ongoing.

Studies using cancer and non-cancer cell lines showed differential responses to C8: cells that can recover from FEN1 inhibition and cells such as *BRCA1* and *BRCA2* mutants that cannot recover. To mitigate toxicity from FEN1 inhibitors, though, cycles of drug treatment and recovery may be a useful approach.

Lastly, the C8-sensitive, olaparib-resistant cell lines used in our studies suggest that FEN1 inhibitors can be used to treat cancer cells that have acquired some kinds of resistance to PARP inhibitors or used in combination with PARPi. Mechanisms of resistance to PARPi include secondary mutations that restore the wildtype function of HR proteins such as BRCA1/2, loss of 53BP1 that shifts the balance of repair from NHEJ to HR, over-expression of drug efflux transporters, and PARP1 mutations that decrease PARPi binding and/ or trapping. While FEN1 inhibitors will not likely kill cells that become resistant to PARPi due to genetic or epigenetic alterations that restore HR or increase HR activity, they may be able to target cells harboring different PARPi resistance pathways.

REFERENCES

1.   Hall JM, Lee MK, Newman B, Morrow JE, Anderson LA, Huey B, King MC. Linkage of early-onset familial breast cancer to chromosome 17q21. Science. 1990;250(4988):1684-9. PubMed PMID: 2270482.

2.   Miki Y, Swensen J, Shattuck-Eidens D, Futreal PA, Harshman K, Tavtigian S, Liu Q, Cochran C, Bennett LM, Ding W, et al. A strong candidate for the breast and ovarian cancer susceptibility gene BRCA1. Science. 1994;266(5182):66-71. PubMed PMID: 7545954.

3.   Venkitaraman AR. Cancer suppression by the chromosome custodians, BRCA1 and BRCA2. Science. 2014;343(6178):1470-5. doi: 10.1126/science.1252230. PubMed PMID: 24675954.

4.   Huen MS, Sy SM, Chen J. BRCA1 and its toolbox for the maintenance of genome integrity. Nat Rev Mol Cell Biol. 2010;11(2):138-48. Epub 2009/12/24. doi: 10.1038/nrm2831. PubMed PMID: 20029420; PMCID: PMC3899800.

5.   Deng CX, Brodie SG. Roles of BRCA1 and its interacting proteins. Bioessays. 2000;22(8):728-37. Epub 2000/08/05. doi: 10.1002/1521-1878(200008)22:8<728::AID-BIES6>3.0.CO;2-B. PubMed PMID: 10918303.

6.   Roy R, Chun J, Powell SN. BRCA1 and BRCA2: different roles in a common pathway of genome protection. Nat Rev Cancer. 2012;12(1):68-78. doi: 10.1038/nrc3181. PubMed PMID: 22193408.

7.   Wu LC, Wang ZW, Tsan JT, Spillman MA, Phung A, Xu XL, Yang MC, Hwang LY, Bowcock AM, Baer R. Identification of a RING protein that can interact in vivo with the BRCA1 gene product. Nat Genet. 1996;14(4):430-40. doi: 10.1038/ng1296-430. PubMed PMID: 8944023.

8.   Trauernicht AM, Boyer TG. BRCA1 and estrogen signaling in breast cancer. Breast Dis. 2003;18:11-20. Epub 2005/02/03. doi: 10.3233/bd-2003-18103. PubMed PMID: 15687685.

9.   Mallery DL, Vandenberg CJ, Hiom K. Activation of the E3 ligase function of the BRCA1/BARD1 complex by polyubiquitin chains. EMBO J. 2002;21(24):6755-62. Epub 2002/12/18. doi: 10.1093/emboj/cdf691. PubMed PMID: 12485996; PMCID: PMC139111.

10.   Eakin CM, Maccoss MJ, Finney GL, Klevit RE. Estrogen receptor alpha is a putative substrate for the BRCA1 ubiquitin ligase. Proc Natl Acad Sci U S A. 2007;104(14):5794-9. doi: 10.1073/pnas.0610887104. PubMed PMID: 17392432; PMCID: PMC1851571.

11.   Dizin E, Irminger-Finger I. Negative feedback loop of BRCA1-BARD1 ubiquitin ligase on estrogen receptor alpha stability and activity antagonized by cancer-associated isoform of BARD1. Int J Biochem Cell Biol. 2010;42(5):693-700. Epub 2010/01/12. doi: 10.1016/j.biocel.2009.12.025. PubMed PMID: 20060929.

12.   Zhang J, Willers H, Feng Z, Ghosh JC, Kim S, Weaver DT, Chung JH, Powell SN, Xia F. Chk2 phosphorylation of BRCA1 regulates DNA double-strand break repair. Mol Cell Biol. 2004;24(2):708-18. Epub 2004/01/01. doi: 10.1128/mcb.24.2.708-718.2004. PubMed PMID: 14701743; PMCID: PMC343805.

13.   Cortez D, Wang Y, Qin J, Elledge SJ. Requirement of ATM-dependent phosphorylation of brca1 in the DNA damage response to double-strand breaks. Science. 1999;286(5442):1162-6. Epub 1999/11/05. doi: 10.1126/science.286.5442.1162. PubMed PMID: 10550055.

14.   Xu B, O'Donnell AH, Kim ST, Kastan MB. Phosphorylation of serine 1387 in Brca1 is specifically required for the Atm-mediated S-phase checkpoint after ionizing irradiation. Cancer Res. 2002;62(16):4588-91. Epub 2002/08/17. PubMed PMID: 12183412.

15.   Zhang F, Fan Q, Ren K, Andreassen PR. PALB2 functionally connects the breast cancer susceptibility proteins BRCA1 and BRCA2. Mol Cancer Res. 2009;7(7):1110-8. doi: 10.1158/1541-7786.MCR-09-0123. PubMed PMID: 19584259; PMCID: PMC4928587.

16.   Zhang F, Ma J, Wu J, Ye L, Cai H, Xia B, Yu X. PALB2 links BRCA1 and BRCA2 in the DNA-damage response. Curr Biol. 2009;19(6):524-9. doi: 10.1016/j.cub.2009.02.018. PubMed PMID: 19268590; PMCID: PMC2750839.

17.   Mohammad DH, Yaffe MB. 14-3-3 proteins, FHA domains and BRCT domains in the DNA damage response. DNA Repair (Amst). 2009;8(9):1009-17. Epub 2009/06/02. doi: 10.1016/j.dnarep.2009.04.004. PubMed PMID: 19481982; PMCID: PMC3263375.

18.   Wang B, Matsuoka S, Ballif BA, Zhang D, Smogorzewska A, Gygi SP, Elledge SJ. Abraxas and RAP80 form a BRCA1 protein complex required for the DNA damage response. Science. 2007;316(5828):1194-8. doi: 10.1126/science.1139476. PubMed PMID: 17525340; PMCID: PMC3573690.

19.   Kim H, Chen J, Yu X. Ubiquitin-binding protein RAP80 mediates BRCA1-dependent DNA damage response. Science. 2007;316(5828):1202-5. doi: 10.1126/science.1139621. PubMed PMID: 17525342.

20.   Liu Z, Wu J, Yu X. CCDC98 targets BRCA1 to DNA damage sites. Nat Struct Mol Biol. 2007;14(8):716-20. Epub 2007/07/24. doi: 10.1038/nsmb1279. PubMed PMID: 17643121.

21.   Sobhian B, Shao G, Lilli DR, Culhane AC, Moreau LA, Xia B, Livingston DM, Greenberg RA. RAP80 targets BRCA1 to specific ubiquitin structures at DNA damage sites. Science. 2007;316(5828):1198-202. Epub 2007/05/26. doi: 10.1126/science.1139516. PubMed PMID: 17525341; PMCID: PMC2706583.

22.   Cantor SB, Bell DW, Ganesan S, Kass EM, Drapkin R, Grossman S, Wahrer DC, Sgroi DC, Lane WS, Haber DA, Livingston DM. BACH1, a novel helicase-like protein, interacts directly with BRCA1 and contributes to its DNA repair function. Cell. 2001;105(1):149-60. Epub 2001/04/13. doi: 10.1016/s0092-8674(01)00304-x. PubMed PMID: 11301010.

23.   Litman R, Peng M, Jin Z, Zhang F, Zhang JR, Powell S, Andreassen PR, Cantor SB. BACH1 is critical for homologous recombination and appears to be the Fanconi anemia gene product FANCJ. Cancer Cell. 2005;8(3):255-65. doi: 10.1016/j.ccr.2005.08.004. PubMed PMID: WOS:000232199900011.

24.   Yu X, Wu LC, Bowcock AM, Aronheim A, Baer R. The C-terminal (BRCT) domains of BRCA1 interact in vivo with CtIP, a protein implicated in the CtBP pathway of transcriptional repression. J Biol Chem. 1998;273(39):25388-92. Epub 1998/09/17. doi: 10.1074/jbc.273.39.25388. PubMed PMID: 9738006.

25.   Yun MH, Hiom K. CtIP-BRCA1 modulates the choice of DNA double-strand-break repair pathway throughout the cell cycle. Nature. 2009;459(7245):460-3. doi: 10.1038/nature07955. PubMed PMID: 19357644; PMCID: PMC2857324.

26.   Knudson AG, Jr. Mutation and cancer: statistical study of retinoblastoma. Proc Natl Acad Sci U S A. 1971;68(4):820-3. PubMed PMID: 5279523; PMCID: PMC389051.

27.   Petrucelli N, Daly MB, Pal T. BRCA1- and BRCA2-Associated Hereditary Breast and Ovarian Cancer. In: Pagon RA, Adam MP, Ardinger HH, Wallace SE, Amemiya A, Bean LJH, Bird TD, Ledbetter N, Mefford HC, Smith RJH, Stephens K, editors. GeneReviews(R). Seattle (WA)1993.

28.   Friedman LS, Ostermeyer EA, Szabo CI, Dowd P, Lynch ED, Rowell SE, King MC. Confirmation of BRCA1 by analysis of germline mutations linked to breast and ovarian cancer in ten families. Nat Genet. 1994;8(4):399-404. doi: 10.1038/ng1294-399. PubMed PMID: 7894493.

29.   Couch FJ, Weber BL. Mutations and polymorphisms in the familial early-onset breast cancer (BRCA1) gene. Breast Cancer Information Core. Hum Mutat. 1996;8(1):8-18. Epub 1996/01/01. doi: 10.1002/humu.1380080102. PubMed PMID: 8807330.

30.   Shattuck-Eidens D, McClure M, Simard J, Labrie F, Narod S, Couch F, Hoskins K, Weber B, Castilla L, Erdos M, et al. A collaborative survey of 80 mutations in the BRCA1 breast and ovarian cancer susceptibility gene. Implications for presymptomatic testing and screening. JAMA. 1995;273(7):535-41. Epub 1995/02/15. PubMed PMID: 7837387.

31.   Brzovic PS, Meza JE, King MC, Klevit RE. BRCA1 RING domain cancer-predisposing mutations. Structural consequences and effects on protein-protein interactions. J Biol Chem. 2001;276(44):41399-406. Epub 2001/08/30. doi: 10.1074/jbc.M106551200. PubMed PMID: 11526114.

32.   Hashizume R, Fukuda M, Maeda I, Nishikawa H, Oyake D, Yabuki Y, Ogata H, Ohta T. The RING heterodimer BRCA1-BARD1 is a ubiquitin ligase inactivated by a breast cancer-derived mutation. J Biol Chem. 2001;276(18):14537-40. Epub 2001/03/30. doi: 10.1074/jbc.C000881200. PubMed PMID: 11278247.

33.   Ruffner H, Joazeiro CA, Hemmati D, Hunter T, Verma IM. Cancer-predisposing mutations within the RING domain of BRCA1: loss of ubiquitin protein ligase activity and protection from radiation hypersensitivity. Proc Natl Acad Sci U S A. 2001;98(9):5134-9. Epub 2001/04/26. doi: 10.1073/pnas.081068398. PubMed PMID: 11320250; PMCID: PMC33176.

34.   Vallon-Christersson J, Cayanan C, Haraldsson K, Loman N, Bergthorsson JT, Brondum-Nielsen K, Gerdes AM, Moller P, Kristoffersson U, Olsson H, Borg A, Monteiro AN. Functional analysis of BRCA1 C-terminal missense mutations identified in breast and ovarian cancer families. Hum Mol Genet. 2001;10(4):353-60. Epub 2001/02/07. doi: 10.1093/hmg/10.4.353. PubMed PMID: 11157798; PMCID: PMC4756649.

35.   Williams RS, Chasman DI, Hau DD, Hui B, Lau AY, Glover JN. Detection of protein folding defects caused by BRCA1-BRCT truncation and missense mutations. J Biol Chem. 2003;278(52):53007-16. Epub 2003/10/10. doi: 10.1074/jbc.M310182200. PubMed PMID: 14534301.

36. Easton DF, Bishop DT, Ford D, Crockford GP. Genetic linkage analysis in familial breast and ovarian cancer: results from 214 families. The Breast Cancer Linkage Consortium. Am J Hum Genet. 1993;52(4):678-701. PubMed PMID: 8460634; PMCID: PMC1682082.

37. Wooster R, Bignell G, Lancaster J, Swift S, Seal S, Mangion J, Collins N, Gregory S, Gumbs C, Micklem G. Identification of the breast cancer susceptibility gene BRCA2. Nature. 1995;378(6559):789-92. doi: 10.1038/378789a0. PubMed PMID: 8524414.

38. Oliver AW, Swift S, Lord CJ, Ashworth A, Pearl LH. Structural basis for recruitment of BRCA2 by PALB2. EMBO Rep. 2009;10(9):990-6. Epub 2009/07/18. doi: 10.1038/embor.2009.126. PubMed PMID: 19609323; PMCID: PMC2750052.

39. Yuan SS, Lee SY, Chen G, Song M, Tomlinson GE, Lee EY. BRCA2 is required for ionizing radiation-induced assembly of Rad51 complex in vivo. Cancer Res. 1999;59(15):3547-51. PubMed PMID: 10446958.

40. Tarsounas M, Davies AA, West SC. RAD51 localization and activation following DNA damage. Philos Trans R Soc Lond B Biol Sci. 2004;359(1441):87-93. Epub 2004/04/07. doi: 10.1098/rstb.2003.1368. PubMed PMID: 15065660; PMCID: PMC1693300.

41. Carreira A, Hilario J, Amitani I, Baskin RJ, Shivji MK, Venkitaraman AR, Kowalczykowski SC. The BRC repeats of BRCA2 modulate the DNA-binding selectivity of RAD51. Cell. 2009;136(6):1032-43. doi: 10.1016/j.cell.2009.02.019. PubMed PMID: 19303847; PMCID: PMC2669112.

42. Thorslund T, McIlwraith MJ, Compton SA, Lekomtsev S, Petronczki M, Griffith JD, West SC. The breast cancer tumor suppressor BRCA2 promotes the specific targeting of RAD51 to single-stranded DNA. Nat Struct Mol Biol. 2010;17(10):1263-5. doi: 10.1038/nsmb.1905. PubMed PMID: 20729858; PMCID: PMC4041013.

43. Yang H, Jeffrey PD, Miller J, Kinnucan E, Sun Y, Thoma NH, Zheng N, Chen PL, Lee WH, Pavletich NP. BRCA2 function in DNA binding and recombination from a BRCA2-DSS1-ssDNA structure. Science. 2002;297(5588):1837-48. doi: 10.1126/science.297.5588.1837. PubMed PMID: 12228710.

44. Yang H, Li Q, Fan J, Holloman WK, Pavletich NP. The BRCA2 homologue Brh2 nucleates RAD51 filament formation at a dsDNA-ssDNA junction. Nature. 2005;433(7026):653-7. doi: 10.1038/nature03234. PubMed PMID: 15703751.

45.   Saeki H, Siaud N, Christ N, Wiegant WW, van Buul PP, Han M, Zdzienicka MZ, Stark JM, Jasin M. Suppression of the DNA repair defects of BRCA2-deficient cells with heterologous protein fusions. Proc Natl Acad Sci U S A. 2006;103(23):8768-73. Epub 2006/05/30. doi: 10.1073/pnas.0600298103. PubMed PMID: 16731627; PMCID: PMC1482653.

46.   Esashi F, Christ N, Gannon J, Liu Y, Hunt T, Jasin M, West SC. CDK-dependent phosphorylation of BRCA2 as a regulatory mechanism for recombinational repair. Nature. 2005;434(7033):598-604. Epub 2005/04/01. doi: 10.1038/nature03404. PubMed PMID: 15800615.

47.   Venkitaraman AR. Linking the cellular functions of BRCA genes to cancer pathogenesis and treatment. Annu Rev Pathol. 2009;4:461-87. doi: 10.1146/annurev.pathol.3.121806.151422. PubMed PMID: 18954285.

48.   Rebbeck TR, Mitra N, Wan F, Sinilnikova OM, Healey S, McGuffog L, Mazoyer S, Chenevix-Trench G, Easton DF, Antoniou AC, Nathanson KL, Consortium C, Laitman Y, Kushnir A, Paluch-Shimon S, Berger R, Zidan J, Friedman E, Ehrencrona H, Stenmark-Askmalm M, Einbeigi Z, Loman N, Harbst K, Rantala J, Melin B, Huo D, Olopade OI, Seldon J, Ganz PA, Nussbaum RL, Chan SB, Odunsi K, Gayther SA, Domchek SM, Arun BK, Lu KH, Mitchell G, Karlan BY, Walsh C, Lester J, Godwin AK, Pathak H, Ross E, Daly MB, Whittemore AS, John EM, Miron A, Terry MB, Chung WK, Goldgar DE, Buys SS, Janavicius R, Tihomirova L, Tung N, Dorfling CM, van Rensburg EJ, Steele L, Neuhausen SL, Ding YC, Ejlertsen B, Gerdes AM, Hansen T, Ramon y Cajal T, Osorio A, Benitez J, Godino J, Tejada MI, Duran M, Weitzel JN, Bobolis KA, Sand SR, Fontaine A, Savarese A, Pasini B, Peissel B, Bonanni B, Zaffaroni D, Vignolo-Lutati F, Scuvera G, Giannini G, Bernard L, Genuardi M, Radice P, Dolcetti R, Manoukian S, Pensotti V, Gismondi V, Yannoukakos D, Fostira F, Garber J, Torres D, Rashid MU, Hamann U, Peock S, Frost D, Platte R, Evans DG, Eeles R, Davidson R, Eccles D, Cole T, Cook J, Brewer C, Hodgson S, Morrison PJ, Walker L, Porteous ME, Kennedy MJ, Izatt L, Adlard J, Donaldson A, Ellis S, Sharma P, Schmutzler RK, Wappenschmidt B, Becker A, Rhiem K, Hahnen E, Engel C, Meindl A, Engert S, Ditsch N, Arnold N, Plendl HJ, Mundhenke C, Niederacher D, Fleisch M, Sutter C, Bartram CR, Dikow N, Wang-Gohrke S, Gadzicki D, Steinemann D, Kast K, Beer M, Varon-Mateeva R, Gehrig A, Weber BH, Stoppa-Lyonnet D, Sinilnikova OM, Mazoyer S, Houdayer C, Belotti M, Gauthier-Villars M, Damiola F, Boutry-Kryza N, Lasset C, Sobol H, Peyrat JP, Muller D, Fricker JP, Collonge-Rame MA, Mortemousque I, Nogues C, Rouleau E, Isaacs C, De Paepe A, Poppe B, Claes K, De Leeneer K, Piedmonte M, Rodriguez G, Wakely K, Boggess J, Blank SV, Basil J, Azodi M, Phillips KA, Caldes T, de la Hoya M, Romero A, Nevanlinna H, Aittomaki K, van der Hout AH, Hogervorst FB, Verhoef S, Collee JM, Seynaeve C, Oosterwijk JC, Gille JJ, Wijnen JT, Gomez Garcia EB, Kets CM, Ausems MG, Aalfs CM, Devilee P, Mensenkamp AR, Kwong A, Olah E, Papp J, Diez O, Lazaro C, Darder E, Blanco I, Salinas M, Jakubowska A, Lubinski J, Gronwald J, Jaworska-Bieniek K, Durda K, Sukiennicki G, Huzarski T, Byrski T, Cybulski C, Toloczko-Grabarek A, Zlowocka-Perlowska E,

Menkiszak J, Arason A, Barkardottir RB, Simard J, Laframboise R, Montagna M, Agata S, Alducci E, Peixoto A, Teixeira MR, Spurdle AB, Lee MH, Park SK, Kim SW, Friebel TM, Couch FJ, Lindor NM, Pankratz VS, Guidugli L, Wang X, Tischkowitz M, Foretova L, Vijai J, Offit K, Robson M, Rau-Murthy R, Kauff N, Fink-Retter A, Singer CF, Rappaport C, Gschwantler-Kaulich D, Pfeiler G, Tea MK, Berger A, Greene MH, Mai PL, Imyanitov EN, Toland AE, Senter L, Bojesen A, Pedersen IS, Skytte AB, Sunde L, Thomassen M, Moeller ST, Kruse TA, Jensen UB, Caligo MA, Aretini P, Teo SH, Selkirk CG, Hulick PJ, Andrulis I. Association of type and location of BRCA1 and BRCA2 mutations with risk of breast and ovarian cancer. JAMA. 2015;313(13):1347-61. doi: 10.1001/jama.2014.5985. PubMed PMID: 25849179; PMCID: PMC4537700.

49.   Guidugli L, Carreira A, Caputo SM, Ehlen A, Galli A, Monteiro AN, Neuhausen SL, Hansen TV, Couch FJ, Vreeswijk MP, consortium E. Functional assays for analysis of variants of uncertain significance in BRCA2. Hum Mutat. 2014;35(2):151-64. Epub 2013/12/11. doi: 10.1002/humu.22478. PubMed PMID: 24323938; PMCID: PMC3995136.

50.   Evers B, Jonkers J. Mouse models of BRCA1 and BRCA2 deficiency: past lessons, current understanding and future prospects. Oncogene. 2006;25(43):5885-97. doi: 10.1038/sj.onc.1209871. PubMed PMID: 16998503.

51.   Deng CX, Scott F. Role of the tumor suppressor gene Brca1 in genetic stability and mammary gland tumor formation. Oncogene. 2000;19(8):1059-64. doi: 10.1038/sj.onc.1203269. PubMed PMID: 10713690.

52.   Tsuzuki T, Fujii Y, Sakumi K, Tominaga Y, Nakao K, Sekiguchi M, Matsushiro A, Yoshimura Y, MoritaT. Targeted disruption of the Rad51 gene leads to lethality in embryonic mice. Proc Natl Acad Sci U S A. 1996;93(13):6236-40. PubMed PMID: 8692798; PMCID: PMC39005.

53.   Lim DS, Hasty P. A mutation in mouse rad51 results in an early embryonic lethal that is suppressed by a mutation in p53. Mol Cell Biol. 1996;16(12):7133-43. PubMed PMID: 8943369; PMCID: PMC231717.

54.   San Filippo J, Sung P, Klein H. Mechanism of eukaryotic homologous recombination. Annu Rev Biochem. 2008;77:229-57. doi: 10.1146/annurev.biochem.77.061306.125255. PubMed PMID: 18275380.

55.   Lord CJ, Ashworth A. BRCAness revisited. Nat Rev Cancer. 2016;16(2):110-20. doi: 10.1038/nrc.2015.21. PubMed PMID: 26775620.

56.   Sugiyama T, Zaitseva EM, Kowalczykowski SC. A single-stranded DNA-binding protein is needed for efficient presynaptic complex formation by the Saccharomyces cerevisiae Rad51 protein. J Biol Chem. 1997;272(12):7940-5. PubMed PMID: 9065463.

57.   Eggler AL, Inman RB, Cox MM. The Rad51-dependent pairing of long DNA substrates is stabilized by replication protein A. J Biol Chem. 2002;277(42):39280-8. doi: 10.1074/jbc.M204328200. PubMed PMID: 12169690.

58.   Sigurdsson S, Van Komen S, Petukhova G, Sung P. Homologous DNA pairing by human recombination factors Rad51 and Rad54. J Biol Chem. 2002;277(45):42790-4. doi: 10.1074/jbc.M208004200. PubMed PMID: 12205100.

59.   Sung P. Function of yeast Rad52 protein as a mediator between replication protein A and the Rad51 recombinase. J Biol Chem. 1997;272(45):28194-7. PubMed PMID: 9353267.

60.   Shinohara A, Ogawa T. Stimulation by Rad52 of yeast Rad51-mediated recombination. Nature. 1998;391(6665):404-7. doi: 10.1038/34943. PubMed PMID: 9450759.

61.   Kim H, Huang J, Chen J. CCDC98 is a BRCA1-BRCT domain-binding protein involved in the DNA damage response. Nat Struct Mol Biol. 2007;14(8):710-5. doi: 10.1038/nsmb1277. PubMed PMID: 17643122.

62.   Chen L, Nievera CJ, Lee AY, Wu X. Cell cycle-dependent complex formation of BRCA1.CtIP.MRN is important for DNA double-strand break repair. J Biol Chem. 2008;283(12):7713-20. Epub 2008/01/04. doi: 10.1074/jbc.M710245200. PubMed PMID: 18171670.

63.   Sy SM, Huen MS, Chen J. PALB2 is an integral component of the BRCA complex required for homologous recombination repair. Proc Natl Acad Sci U S A. 2009;106(17):7155-60. doi: 10.1073/pnas.0811159106. PubMed PMID: 19369211; PMCID: PMC2678481.

64.   Xia B, Sheng Q, Nakanishi K, Ohashi A, Wu J, Christ N, Liu X, Jasin M, Couch FJ, Livingston DM. Control of BRCA2 cellular and clinical functions by a nuclear partner, PALB2. Mol Cell. 2006;22(6):719-29. doi: 10.1016/j.molcel.2006.05.022. PubMed PMID: 16793542.

65.   San Filippo J, Chi P, Sehorn MG, Etchin J, Krejci L, Sung P. Recombination mediator and Rad51 targeting activities of a human BRCA2 polypeptide. J Biol Chem. 2006;281(17):11649-57. doi: 10.1074/jbc.M601249200. PubMed PMID: 16513631; PMCID: PMC2077811.

66.   Jasin M. Homologous repair of DNA damage and tumorigenesis: the BRCA connection. Oncogene. 2002;21(58):8981-93. doi: 10.1038/sj.onc.1206176. PubMed PMID: 12483514.

67.   Chen PL, Chen CF, Chen Y, Xiao J, Sharp ZD, Lee WH. The BRC repeats in BRCA2 are critical for RAD51 binding and resistance to methyl methanesulfonate treatment. Proc Natl Acad Sci U S A. 1998;95(9):5287-92. PubMed PMID: 9560268; PMCID: PMC20253.

68.   Wong AK, Pero R, Ormonde PA, Tavtigian SV, Bartel PL. RAD51 interacts with the evolutionarily conserved BRC motifs in the human breast cancer susceptibility gene brca2. J Biol Chem. 1997;272(51):31941-4. PubMed PMID: 9405383.

69.   Bork P, Blomberg N, Nilges M. Internal repeats in the BRCA2 protein sequence. Nat Genet. 1996;13(1):22-3. doi: 10.1038/ng0596-22. PubMed PMID: 8673099.

70.   Sharan SK, Morimatsu M, Albrecht U, Lim DS, Regel E, Dinh C, Sands A, Eichele G, Hasty P, Bradley A. Embryonic lethality and radiation hypersensitivity mediated by Rad51 in mice lacking Brca2. Nature. 1997;386(6627):804-10. doi: 10.1038/386804a0. PubMed PMID: 9126738.

71.   Mizuta R, LaSalle JM, Cheng HL, Shinohara A, Ogawa H, Copeland N, Jenkins NA, Lalande M, Alt FW. RAB22 and RAB163/mouse BRCA2: proteins that specifically interact with the RAD51 protein. Proc Natl Acad Sci U S A. 1997;94(13):6927-32. PubMed PMID: 9192668; PMCID: PMC21261.

72.   Xia F, Taghian DG, DeFrank JS, Zeng ZC, Willers H, Iliakis G, Powell SN. Deficiency of human BRCA2 leads to impaired homologous recombination but maintains normal nonhomologous end joining. Proc Natl Acad Sci U S A. 2001;98(15):8644-9. doi: 10.1073/pnas.151253498. PubMed PMID: 11447276; PMCID: PMC37489.

73.   Moynahan ME, Pierce AJ, Jasin M. BRCA2 is required for homology-directed repair of chromosomal breaks. Mol Cell. 2001;7(2):263-72. PubMed PMID: 11239455.

74.   Davies AA, Masson JY, McIlwraith MJ, Stasiak AZ, Stasiak A, Venkitaraman AR, West SC. Role of BRCA2 in control of the RAD51 recombination and DNA repair protein. Mol Cell. 2001;7(2):273-82. PubMed PMID: 11239456.

75.   Zeman MK, Cimprich KA. Causes and consequences of replication stress. Nat Cell Biol. 2014;16(1):2-9. Epub 2013/12/25. doi: 10.1038/ncb2897. PubMed PMID: 24366029; PMCID: PMC4354890.

76.   Mirkin EV, Mirkin SM. Replication fork stalling at natural impediments. Microbiol Mol Biol Rev. 2007;71(1):13-35. Epub 2007/03/10. doi: 10.1128/MMBR.00030-06. PubMed PMID: 17347517; PMCID: PMC1847372.

77.   Sidorova J. A game of substrates: replication fork remodeling and its roles in genome stability and chemo-resistance. Cell Stress. 2017;1(3):115-33. Epub 2018/01/23. doi: 10.15698/cst2017.12.114. PubMed PMID: 29355244; PMCID: PMC5771654.

78.   Cantor SB, Calvo JA. Fork Protection and Therapy Resistance in Hereditary Breast Cancer. Cold Spring Harb Symp Quant Biol. 2017;82:339-48. Epub 2018/02/24. doi: 10.1101/sqb.2017.82.034413. PubMed PMID: 29472318; PMCID: PMC6041132.

79.   Hashimoto Y, Chaudhuri AR, Lopes M, Costanzo V. Rad51 protects nascent DNA from Mre11-dependent degradation and promotes continuous DNA synthesis. Nature Structural & Molecular Biology. 2010;17(11):1305-U268. doi: 10.1038/nsmb.1927. PubMed PMID: WOS:000283773200006.

80.   Schlacher K, Christ N, Siaud N, Egashira A, Wu H, Jasin M. Double-strand break repair-independent role for BRCA2 in blocking stalled replication fork degradation by MRE11. Cell. 2011;145(4):529-42. doi: 10.1016/j.cell.2011.03.041. PubMed PMID: 21565612; PMCID: PMC3261725.

81.   Zadorozhny K, Sannino V, Belan O, Mlcouskova J, Spirek M, Costanzo V, Krejci L. Fanconi-Anemia-Associated Mutations Destabilize RAD51 Filaments and Impair Replication Fork Protection. Cell Rep. 2017;21(2):333-40. doi: 10.1016/j.celrep.2017.09.062. PubMed PMID: WOS:000412686100005.

82.   Chen CC, Feng WR, Lim PX, Kass EM, Jasin M. Homology-Directed Repair and the Role of BRCA1, BRCA2, and Related Proteins in Genome Integrity and Cancer. Annu Rev Canc Biol. 2018;2:313-36. doi: 10.1146/annurev-cancerbio-030617-050502. PubMed PMID: WOS:000462706100017.

83.   Dungrawala H, Cortez D. Purification of Proteins on Newly Synthesized DNA Using iPOND. Nucleus, 2nd Edition. 2015;1228:123-31. doi: 10.1007/978-1-4939-1680-1_10. PubMed PMID: WOS:000343313300011.

84.   Sirbu BM, McDonald WH, Dungrawala H, Badu-Nkansah A, Kavanaugh GM, Chen YY, Tabb DL, Cortez D. Identification of Proteins at Active, Stalled, and Collapsed Replication Forks Using Isolation of Proteins on Nascent DNA (iPOND) Coupled with Mass Spectrometry. Journal of Biological Chemistry. 2013;288(44):31458-67. doi: 10.1074/jbc.M113.511337. PubMed PMID: WOS:000330596200005.

85.   Daza-Martin M, Starowicz K, Jamshad M, Tye S, Ronson GE, MacKay HL, Chauhan AS, Walker AK, Stone HR, Beesley JFJ, Coles JL, Garvin AJ, Stewart GS, McCorvie TJ, Zhang X, Densham RM, Morris JR. Isomerization of BRCA1-BARD1 promotes replication fork protection. Nature. 2019;571(7766):521-7. Epub 2019/07/05. doi: 10.1038/s41586-019-1363-4. PubMed PMID: 31270457.

86.   Schlacher K, Wu H, Jasin M. A distinct replication fork protection pathway connects Fanconi anemia tumor suppressors to RAD51-BRCA1/2. Cancer Cell. 2012;22(1):106-16. Epub 2012/07/14. doi: 10.1016/j.ccr.2012.05.015. PubMed PMID: 22789542; PMCID: PMC3954744.

87.   BRCA1 Phosphorylation and Isomerization Enhances Replication Fork Protection. Cancer Discov. 2019;9(9):OF9. Epub 2019/07/22. doi: 10.1158/2159-8290.CD-RW2019-108. PubMed PMID: 31324612.

88.   Kolinjivadi AM, Sannino V, de Antoni A, Techer H, Baldi G, Costanzo V. Moonlighting at replication forks - a new life for homologous recombination proteins BRCA1, BRCA2 and RAD51. FEBS Lett. 2017;591(8):1083-100. Epub 2017/01/13. doi: 10.1002/1873-3468.12556. PubMed PMID: 28079255.

89.   Ying S, Hamdy FC, Helleday T. Mre11-dependent degradation of stalled DNA replication forks is prevented by BRCA2 and PARP1. Cancer Res. 2012;72(11):2814-21. Epub 2012/03/27. doi: 10.1158/0008-5472.CAN-11-3417. PubMed PMID: 22447567.

90.   McPherson JP, Hande MP, Poonepalli A, Lemmers B, Zablocki E, Migon E, Shehabeldin A, Porras A, Karaskova J, Vukovic B, Squire J, Hakem R. A role for Brca1 in chromosome end maintenance. Hum Mol Genet. 2006;15(6):831-8. Epub 2006/02/01. doi: 10.1093/hmg/ddl002. PubMed PMID: 16446310.

91.   Patel KJ, Yu VP, Lee H, Corcoran A, Thistlethwaite FC, Evans MJ, Colledge WH, Friedman LS, Ponder BA, Venkitaraman AR. Involvement of Brca2 in DNA repair. Mol

Cell. 1998;1(3):347-57. Epub 1998/07/14. doi: 10.1016/s1097-2765(00)80035-0. PubMed PMID: 9660919.

92.   Deng CX, Brodie SG. Knockout mouse models and mammary tumorigenesis. Semin Cancer Biol. 2001;11(5):387-94. Epub 2001/09/20. doi: 10.1006/scbi.2001.0394. PubMed PMID: 11562181.

93.   Farmer H, McCabe N, Lord CJ, Tutt AN, Johnson DA, Richardson TB, Santarosa M, Dillon KJ, Hickson I, Knights C, Martin NM, Jackson SP, Smith GC, Ashworth A. Targeting the DNA repair defect in BRCA mutant cells as a therapeutic strategy. Nature. 2005;434(7035):917-21. doi: 10.1038/nature03445. PubMed PMID: 15829967.

94.   Bryant HE, Schultz N, Thomas HD, Parker KM, Flower D, Lopez E, Kyle S, Meuth M, Curtin NJ, Helleday T. Specific killing of BRCA2-deficient tumours with inhibitors of poly(ADP-ribose) polymerase. Nature. 2005;434(7035):913-7. doi: 10.1038/nature03443. PubMed PMID: 15829966.

95.   de Murcia G, Menissier-de Murcia J, Schreiber V. Poly(ADP-ribose) polymerase: molecular biological aspects. Bioessays. 1991;13(9):455-62. doi: 10.1002/bies.950130905. PubMed PMID: 1796908.

96.   Althaus FR, Richter C. ADP-ribosylation of proteins. Enzymology and biological significance. Mol Biol Biochem Biophys. 1987;37:1-237. PubMed PMID: 3118181.

97.   Cleaver JE, Morgan WF. Poly(ADP-ribose)polymerase: a perplexing participant in cellular responses to DNA breakage. Mutat Res. 1991;257(1):1-18. PubMed PMID: 1898983.

98.   Yelamos J, Farres J, Llacuna L, Ampurdanes C, Martin-Caballero J. PARP-1 and PARP-2: New players in tumour development. Am J Cancer Res. 2011;1(3):328-46. Epub 2011/10/05. PubMed PMID: 21968702; PMCID: PMC3180065.

99.   Satoh MS, Lindahl T. Role of poly(ADP-ribose) formation in DNA repair. Nature. 1992;356(6367):356-8. doi: 10.1038/356356a0. PubMed PMID: 1549180.

100.   Eustermann S, Wu WF, Langelier MF, Yang JC, Easton LE, Riccio AA, Pascal JM, Neuhaus D. Structural Basis of Detection and Signaling of DNA Single-Strand Breaks by Human PARP-1. Mol Cell. 2015;60(5):742-54. doi: 10.1016/j.molcel.2015.10.032. PubMed PMID: 26626479; PMCID: PMC4678113.

101.   Krishnakumar R, Kraus WL. The PARP side of the nucleus: molecular actions, physiological outcomes, and clinical targets. Mol Cell. 2010;39(1):8-24. doi: 10.1016/j.molcel.2010.06.017. PubMed PMID: 20603072; PMCID: PMC2923840.

102.   Wang ZQ, Auer B, Stingl L, Berghammer H, Haidacher D, Schweiger M, Wagner EF. Mice lacking ADPRT and poly(ADP-ribosyl)ation develop normally but are susceptible to skin disease. Genes Dev. 1995;9(5):509-20. PubMed PMID: 7698643.

103.   de Murcia JM, Niedergang C, Trucco C, Ricoul M, Dutrillaux B, Mark M, Oliver FJ, Masson M, Dierich A, LeMeur M, Walztinger C, Chambon P, de Murcia G. Requirement of poly(ADP-ribose) polymerase in recovery from DNA damage in mice and in cells. Proc Natl Acad Sci U S A. 1997;94(14):7303-7. PubMed PMID: 9207086; PMCID: PMC23816.

104.   Rongvaux A, Andris F, Van Gool F, Leo O. Reconstructing eukaryotic NAD metabolism. Bioessays. 2003;25(7):683-90. doi: 10.1002/bies.10297. PubMed PMID: 12815723.

105.   Murai J, Huang SY, Das BB, Renaud A, Zhang Y, Doroshow JH, Ji J, Takeda S, Pommier Y. Trapping of PARP1 and PARP2 by Clinical PARP Inhibitors. Cancer Res. 2012;72(21):5588-99. doi: 10.1158/0008-5472.CAN-12-2753. PubMed PMID: 23118055; PMCID: PMC3528345.

106.   Murai J, Huang SY, Renaud A, Zhang Y, Ji J, Takeda S, Morris J, Teicher B, Doroshow JH, Pommier Y. Stereospecific PARP trapping by BMN 673 and comparison with olaparib and rucaparib. Mol Cancer Ther. 2014;13(2):433-43. doi: 10.1158/1535-7163.MCT-13-0803. PubMed PMID: 24356813; PMCID: PMC3946062.

107.   Pommier Y, O'Connor MJ, de Bono J. Laying a trap to kill cancer cells: PARP inhibitors and their mechanisms of action. Sci Transl Med. 2016;8(362):362ps17. doi: 10.1126/scitranslmed.aaf9246. PubMed PMID: 27797957.

108.   Pettitt SJ, Rehman FL, Bajrami I, Brough R, Wallberg F, Kozarewa I, Fenwick K, Assiotis I, Chen L, Campbell J, Lord CJ, Ashworth A. A genetic screen using the PiggyBac transposon in haploid cells identifies Parp1 as a mediator of olaparib toxicity. PLoS One. 2013;8(4):e61520. doi: 10.1371/journal.pone.0061520. PubMed PMID: 23634208; PMCID: PMC3636235.

109.   Shen Y, Rehman FL, Feng Y, Boshuizen J, Bajrami I, Elliott R, Wang B, Lord CJ, Post LE, Ashworth A. BMN 673, a novel and highly potent PARP1/2 inhibitor for the treatment of human cancers with DNA repair deficiency. Clin Cancer Res. 2013;19(18):5003-15. doi: 10.1158/1078-0432.CCR-13-1391. PubMed PMID: 23881923.

110. Saleh-Gohari N, Bryant HE, Schultz N, Parker KA, Cassel TN, Helleday T. Spontaneous homologous recombination is induced by collapsed replication forks that are caused by endogenous DNA single-strand breaks. Molecular and Cellular Biology. 2005;25(16):7158-69. doi: 10.1128/Mcb.25.16.7158-7169.2005. PubMed PMID: WOS:000231000800026.

111. Fong PC, Boss DS, Yap TA, Tutt A, Wu P, Mergui-Roelvink M, Mortimer P, Swaisland H, Lau A, O'Connor MJ, Ashworth A, Carmichael J, Kaye SB, Schellens JH, de Bono JS. Inhibition of poly(ADP-ribose) polymerase in tumors from BRCA mutation carriers. N Engl J Med. 2009;361(2):123-34. doi: 10.1056/NEJMoa0900212. PubMed PMID: 19553641.

112. Audeh MW, Carmichael J, Penson RT, Friedlander M, Powell B, Bell-McGuinn KM, Scott C, Weitzel JN, Oaknin A, Loman N, Lu K, Schmutzler RK, Matulonis U, Wickens M, Tutt A. Oral poly(ADP-ribose) polymerase inhibitor olaparib in patients with BRCA1 or BRCA2 mutations and recurrent ovarian cancer: a proof-of-concept trial. Lancet. 2010;376(9737):245-51. doi: 10.1016/S0140-6736(10)60893-8. PubMed PMID: 20609468.

113. Tutt A, Robson M, Garber JE, Domchek SM, Audeh MW, Weitzel JN, Friedlander M, Arun B, Loman N, Schmutzler RK, Wardley A, Mitchell G, Earl H, Wickens M, Carmichael J. Oral poly(ADP-ribose) polymerase inhibitor olaparib in patients with BRCA1 or BRCA2 mutations and advanced breast cancer: a proof-of-concept trial. Lancet. 2010;376(9737):235-44. doi: 10.1016/S0140-6736(10)60892-6. PubMed PMID: 20609467.

114. Kaufman B, Shapira-Frommer R, Schmutzler RK, Audeh MW, Friedlander M, Balmana J, Mitchell G, Fried G, Stemmer SM, Hubert A, Rosengarten O, Steiner M, Loman N, Bowen K, Fielding A, Domchek SM. Olaparib monotherapy in patients with advanced cancer and a germline BRCA1/2 mutation. J Clin Oncol. 2015;33(3):244-50. doi: 10.1200/JCO.2014.56.2728. PubMed PMID: 25366685.

115. Edwards SL, Brough R, Lord CJ, Natrajan R, Vatcheva R, Levine DA, Boyd J, Reis-Filho JS, Ashworth A. Resistance to therapy caused by intragenic deletion in BRCA2. Nature. 2008;451(7182):1111-5. doi: 10.1038/nature06548. PubMed PMID: 18264088.

116. Barber LJ, Sandhu S, Chen L, Campbell J, Kozarewa I, Fenwick K, Assiotis I, Rodrigues DN, Reis Filho JS, Moreno V, Mateo J, Molife LR, De Bono J, Kaye S, Lord CJ, Ashworth A. Secondary mutations in BRCA2 associated with clinical resistance to a PARP inhibitor. J Pathol. 2013;229(3):422-9. doi: 10.1002/path.4140. PubMed PMID: 23165508.

117.   Jaspers JE, Kersbergen A, Boon U, Sol W, van Deemter L, Zander SA, Drost R, Wientjens E, Ji J, Aly A, Doroshow JH, Cranston A, Martin NM, Lau A, O'Connor MJ, Ganesan S, Borst P, Jonkers J, Rottenberg S. Loss of 53BP1 causes PARP inhibitor resistance in Brca1-mutated mouse mammary tumors. Cancer Discov. 2013;3(1):68-81. doi: 10.1158/2159-8290.CD-12-0049. PubMed PMID: 23103855.

118.   Xu G, Chapman JR, Brandsma I, Yuan J, Mistrik M, Bouwman P, Bartkova J, Gogola E, Warmerdam D, Barazas M, Jaspers JE, Watanabe K, Pieterse M, Kersbergen A, Sol W, Celie PH, Schouten PC, van den Broek B, Salman A, Nieuwland M, de Rink I, de Ronde J, Jalink K, Boulton SJ, Chen J, van Gent DC, Bartek J, Jonkers J, Borst P, Rottenberg S. REV7 counteracts DNA double-strand break resection and affects PARP inhibition. Nature. 2015;521(7553):541-4. doi: 10.1038/nature14328. PubMed PMID: 25799992; PMCID: PMC4671316.

119.   Ashworth A, Lord CJ, Reis-Filho JS. Genetic interactions in cancer progression and treatment. Cell. 2011;145(1):30-8. doi: 10.1016/j.cell.2011.03.020. PubMed PMID: 21458666.

120.   Nijman SM. Synthetic lethality: general principles, utility and detection using genetic screens in human cells. FEBS Lett. 2011;585(1):1-6. doi: 10.1016/j.febslet.2010.11.024. PubMed PMID: 21094158; PMCID: PMC3018572.

121.   Tong AH, Boone C. Synthetic genetic array analysis in Saccharomyces cerevisiae. Methods Mol Biol. 2006;313:171-92. PubMed PMID: 16118434.

122.   Putnam CD, Srivatsan A, Nene RV, Martinez SL, Clotfelter SP, Bell SN, Somach SB, de Souza JE, Fonseca AF, de Souza SJ, Kolodner RD. A genetic network that suppresses genome rearrangements in Saccharomyces cerevisiae and contains defects in cancers. Nat Commun. 2016;7:11256. doi: 10.1038/ncomms11256. PubMed PMID: 27071721; PMCID: PMC4833866.

123.   Srivatsan A, Li B, Sanchez DN, Somach SB, da Silva VL, de Souza SJ, Putnam CD, Kolodner RD. Essential Saccharomyces cerevisiae genome instability suppressing genes identify potential human tumor suppressors. Proc Natl Acad Sci U S A. 2019;116(35):17377-82. Epub 2019/08/15. doi: 10.1073/pnas.1906921116. PubMed PMID: 31409704; PMCID: PMC6717276.

124.   Tishkoff DX, Filosi N, Gaida GM, Kolodner RD. A novel mutation avoidance mechanism dependent on S-cerevisiae RAD27 is distinct from DNA mismatch repair. Cell. 1997;88(2):253-63. doi: Doi 10.1016/S0092-8674(00)81846-2. PubMed PMID: WOS:A1997WE97000014.

125.   Tishkoff DX, Filosi N, Gaida GM, Kolodner RD. A novel mutation avoidance mechanism dependent on S. cerevisiae RAD27 is distinct from DNA mismatch repair. Cell. 1997;88(2):253-63. PubMed PMID: 9008166.

126.   Symington LS. Homologous recombination is required for the viability of rad27 mutants. Nucleic Acids Res. 1998;26(24):5589-95. PubMed PMID: 9837987; PMCID: PMC148039.

127.   Ishimi Y, Claude A, Bullock P, Hurwitz J. Complete enzymatic synthesis of DNA containing the SV40 origin of replication. J Biol Chem. 1988;263(36):19723-33. PubMed PMID: 2848839.

128.   Goulian M, Richards SH, Heard CJ, Bigsby BM. Discontinuous DNA synthesis by purified mammalian proteins. J Biol Chem. 1990;265(30):18461-71. PubMed PMID: 2170412.

129.   Turchi JJ, Bambara RA. Completion of mammalian lagging strand DNA replication using purified proteins. J Biol Chem. 1993;268(20):15136-41. PubMed PMID: 8392066.

130.   Turchi JJ, Huang L, Murante RS, Kim Y, Bambara RA. Enzymatic completion of mammalian lagging-strand DNA replication. Proc Natl Acad Sci U S A. 1994;91(21):9803-7. PubMed PMID: 7524089; PMCID: PMC44905.

131.   Waga S, Bauer G, Stillman B. Reconstitution of complete SV40 DNA replication with purified replication factors. J Biol Chem. 1994;269(14):10923-34. PubMed PMID: 8144677.

132.   Robins P, Pappin DJ, Wood RD, Lindahl T. Structural and functional homology between mammalian DNase IV and the 5'-nuclease domain of Escherichia coli DNA polymerase I. J Biol Chem. 1994;269(46):28535-8. PubMed PMID: 7961795.

133.   Johnson RE, Kovvali GK, Prakash L, Prakash S. Requirement of the yeast RTH1 5' to 3' exonuclease for the stability of simple repetitive DNA. Science. 1995;269(5221):238-40. PubMed PMID: 7618086.

134.   Wu X, Li J, Li X, Hsieh CL, Burgers PM, Lieber MR. Processing of branched DNA intermediates by a complex of human FEN-1 and PCNA. Nucleic Acids Res. 1996;24(11):2036-43. PubMed PMID: 8668533; PMCID: PMC145902.

135.   Harrington JJ, Lieber MR. The characterization of a mammalian DNA structure-specific endonuclease. EMBO J. 1994;13(5):1235-46. PubMed PMID: 8131753; PMCID: PMC394933.

136.   Harrington JJ, Lieber MR. Functional domains within FEN-1 and RAD2 define a family of structure-specific endonucleases: implications for nucleotide excision repair. Genes Dev. 1994;8(11):1344-55. PubMed PMID: 7926735.

137.   Barnes CJ, Wahl AF, Shen B, Park MS, Bambara RA. Mechanism of tracking and cleavage of adduct-damaged DNA substrates by the mammalian 5'- to 3'-exonuclease/endonuclease RAD2 homologue 1 or flap endonuclease 1. J Biol Chem. 1996;271(47):29624-31. Epub 1996/11/22. doi: 10.1074/jbc.271.47.29624. PubMed PMID: 8939893.

138.   Murante RS, Huang L, Turchi JJ, Bambara RA. The Calf 5'-Exonuclease to 3'-Exonuclease Is Also an Endonuclease with Both Activities Dependent on Primers Annealed Upstream of the Point of Cleavage. Journal of Biological Chemistry. 1994;269(2):1191-6. PubMed PMID: WOS:A1994MR22000067.

139.   Murante RS, Rumbaugh JA, Barnes CJ, Norton JR, Bambara RA. Calf RTH-1 nuclease can remove the initiator RNAs of Okazaki fragments by endonuclease activity. Journal of Biological Chemistry. 1996;271(42):25888-97. doi: DOI 10.1074/jbc.271.42.25888. PubMed PMID: WOS:A1996VN18000027.

140.   Turchi JJ, Huang L, Murante RS, Kim Y, Bambara RA. Enzymatic Completion of Mammalian Lagging-Strand DNA-Replication. P Natl Acad Sci USA. 1994;91(21):9803-7. doi: DOI 10.1073/pnas.91.21.9803. PubMed PMID: WOS:A1994PM13800029.

141.   Lusetti SL, Cox MM. The bacterial RecA protein and the recombinational DNA repair of stalled replication forks. Annu Rev Biochem. 2002;71:71-100. Epub 2002/06/05. doi: 10.1146/annurev.biochem.71.083101.133940. PubMed PMID: 12045091.

142.   Sharma S, Otterlei M, Sommers JA, Driscoll HC, Dianov GL, Kao HI, Bambara RA, Brosh RM. WRN helicase and FEN-1 form a complex upon replication arrest and together process branch-migrating DNA structures associated with the replication fork. Mol Biol Cell. 2004;15(2):734-50. doi: 10.1091/mbc.E03-08-0567. PubMed PMID: WOS:000188718900032.

143.   Liu Y, Wilson SH. DNA base excision repair: a mechanism of trinucleotide repeat expansion. Trends Biochem Sci. 2012;37(4):162-72. Epub 2012/01/31. doi: 10.1016/j.tibs.2011.12.002. PubMed PMID: 22285516; PMCID: PMC3323758.

144.   Kunkel TA, Resnick MA, Gordenin DA. Mutator specificity and disease: looking over the FENce. Cell. 1997;88(2):155-8. Epub 1997/01/24. doi: 10.1016/s0092-8674(00)81832-2. PubMed PMID: 9008154.

145.   Reagan MS, Pittenger C, Siede W, Friedberg EC. Characterization of a mutant strain of Saccharomyces cerevisiae with a deletion of the RAD27 gene, a structural homolog of the RAD2 nucleotide excision repair gene. J Bacteriol. 1995;177(2):364-71. PubMed PMID: 7814325; PMCID: PMC176599.

146.   Sommers CH, Miller EJ, Dujon B, Prakash S, Prakash L. Conditional lethality of null mutations in RTH1 that encodes the yeast counterpart of a mammalian 5'- to 3'-exonuclease required for lagging strand DNA synthesis in reconstituted systems. J Biol Chem. 1995;270(9):4193-6. PubMed PMID: 7876174.

147.   Vallen EA, Cross FR. Mutations in RAD27 define a potential link between G1 cyclins and DNA replication. Mol Cell Biol. 1995;15(8):4291-302. PubMed PMID: 7623823; PMCID: PMC230668.

148.   Reagan MS, Pittenger C, Siede W, Friedberg EC. Characterization of a Mutant Strain of Saccharomyces-Cerevisiae with a Deletion of the Rad27 Gene, a Structural Homolog of the Rad2 Nucleotide Excision-Repair Gene. Journal of Bacteriology. 1995;177(2):364-71. doi: DOI 10.1128/jb.177.2.364-371.1995. PubMed PMID: WOS:A1995QB30700012.

149.   Sommers CH, Miller EJ, Dujon B, Prakash S, Prakash L. Conditional Lethality of Null Mutations in Rth1 That Encodes the Yeast Counterpart of a Mammalian 5'-Exonuclease to 3'-Exonuclease Required for Lagging-Strand DNA-Synthesis in Reconstituted Systems. Journal of Biological Chemistry. 1995;270(9):4193-6. doi: DOI 10.1074/jbc.270.9.4193. PubMed PMID: WOS:A1995QK08400004.

150.   Vallen EA, Cross FR. Mutations in Rad27 Define a Potential Link between G(1) Cyclins and DNA-Replication. Molecular and Cellular Biology. 1995;15(8):4291-302. PubMed PMID: WOS:A1995RJ77900033.

151.   Murray JM, Tavassoli M, al-Harithy R, Sheldrick KS, Lehmann AR, Carr AM, Watts FZ. Structural and functional conservation of the human homolog of the Schizosaccharomyces pombe rad2 gene, which is required for chromosome segregation and recovery from DNA damage. Mol Cell Biol. 1994;14(7):4878-88. Epub 1994/07/01. doi: 10.1128/mcb.14.7.4878. PubMed PMID: 8007985; PMCID: PMC358860.

152.   Larsen E, Gran C, Saether BE, Seeberg E, Klungland A. Proliferation failure and gamma radiation sensitivity of Fen1 null mutant mice at the blastocyst stage. Molecular and Cellular Biology. 2003;23(15):5346-53. doi: 10.1128/Mcb.23.15.5346-5353.2003. PubMed PMID: WOS:000184283700022.

153.   Kucherlapati M, Yang K, Kuraguchi M, Zhao J, Lia M, Heyer J, Kane MF, Fan K, Russell R, Brown AM, Kneitz B, Edelmann W, Kolodner RD, Lipkin M, Kucherlapati R. Haploinsufficiency of Flap endonuclease (Fen1) leads to rapid tumor progression. Proc Natl Acad Sci U S A. 2002;99(15):9924-9. doi: 10.1073/pnas.152321699. PubMed PMID: 12119409; PMCID: PMC126601.

154.   Sato M, Girard L, Sekine I, Sunaga N, Ramirez RD, Kamibayashi C, Minna JD. Increased expression and no mutation of the Flap endonuclease (FEN1) gene in human lung cancer. Oncogene. 2003;22(46):7243-6. doi: 10.1038/sj.onc.1206977. PubMed PMID: 14562054.

155.   Lam JS, Seligson DB, Yu H, Li A, Eeva M, Pantuck AJ, Zeng G, Horvath S, Belldegrun AS. Flap endonuclease 1 is overexpressed in prostate cancer and is associated with a high Gleason score. BJU Int. 2006;98(2):445-51. doi: 10.1111/j.1464-410X.2006.06224.x. PubMed PMID: 16879693.

156.   Nikolova T, Christmann M, Kaina B. FEN1 is overexpressed in testis, lung and brain tumors. Anticancer Res. 2009;29(7):2453-9. PubMed PMID: 19596913.

157.   Singh P, Yang M, Dai H, Yu D, Huang Q, Tan W, Kernstine KH, Lin D, Shen B. Overexpression and hypomethylation of flap endonuclease 1 gene in breast and other cancers. Mol Cancer Res. 2008;6(11):1710-7. doi: 10.1158/1541-7786.MCR-08-0269. PubMed PMID: 19010819; PMCID: PMC2948671.

158.   Lenoir WF, Lim TL, Hart T. PICKLES: the database of pooled in-vitro CRISPR knockout library essentiality screens. Nucleic Acids Res. 2018;46(D1):D776-D80. Epub 2017/10/28. doi: 10.1093/nar/gkx993. PubMed PMID: 29077937; PMCID: PMC5753353.

159.   McKinley KL, Cheeseman IM. Large-Scale Analysis of CRISPR/Cas9 Cell-Cycle Knockouts Reveals the Diversity of p53-Dependent Responses to Cell-Cycle Defects. Dev Cell. 2017;40(4):405-20 e2. Epub 2017/02/22. doi: 10.1016/j.devcel.2017.01.012. PubMed PMID: 28216383; PMCID: PMC5345124.

160.   Henneke G, Koundrioukoff S, Hubscher U. Phosphorylation of human Fen1 by cyclin-dependent kinase modulates its role in replication fork regulation. Oncogene.

2003;22(28):4301-13. doi: 10.1038/sj.onc.1206606. PubMed PMID: WOS:000183978900001.

161.   Tumey LN, Bom D, Huck B, Gleason E, Wang J, Silver D, Brunden K, Boozer S, Rundlett S, Sherf B, Murphy S, Dent T, Leventhal C, Bailey A, Harrington J, Bennani YL. The identification and optimization of a N-hydroxy urea series of flap endonuclease 1 inhibitors. Bioorg Med Chem Lett. 2005;15(2):277-81. doi: 10.1016/j.bmcl.2004.10.086. PubMed PMID: 15603939.

162.   Sakai W, Swisher EM, Jacquemont C, Chandramohan KV, Couch FJ, Langdon SP, Wurz K, Higgins J, Villegas E, Taniguchi T. Functional restoration of BRCA2 protein by secondary BRCA2 mutations in BRCA2-mutated ovarian carcinoma. Cancer Res. 2009;69(16):6381-6. doi: 10.1158/0008-5472.CAN-09-1178. PubMed PMID: 19654294; PMCID: PMC2754824.

163.   Barretina J, Caponigro G, Stransky N, Venkatesan K, Margolin AA, Kim S, Wilson CJ, Lehar J, Kryukov GV, Sonkin D, Reddy A, Liu MW, Murray L, Berger MF, Monahan JE, Morais P, Meltzer J, Korejwa A, Jane-Valbuena J, Mapa FA, Thibault J, Bric-Furlong E, Raman P, Shipway A, Engels IH, Cheng J, Yu GYK, Yu JJ, Aspesi P, de Silva M, Jagtap K, Jones MD, Wang L, Hatton C, Palescandolo E, Gupta S, Mahan S, Sougnez C, Onofrio RC, Liefeld T, MacConaill L, Winckler W, Reich M, Li NX, Mesirov JP, Gabriel SB, Getz G, Ardlie K, Chan V, Myer VE, Weber BL, Porter J, Warmuth M, Finan P, Harris JL, Meyerson M, Golub TR, Morrissey MP, Sellers WR, Schlegel R, Garraway LA. The Cancer Cell Line Encyclopedia enables predictive modelling of anticancer drug sensitivity. Nature. 2012;483(7391):603-7. doi: 10.1038/nature11003. PubMed PMID: WOS:000302006100040.

164.   Mertens-Talcott SU, Chintharlapalli S, Li X, Safe S. The oncogenic microRNA-27a targets genes that regulate specificity protein transcription factors and the G2-M checkpoint in MDA-MB-231 breast cancer cells. Cancer Res. 2007;67(22):11001-11. Epub 2007/11/17. doi: 10.1158/0008-5472.CAN-07-2416. PubMed PMID: 18006846.

165.   Li Z, Li J, Mo B, Hu C, Liu H, Qi H, Wang X, Xu J. Genistein induces G2/M cell cycle arrest via stable activation of ERK1/2 pathway in MDA-MB-231 breast cancer cells. Cell Biol Toxicol. 2008;24(5):401-9. Epub 2008/01/29. doi: 10.1007/s10565-008-9054-1. PubMed PMID: 18224451.

166.   Pangon L, Sigglekow ND, Larance M, Al-Sohaily S, Mladenova DN, Selinger CI, Musgrove EA, Kohonen-Corish MR. The "Mutated in Colorectal Cancer" Protein Is a Novel Target of the UV-Induced DNA Damage Checkpoint. Genes Cancer. 2010;1(9):917-26. Epub 2011/07/23. doi: 10.1177/1947601910388937. PubMed PMID: 21779472; PMCID: PMC3092258.

167.   Chung JH, Bunz F. Cdk2 is required for p53-independent G2/M checkpoint control. PLoS Genet. 2010;6(2):e1000863. Epub 2010/03/03. doi: 10.1371/journal.pgen.1000863. PubMed PMID: 20195506; PMCID: PMC2829054.

168.   Voland C, Bord A, Peleraux A, Penarier G, Carriere D, Galiegue S, Cvitkovic E, Jbilo O, Casellas P. Repression of cell cycle-related proteins by oxaliplatin but not cisplatin in human colon cancer cells. Mol Cancer Ther. 2006;5(9):2149-57. Epub 2006/09/21. doi: 10.1158/1535-7163.MCT-05-0212. PubMed PMID: 16985047.

169.   Bunz F, Dutriaux A, Lengauer C, Waldman T, Zhou S, Brown JP, Sedivy JM, Kinzler KW, Vogelstein B. Requirement for p53 and p21 to sustain G2 arrest after DNA damage. Science. 1998;282(5393):1497-501. Epub 1998/11/20. doi: 10.1126/science.282.5393.1497. PubMed PMID: 9822382.

170.   Chan TA, Hermeking H, Lengauer C, Kinzler KW, Vogelstein B. 14-3-3 sigma is required to prevent mitotic catastrophe after DNA damage. Nature. 1999;401(6753):616-20. PubMed PMID: WOS:000083054900058.

171.   Chen Z, Xiao Z, Chen J, Ng SC, Sowin T, Sham H, Rosenberg S, Fesik S, Zhang H. Human Chk1 expression is dispensable for somatic cell death and critical for sustaining G2 DNA damage checkpoint. Mol Cancer Ther. 2003;2(6):543-8. Epub 2003/06/19. PubMed PMID: 12813133.

172.   Jette N, Lees-Miller SP. The DNA-dependent protein kinase: A multifunctional protein kinase with roles in DNA double strand break repair and mitosis. Prog Biophys Mol Bio. 2015;117(2-3):194-205. doi: 10.1016/j.pbiomolbio.2014.12.003. PubMed PMID: WOS:000355025900009.

173.   Andegeko Y, Moyal L, Mittelman L, Tsarfaty I, Shiloh Y, Rotman G. Nuclear retention of ATM at sites of DNA double strand breaks. Journal of Biological Chemistry. 2001;276(41):38224-30. PubMed PMID: WOS:000171526500068.

174.   Bekker-Jensen S, Lukas C, Kitagawa R, Melander F, Kastan MB, Bartek J, Lukas J. Spatial organization of the mammalian genome surveillance machinery in response to DNA strand breaks. J Cell Biol. 2006;173(2):195-206. doi: DOI 10.1083/jcb.200510130. PubMed PMID: WOS:000237055500011.

175.   Bakr A, Oing C, Kocher S, Borgmann K, Dornreiter I, Petersen C, Dikomey E, Mansour WY. Involvement of ATM in homologous recombination after end resection and RAD51 nucleofilament formation. Nucleic Acids Research. 2015;43(6):3154-66. doi: 10.1093/nar/gkv160. PubMed PMID: WOS:000354719300022.

176. Yoshida K, Miki Y. Role of BRCA1 and BRCA2 as regulators of DNA repair, transcription, and cell cycle in response to DNA damage. Cancer Sci. 2004;95(11):866-71. Epub 2004/11/18. doi: 10.1111/j.1349-7006.2004.tb02195.x. PubMed PMID: 15546503.

177. Simhadri S, Vincelli G, Huo YY, Misenko S, Foo TK, Ahlskog J, Sorensen CS, Oakley GG, Ganesan S, Bunting SF, Xia B. PALB2 connects BRCA1 and BRCA2 in the G2/M checkpoint response. Oncogene. 2019;38(10):1585-96. doi: 10.1038/s41388-018-0535-2. PubMed PMID: WOS:000460423800001.

178. Zou L, Elledge SJ. Sensing DNA damage through ATRIP recognition of RPA-ssDNA complexes. Science. 2003;300(5625):1542-8. doi: DOI 10.1126/science.1083430. PubMed PMID: WOS:000183333100046.

179. Bartek J, Lukas J. Mammalian G1- and S-phase checkpoints in response to DNA damage. Current Opinion in Cell Biology. 2001;13(6):738-47. doi: Doi 10.1016/S0955-0674(00)00280-5. PubMed PMID: WOS:000172100700013.

180. Blackford AN, Jackson SP. ATM, ATR, and DNA-PK: The Trinity at the Heart of the DNA Damage Response. Molecular Cell. 2017;66(6):801-17. doi: 10.1016/j.molcel.2017.05.015. PubMed PMID: WOS:000403329400009.

181. Guo Z, Kumagai A, Wang SX, Dunphy WG. Requirement for Atr in phosphorylation of Chk1 and cell cycle regulation in response to DNA replication blocks and UV-damaged DNA in Xenopus egg extracts. Genes Dev. 2000;14(21):2745-56. Epub 2000/11/09. doi: 10.1101/gad.842500. PubMed PMID: 11069891; PMCID: PMC317027.

182. Ahn JY, Schwarz JK, Piwnica-Worms H, Canman CE. Threonine 68 phosphorylation by ataxia telangiectasia mutated is required for efficient activation of Chk2 in response to ionizing radiation. Cancer Research. 2000;60(21):5934-6. PubMed PMID: WOS:000165230300006.

183. Matsuoka S, Rotman G, Ogawa A, Shiloh Y, Tamai K, Elledge SJ. Ataxia telangiectasia-mutated phosphorylates Chk2 in vivo and in vitro. P Natl Acad Sci USA. 2000;97(19):10389-94. doi: DOI 10.1073/pnas.190030497. PubMed PMID: WOS:000089341400020.

184. Zhao H, Piwnica-Worms H. ATR-mediated checkpoint pathways regulate phosphorylation and activation of human Chk1. Mol Cell Biol. 2001;21(13):4129-39. Epub 2001/06/08. doi: 10.1128/MCB.21.13.4129-4139.2001. PubMed PMID: 11390642; PMCID: PMC87074.

185.	Theunissen JWF, Petrini JHJ. Methods for studying the cellular response to DNA damage: Influence of the Mre11 complex on chromosome metabolism. Method Enzymol. 2006;409:251-+.	doi:	10.1016/S0076-6879(05)09015-4.	PubMed	PMID: WOS:000238354800015.

186.	Pierce A, McGowan PM, Cotter M, Mullooly M, O'Donovan N, Rani S, O'Driscoll L, Crown J, Duffy MJ. Comparative antiproliferative effects of iniparib and olaparib on a panel of triple-negative and non-triple-negative breast cancer cell lines. Cancer Biol Ther. 2013;14(6):537-45. Epub 2013/06/14. doi: 10.4161/cbt.24349. PubMed PMID: 23760496; PMCID: PMC3813570.